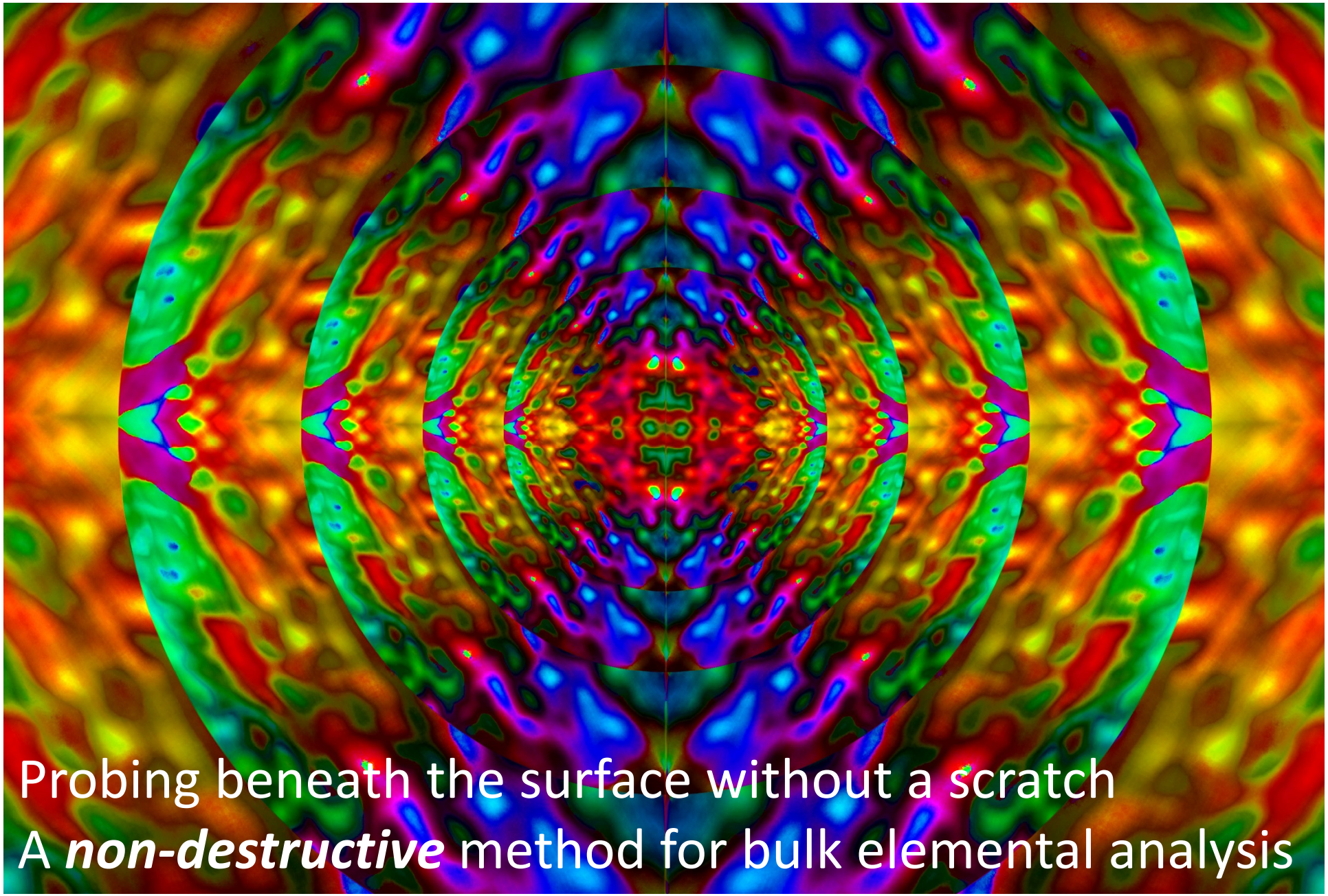

Probing beneath the surface without a scratch
A ***non-destructive*** method for bulk elemental analysis

Adrian Hillier, ISIS muon Group

Outline

- Introduction
- Past Examples
- Current developments and recent results

Elemental analysis

- Determine the composition of a material
- Techniques commonly used are:
  - X-Ray fluorescence
  - Scanning tunnelling microscope
  - Laser ablation
  - Mass spectrometry
  - Neutrons
- Some techniques are destructive
- Some are only surface sensitive

Different probes

Different probes ‘see‘ materials differently, complementary

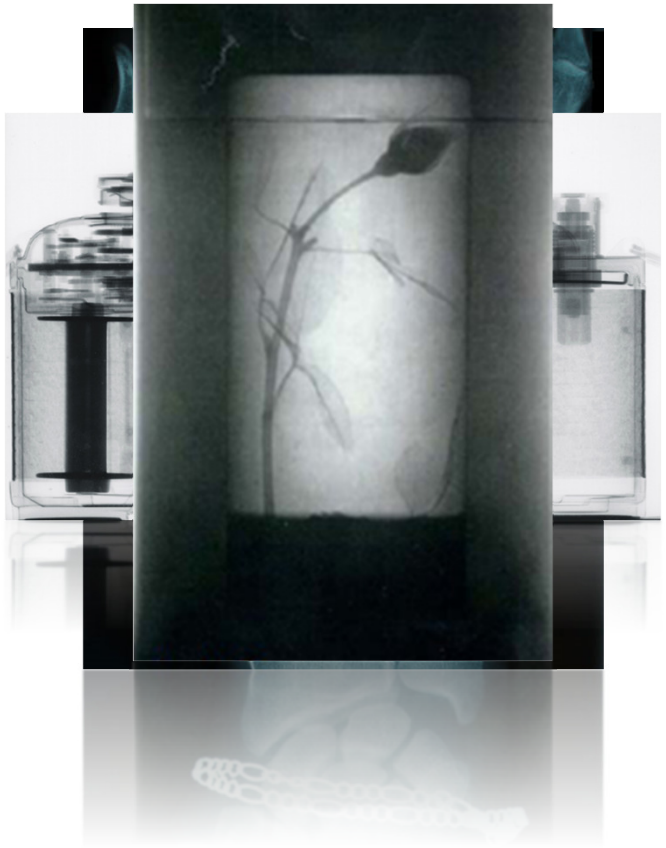

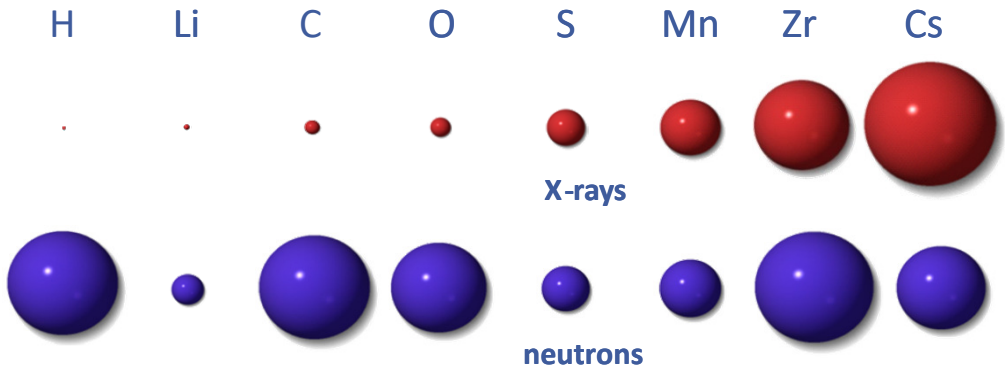

Muon properties

Muons:

- fundamental, charged particles
- heavy electrons
- spin 1/2
- magnetic moment 3.2 x m_p
- mass 0.11 x m_p

- produced from pion decays
- lifetime 2.2 μs (+'ve but varies for -'ve)
- decay into a positron or electron (+ 2xν)

Non destructive probing

Need a method to probe inside materials

- For example, neutrons are highly penetrating
- Neutrons can be used as non-destructive probes

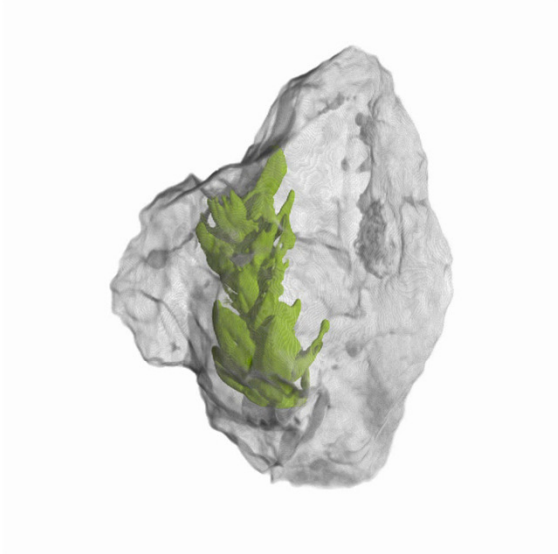

Neutrons in Cultural Heritage

- inorganic material analysis
- metals, ceramics, rocks, pigments
- movable objects

Eneolithic copper axe
Bolzano Museum,
G. Artioli, Padova

16th century gold coins, M. Jones
Mary Rose Trust, Portsmouth

Why?

Non-destructive analysis
Ancient/historic fabrication techniques
Authenticity
Provenance
State of corrosion

Greek coins 1-3 cAD; KHM Vienna;
R Traum; M Griesser

Boettger Stoneware
Staatliche Kunstsammlungen
Dresden, C. Neelmejer

"Striding Nobleman" 16th century,
Rijksmuseum Amsterdam
R. vanLangh

Bronze Age swords from Austria
1500-1000 BC; M. Moedlinger

Koto Age swords; 1000-1500 AD
Stibbert Museum Florence; F Grazzi

Muons at ISIS

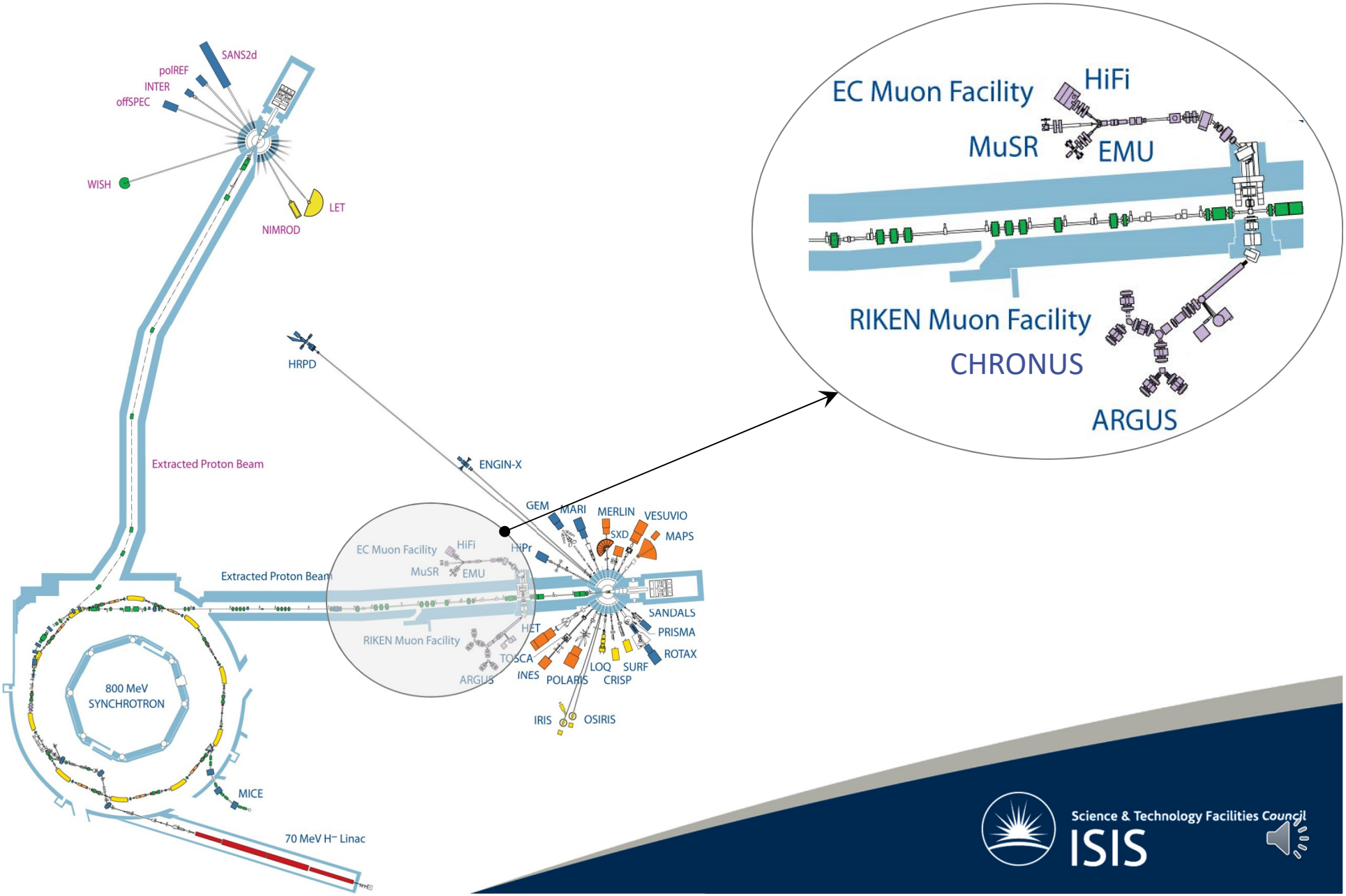

Science & Technology Facilities Council
ISIS

Muons at ISIS

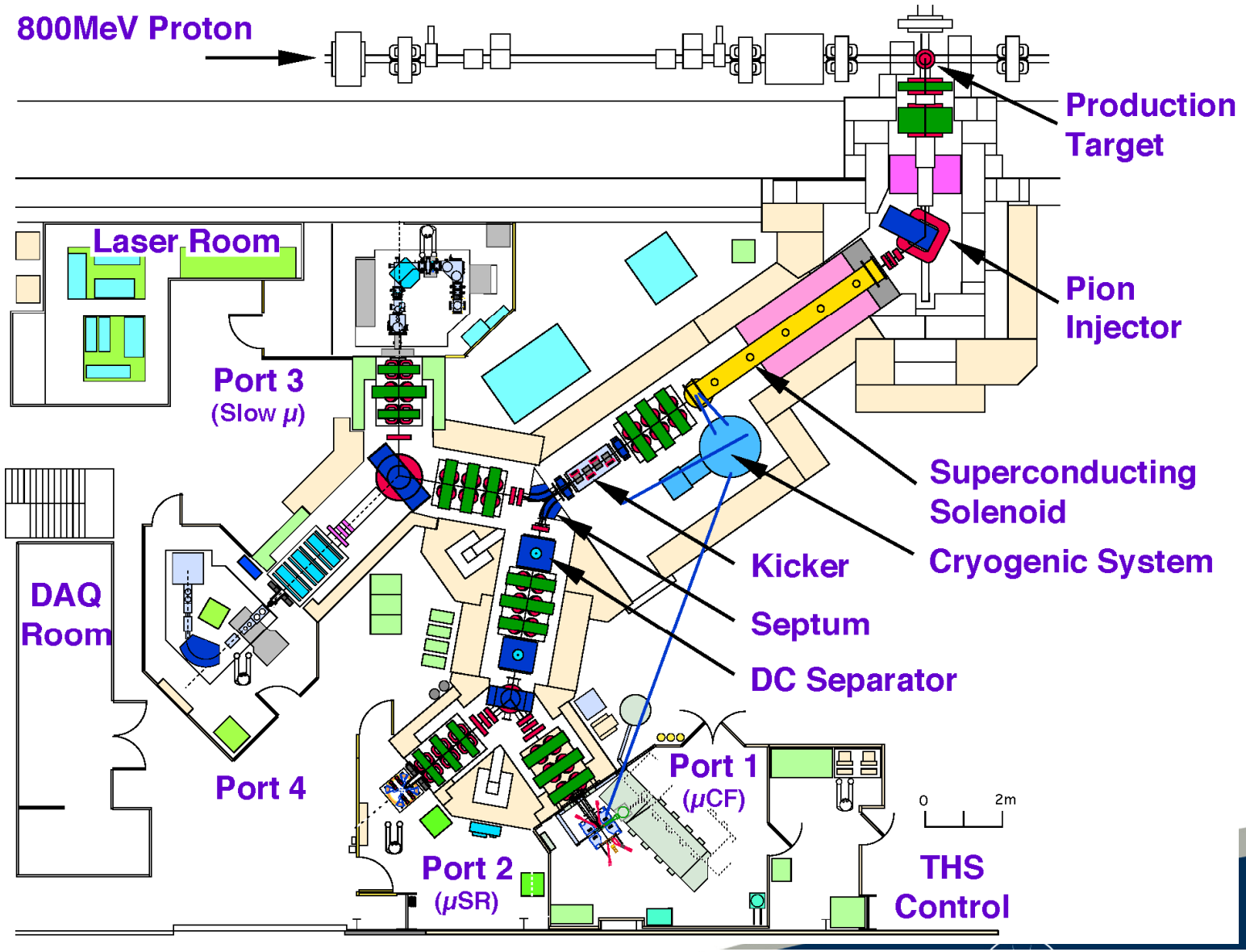

Science & Technology Facilities Council
ISIS

RIKEN

Negative muons

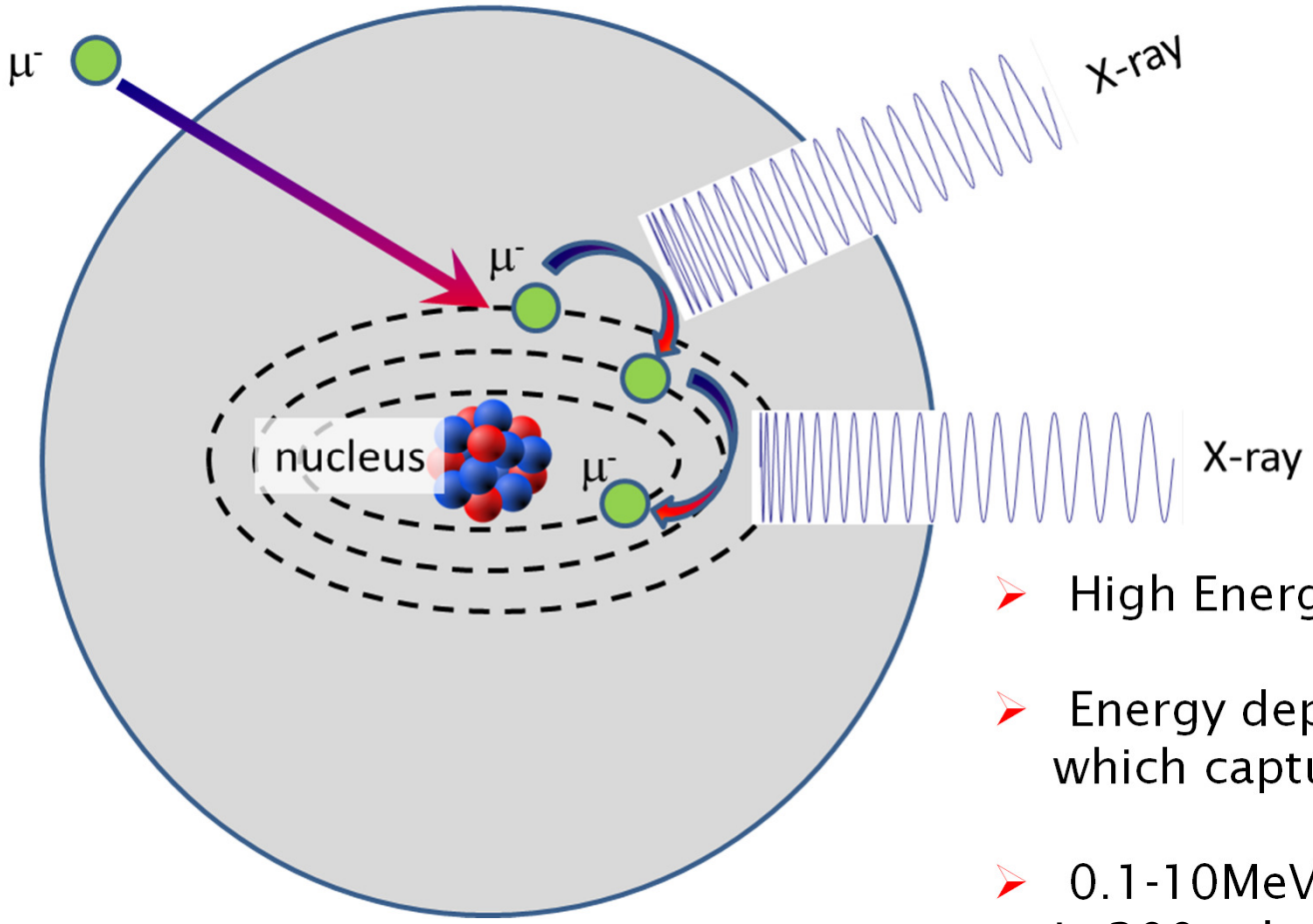

- High Energy X-rays emitted
- Energy dependent of the atom which captures the muon
- 0.1-10MeV – mass of the muon is 200x that of the electron

Negative muons

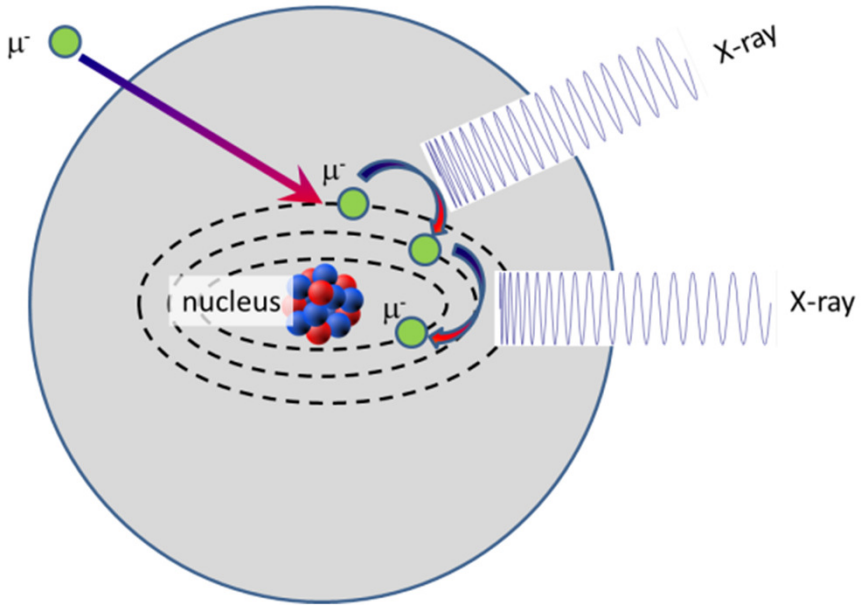

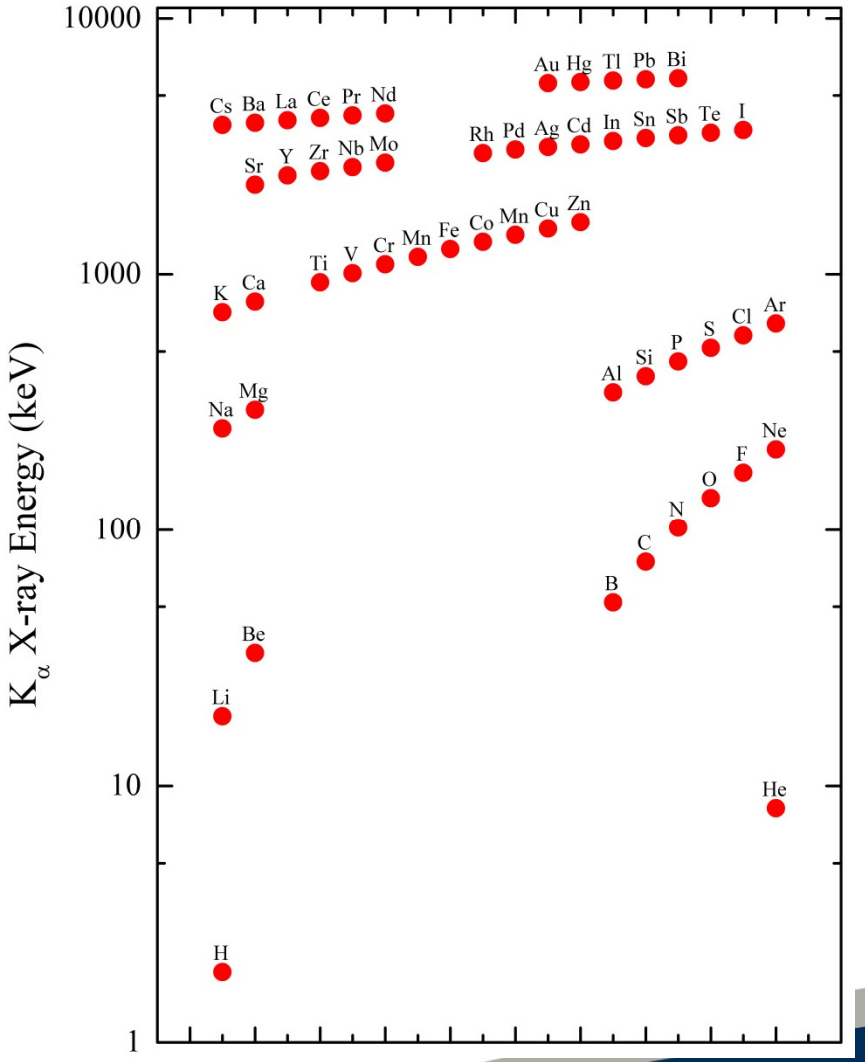

- High Energy X-rays emitted
  - 0.1-10MeV
- Transition Energies are known from measurement and calculation

Negative muons

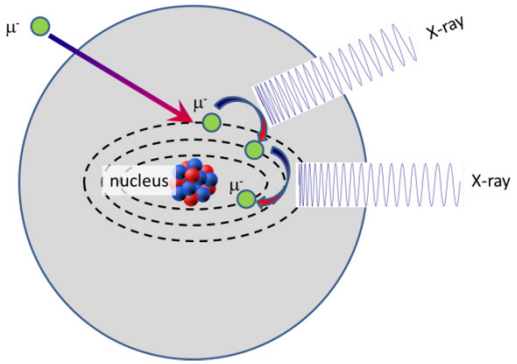

- High Energy X-rays emitted
  - 0.1-10MeV
- Transition Energies are known from measurement and calculation
- Probably of capture known

ATOMIC DATA AND NUCLEAR DATA TABLES **14**, 509–597 (1974)

CHARGE-DISTRIBUTION PARAMETERS, ISOTOPE SHIFTS,

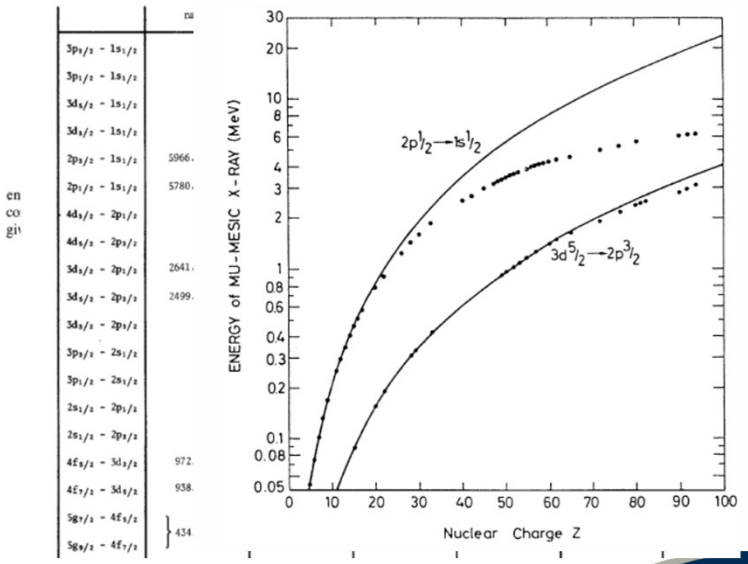

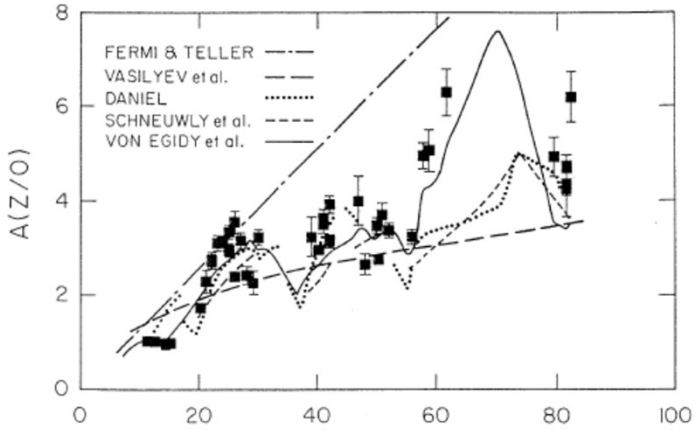

Science & Technology Facilities Council
ISIS

Potential applications for negative muons

- Meteorites
- Energy materials
- Biomaterials
- Welds in Engineering
- Geological samples
- Cultural heritage, coins, arrowheads, mirrors, swords
- Or whatever you would like to know the composition of

Examples - meteorites

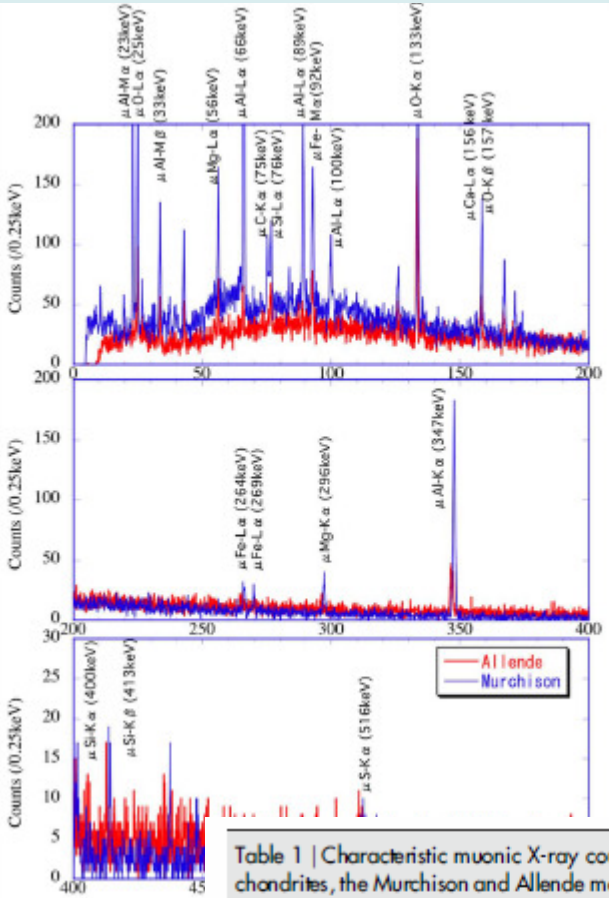

Table 1 | Characteristic muonic X-ray counts from carbonaceous chondrites, the Murchison and Allende meteorites

Characteristic X-ray	Energy (keV)	Murchison	Allende
Ca-Mα	55	n.d.	53 ± 23
Mg-Lα	56	896 ± 66	183 ± 23
Al-Lα	66	10796 ± 130	136 ± 30
C-Kα	75	626 ± 52	6 ± 27
Si-Lα	76	824 ± 58	175 ± 32
Fe-Mα	94	1310 ± 63	265 ± 39
O-Kα	133	4785 ± 111	800 ± 38
K-Lα	140	n.d.	94 ± 27
Ca-Lα	156	213 ± 41	83 ± 28
Al-Kα	346	9542 ± 100	359 ± 27
S-Kα	516	121 ± 33	11 ± 9

n.d.: Not detected.

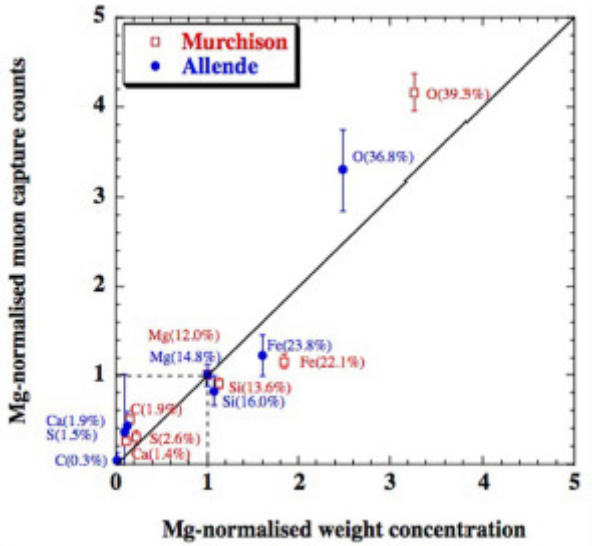

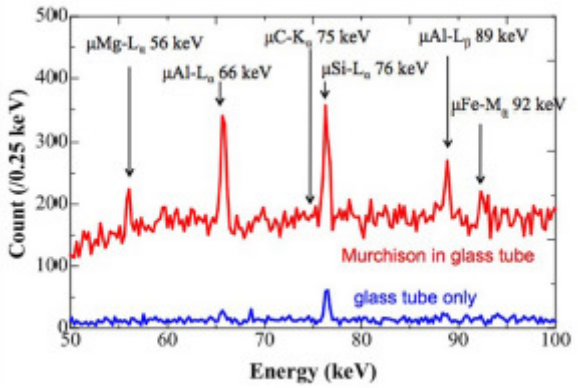

Terada et al Sci. Rep. **4** 5072 (2014)

Science & Technology Facilities Council
ISIS

Examples - bones

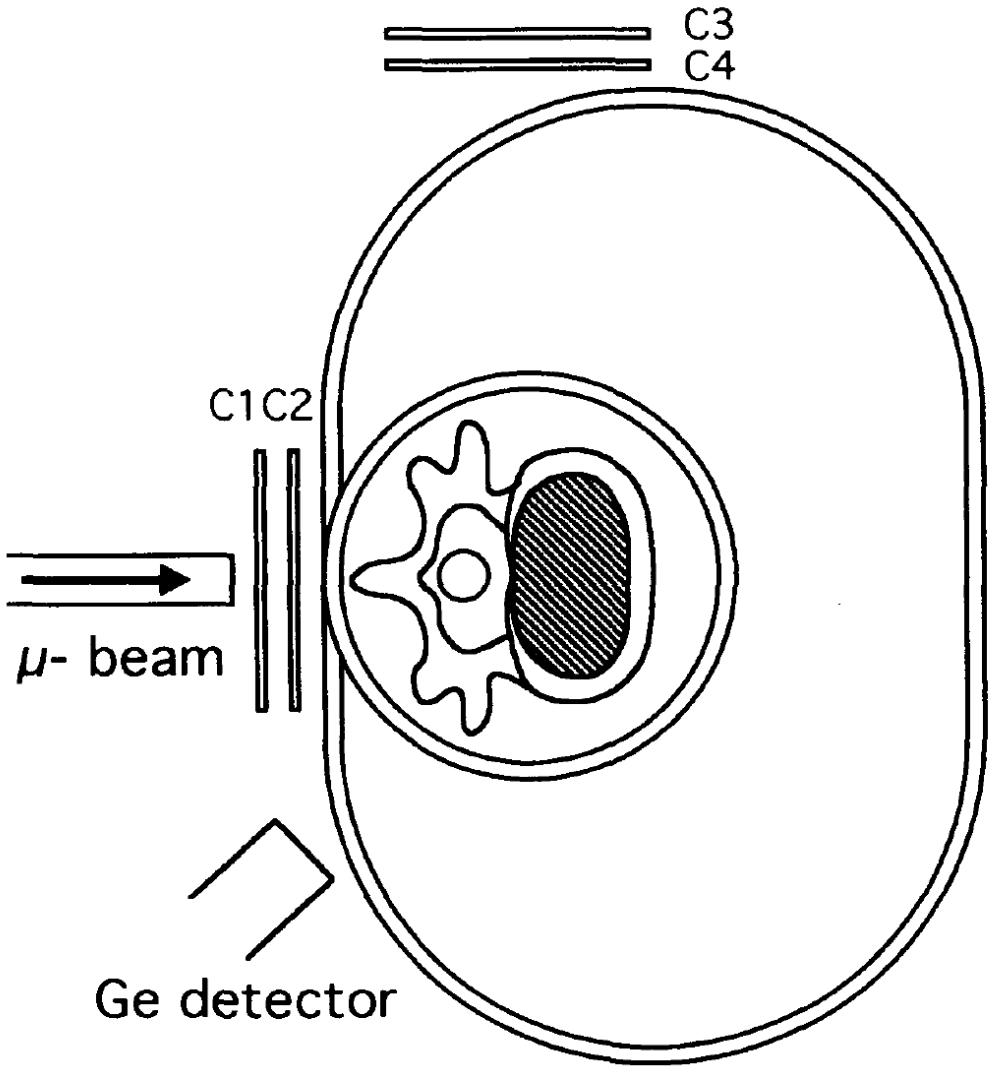

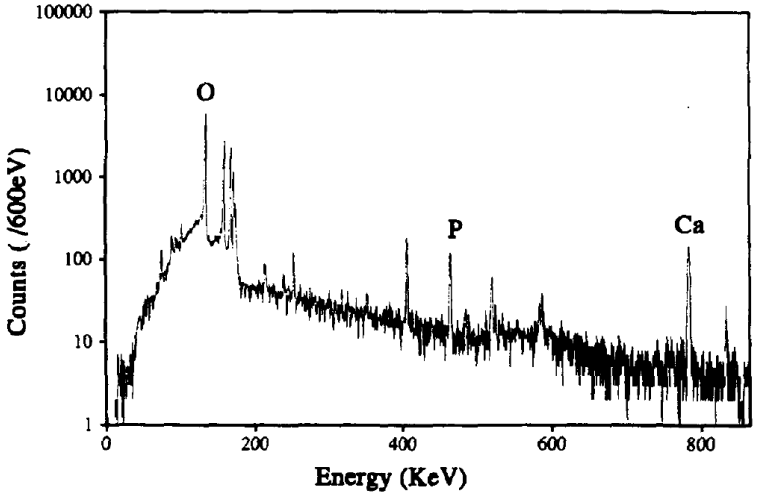

Table III. Elemental composition of bone phantoms

Bone phantom	Ca (mg cm^{-3})	P (mg cm^{-3})
Centre of vertebral body in sample A[a]	70.7	25.7
Centre of vertebral body in sample B[a]	39.3	14.3
Centre of vertebral body in sample C[a]	19.6	7.1
Centre of vertebral body in sample D[a]	0.0	0.0
Non-central portion of vertebral bone A–D[b]	154.9	70.0

Hosoi et al, Radiology, **68**, 1325 (1995)

Examples - biomaterials

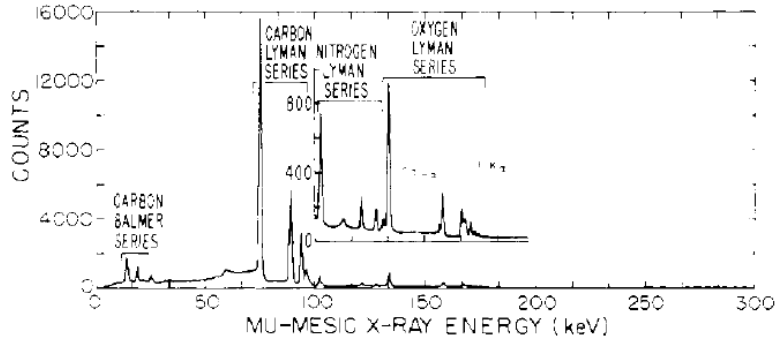

Figure 2. Partial muonic x-ray spectrum from the tissue equivalent plastic sample (Shonka plastic, A-150)

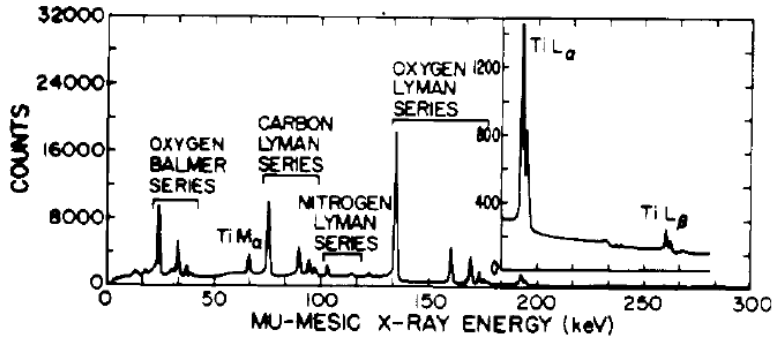

Figure 3. Partial muonic x-ray spectrum from the tissue equivalent liquid sample

Table I. Relative Muonic X-ray Intensities

Element	Transition	Intensity, %[a]
Shonka plastic		
C	2p-1s	55
	3p-1s	20
	4p-1s	11
	5p-1s	3.3
	6p-1s	0.85
N	2p-1s	2.3
	3p-1s	0.76
	4p-1s	0.38
	5p-1s	0.24
O	2p-1s	3.7
	3p-1s	1.3
	4p-1s	0.94
	5p-1s	0.40
F	2p-1s	0.57
Ca	3d-2p	0.30
	2p-1s[b]	0.38
TE-liquid		
C	2p-1s	8.5
	3p-1s	3.5
	4p-1s	1.8
	5p-1s	0.87
N	2p-1s	2.2
	3p-1s	1.1
	4p-1s	0.34
O	2p-1s	48
	3p-1s	14
	4p-1s	12
	5p-1s	5.4
	6p-1s	1.8

[a] See text for a discussion of the uncertainties.
[b] Ca(2p-1s) intensity deduced from Ca(3d-2p) intensity; the uncertainty in this value is approximately 20%.

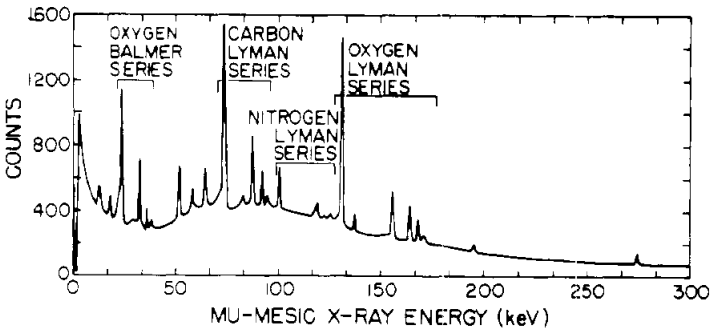

Figure 4. Partial muonic x-ray singles spectrum from a tissue sample, calf liver (singles)

Hosoi et al, Radiology, **68**, 1325 (1995)

ISIS

Examples – Chinese Coins

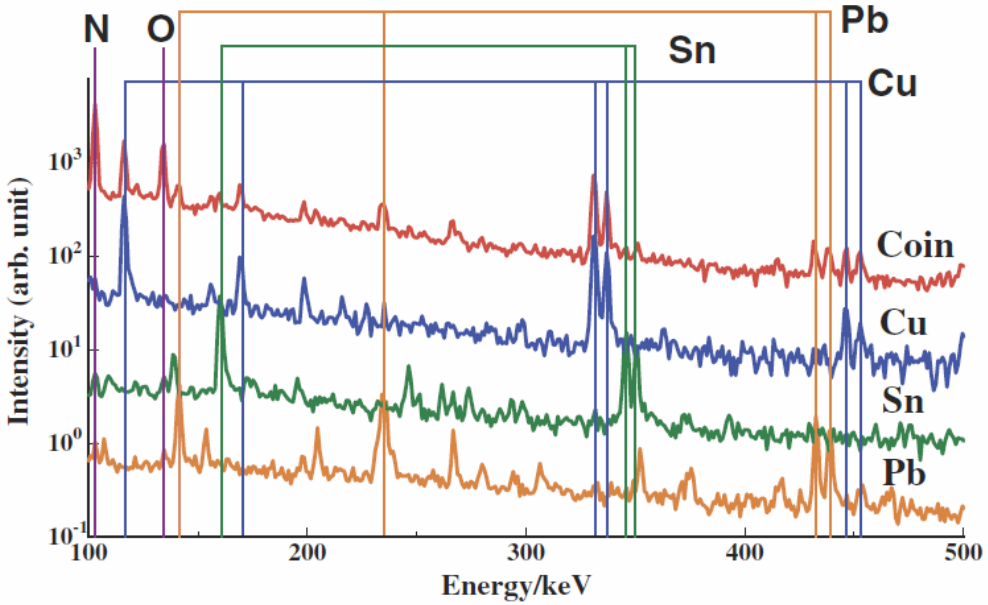

Figure 2. Muonic X-ray spectra measured with the ancient Chinese coin, Cu, Sn, and Pb samples. Muonic X-ray peaks in these spectra originate from muon capture in Cu, Sn, and Pb atoms. In the coin sample, intense N and O muonic X-rays were detected comparing other samples. Because the size of the coin is smaller than the distribution of the muon beam, many muons were stopped in air.

Ninomiya et al Bull. Chem. Soc. Jpn. **85** 228 (2012)

Examples – Chinese Artifacts

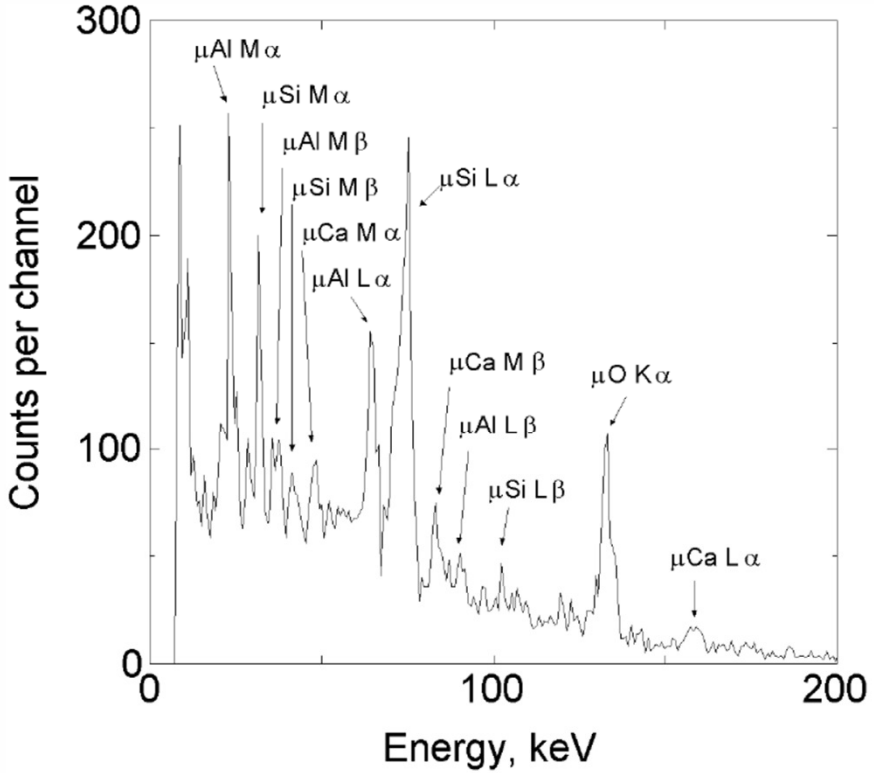

Fig. 4. Muonic X-ray spectrum recorded using a CZT detector of a model Tang San Cai horse

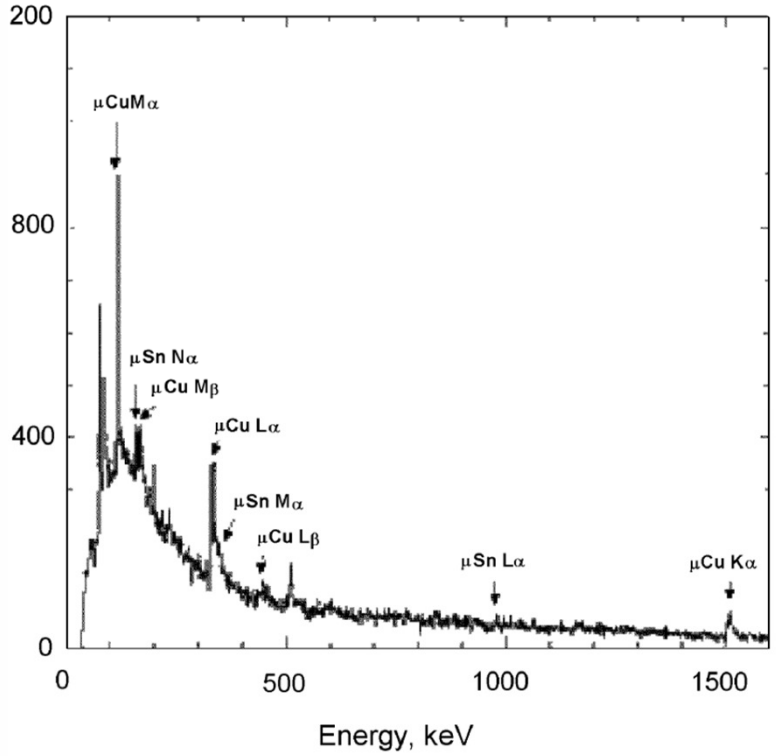

Fig. 2. Muonic X-ray spectrum of an ancient Chinese bronze mirror

Kubo et al J. Rad. Nuc. Chem. **278** 777 (2008)

Test Experiment

In collaboration with RIKEN using port 4

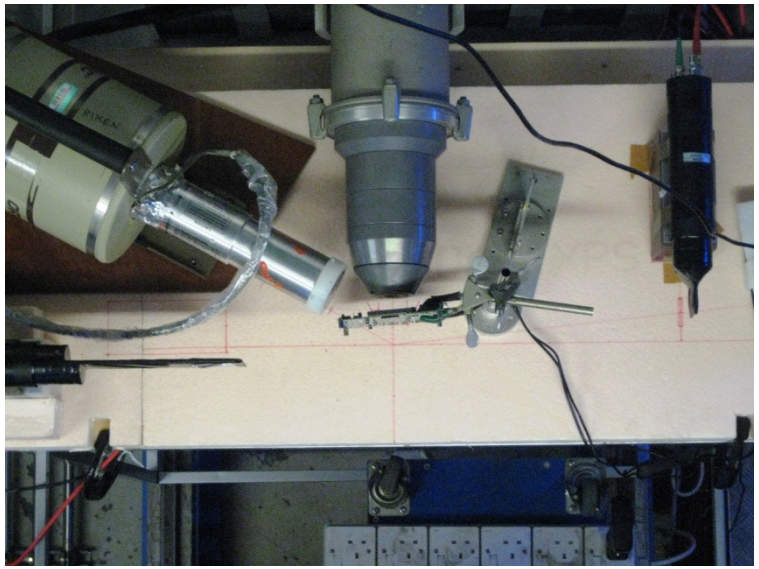

We can use negative muons for elemental analysis

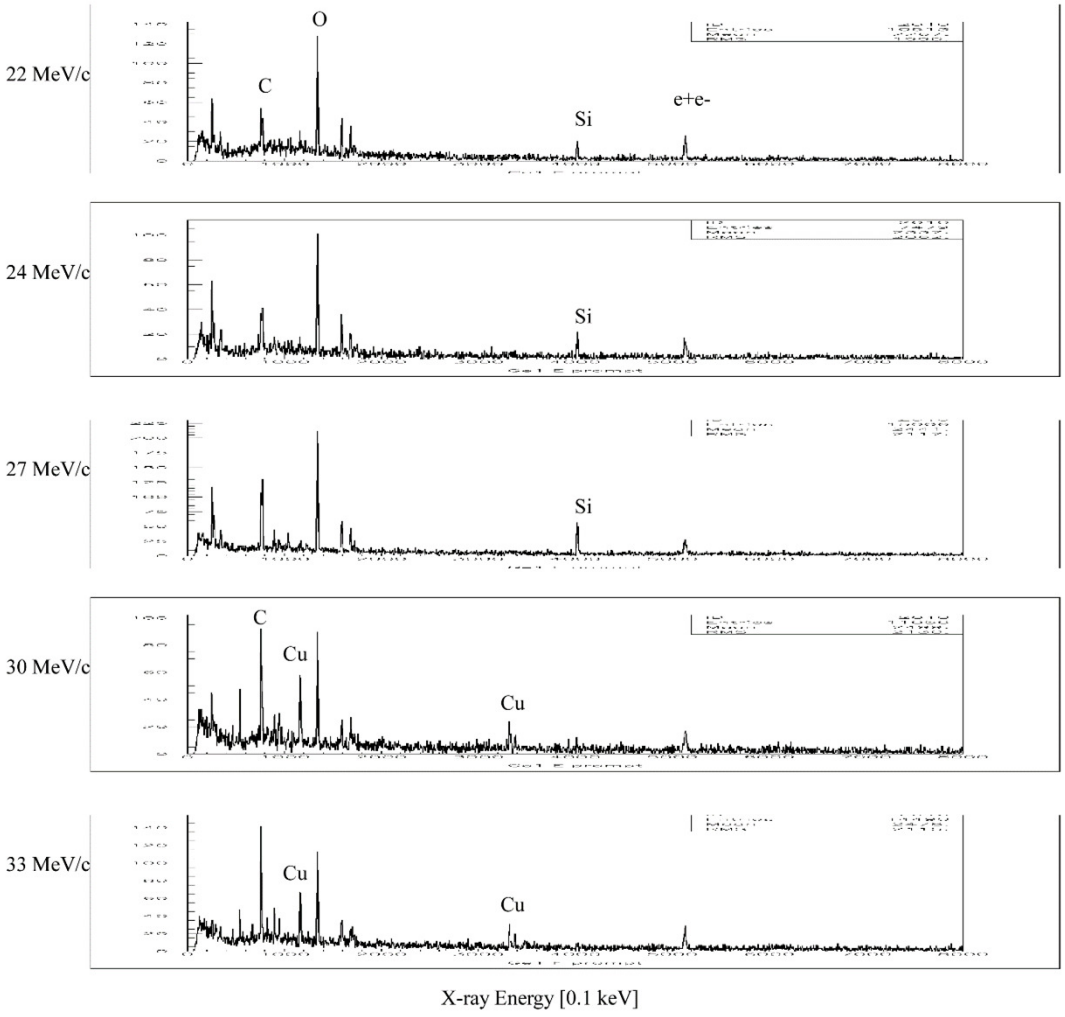

New setup

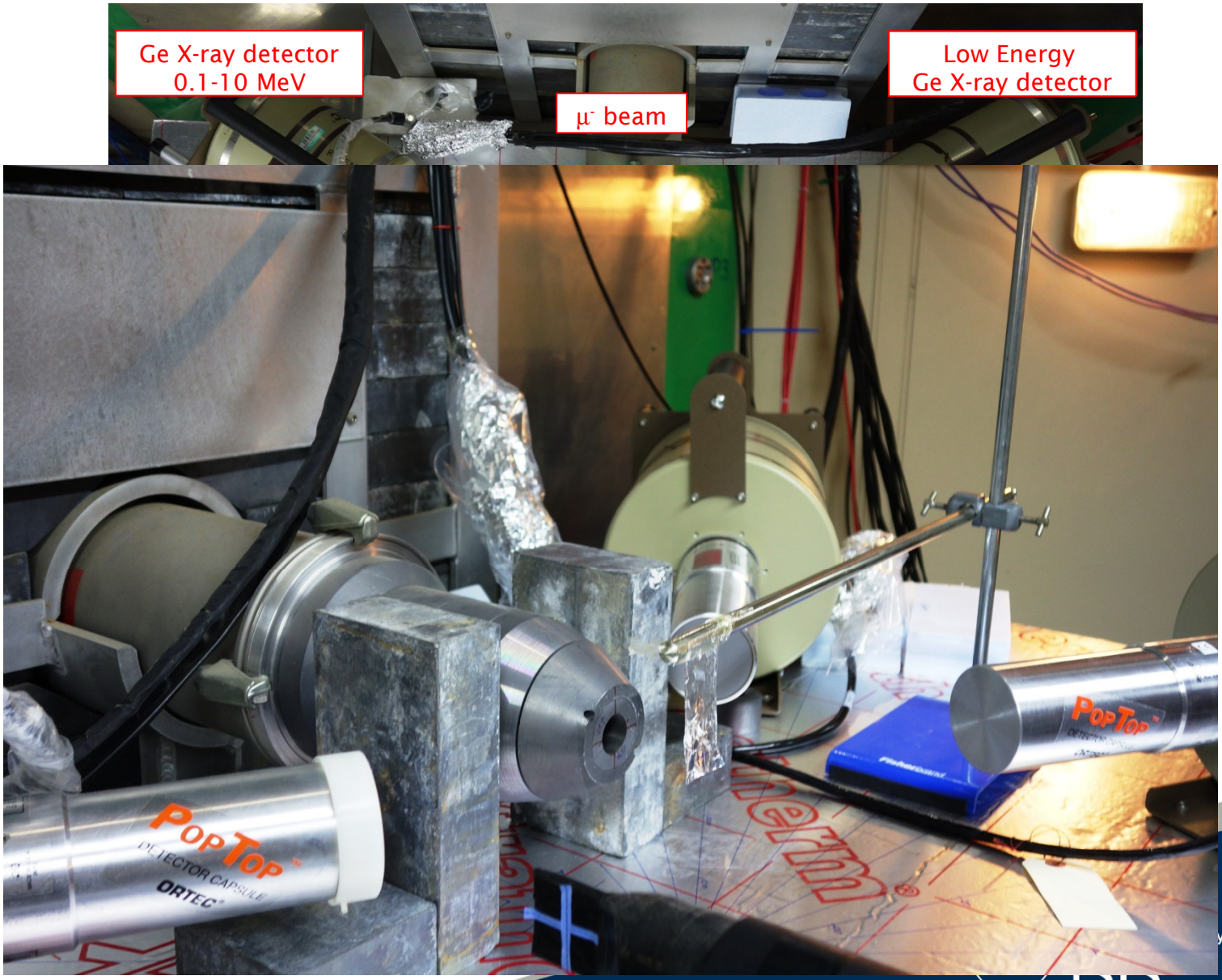
Ge X-ray detector
0.1-10 MeV
μ⁻ beam
Low Energy
Ge X-ray detector
PopTop
DETECTOR CAPSULE
ORTEC

Depth Profiling

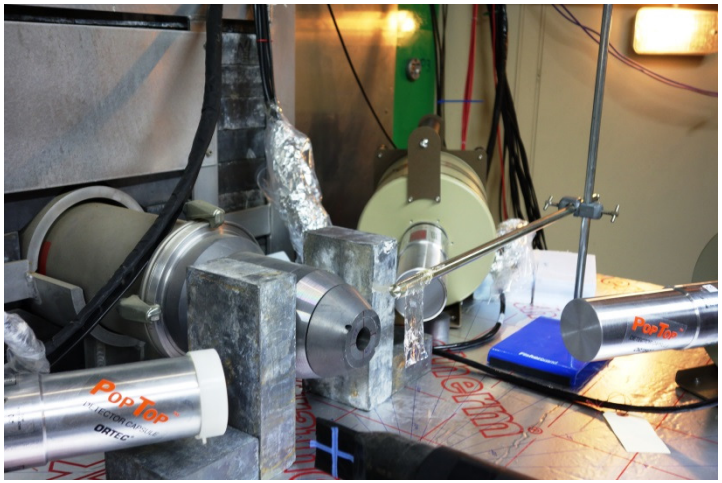

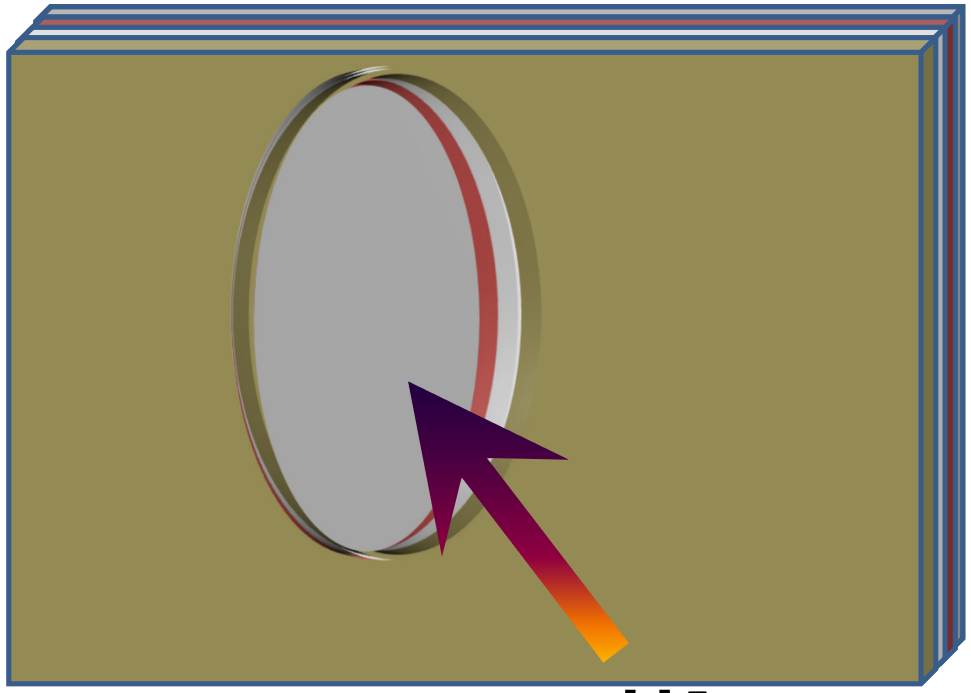

Depth Profiling - Simulations

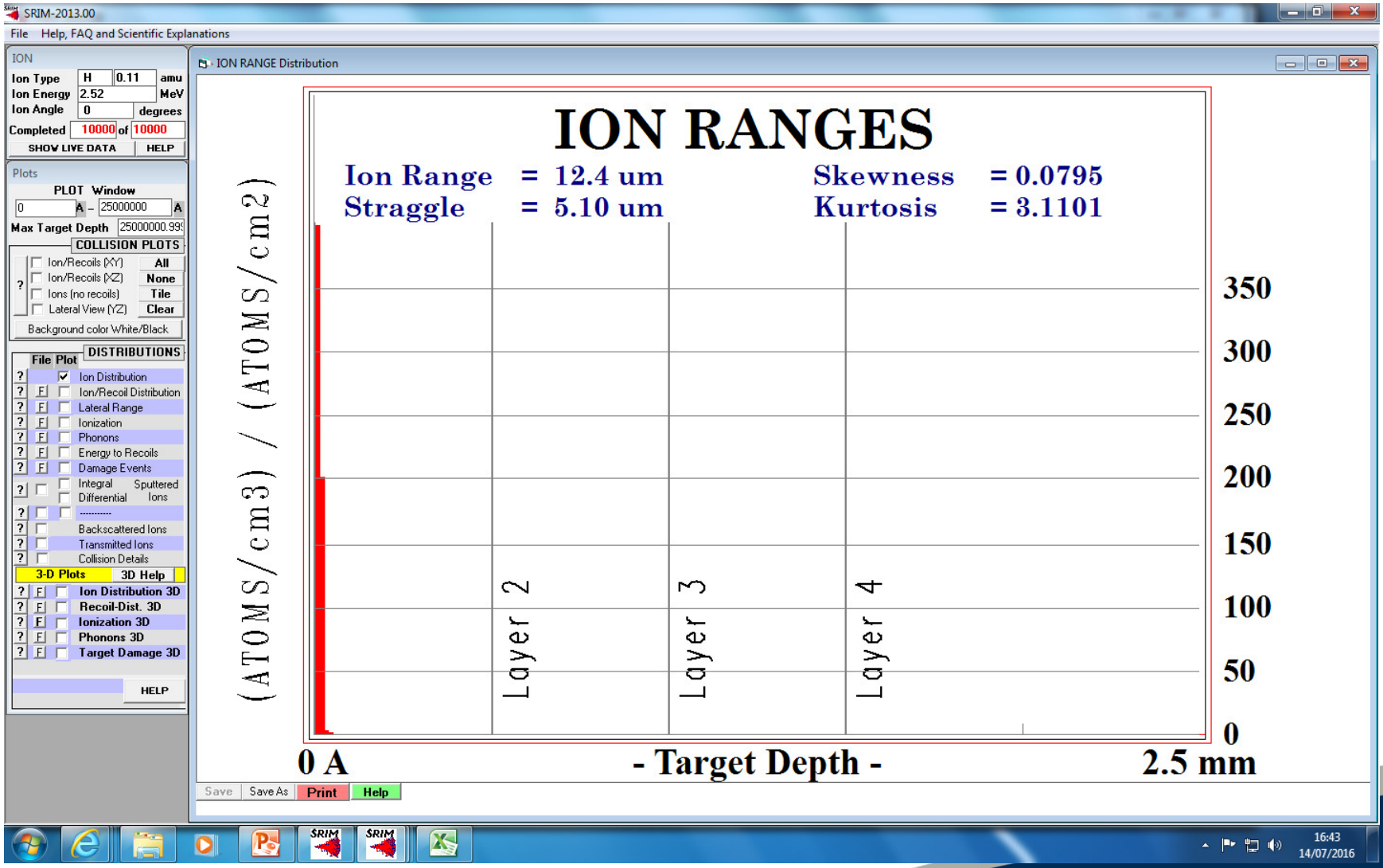

Depth Profiling - Simulations

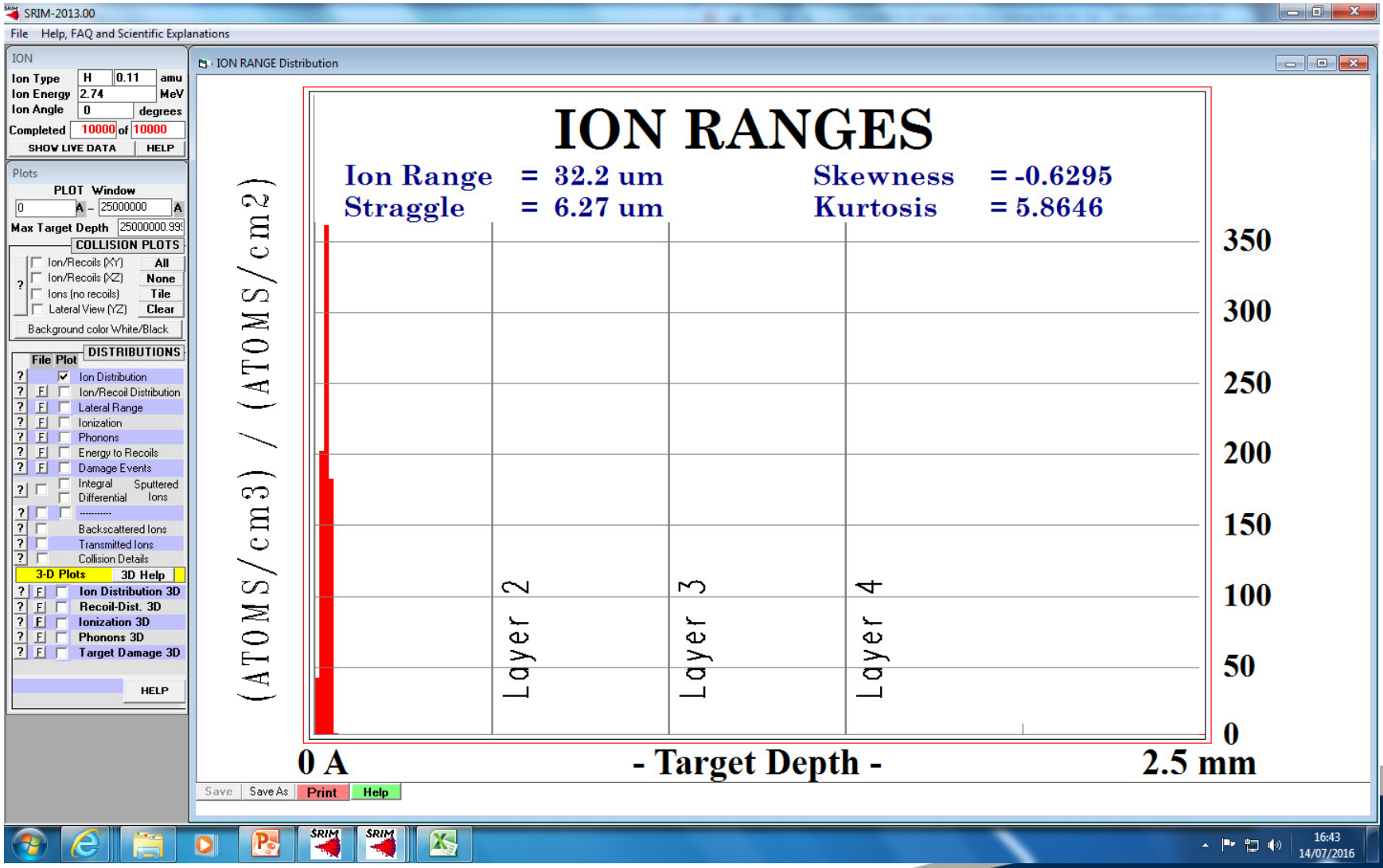

Depth Profiling - Simulations

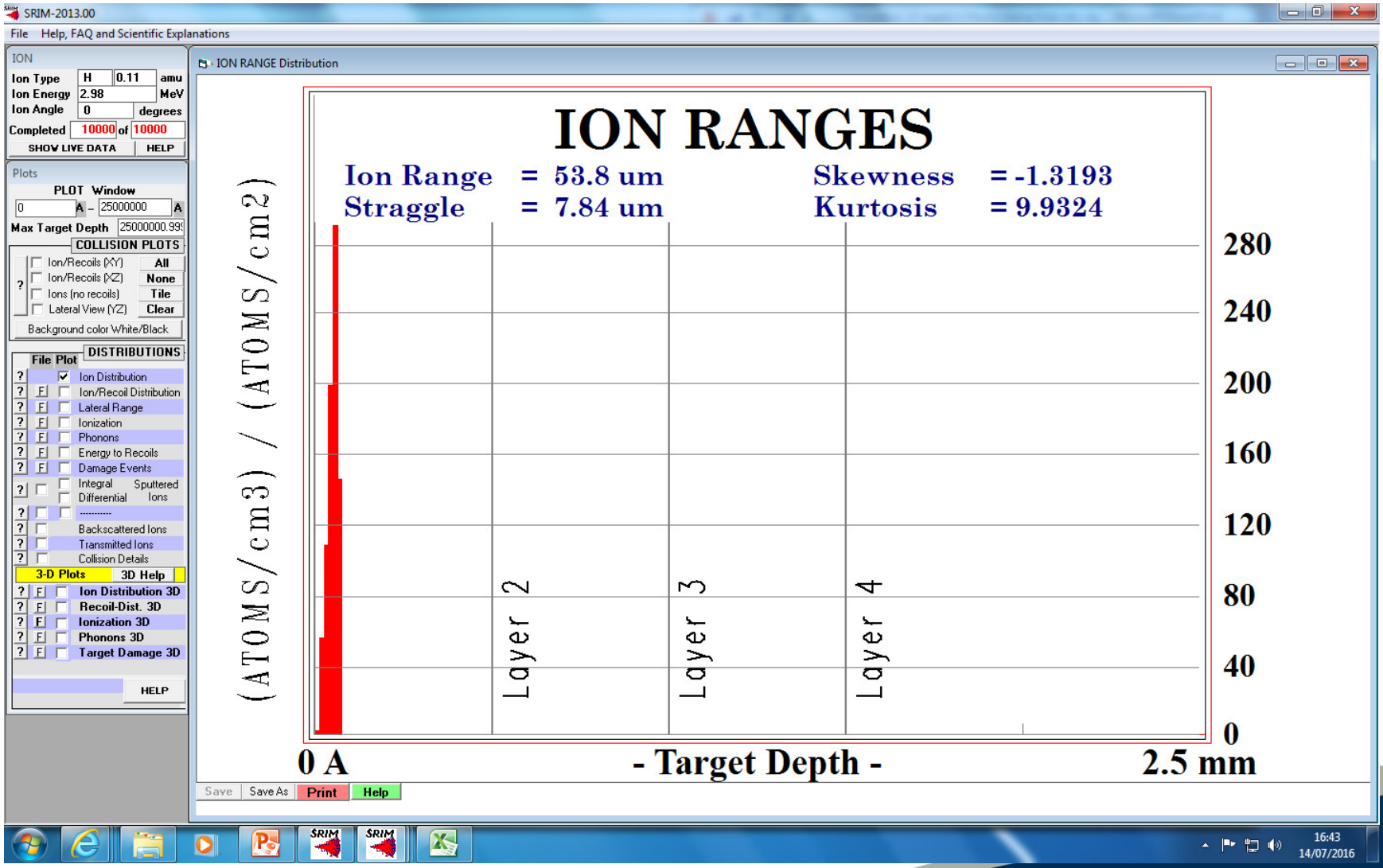

Depth Profiling - Simulations

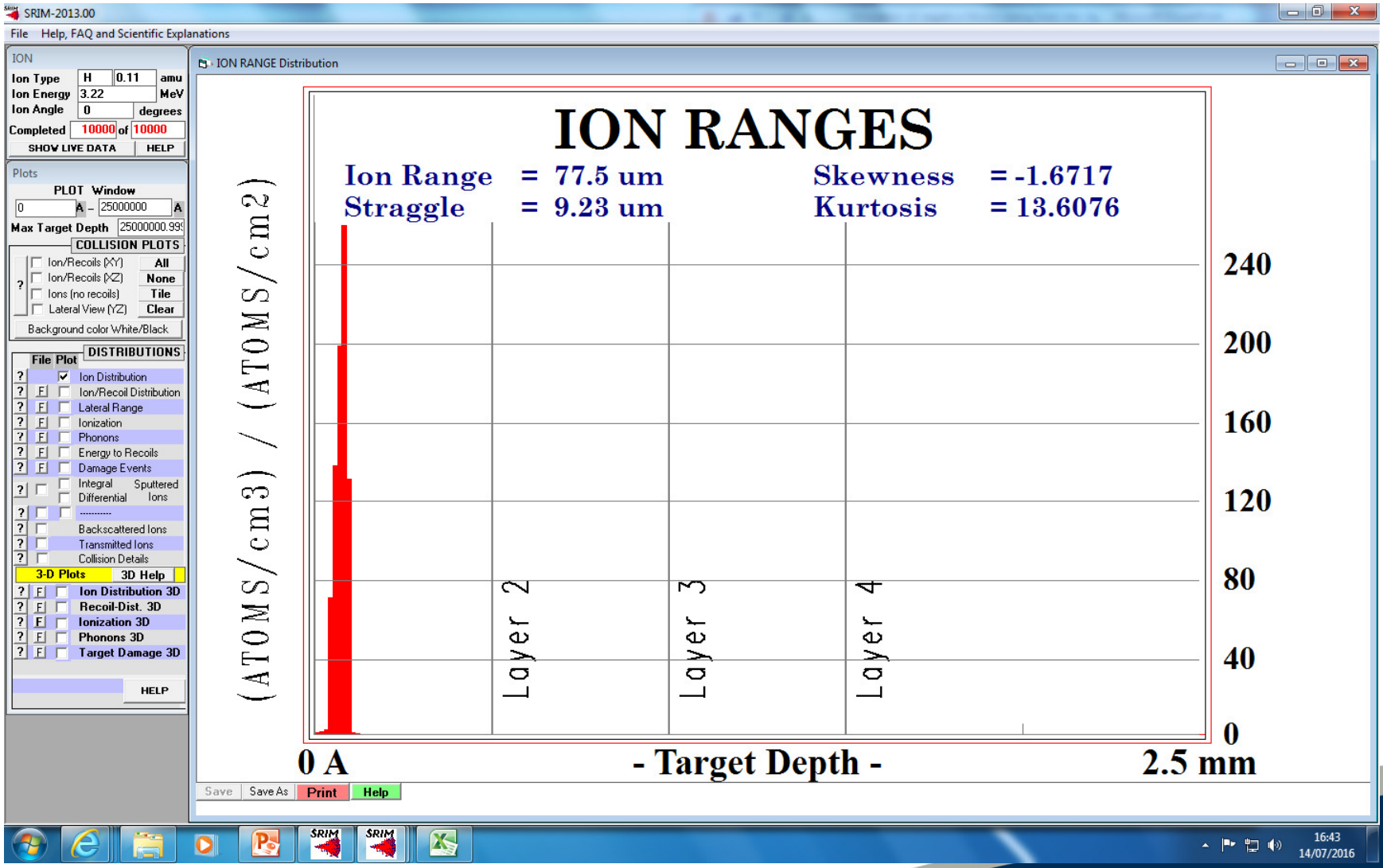

Science & Technology Facilities Council
ISIS

Depth Profiling - Simulations

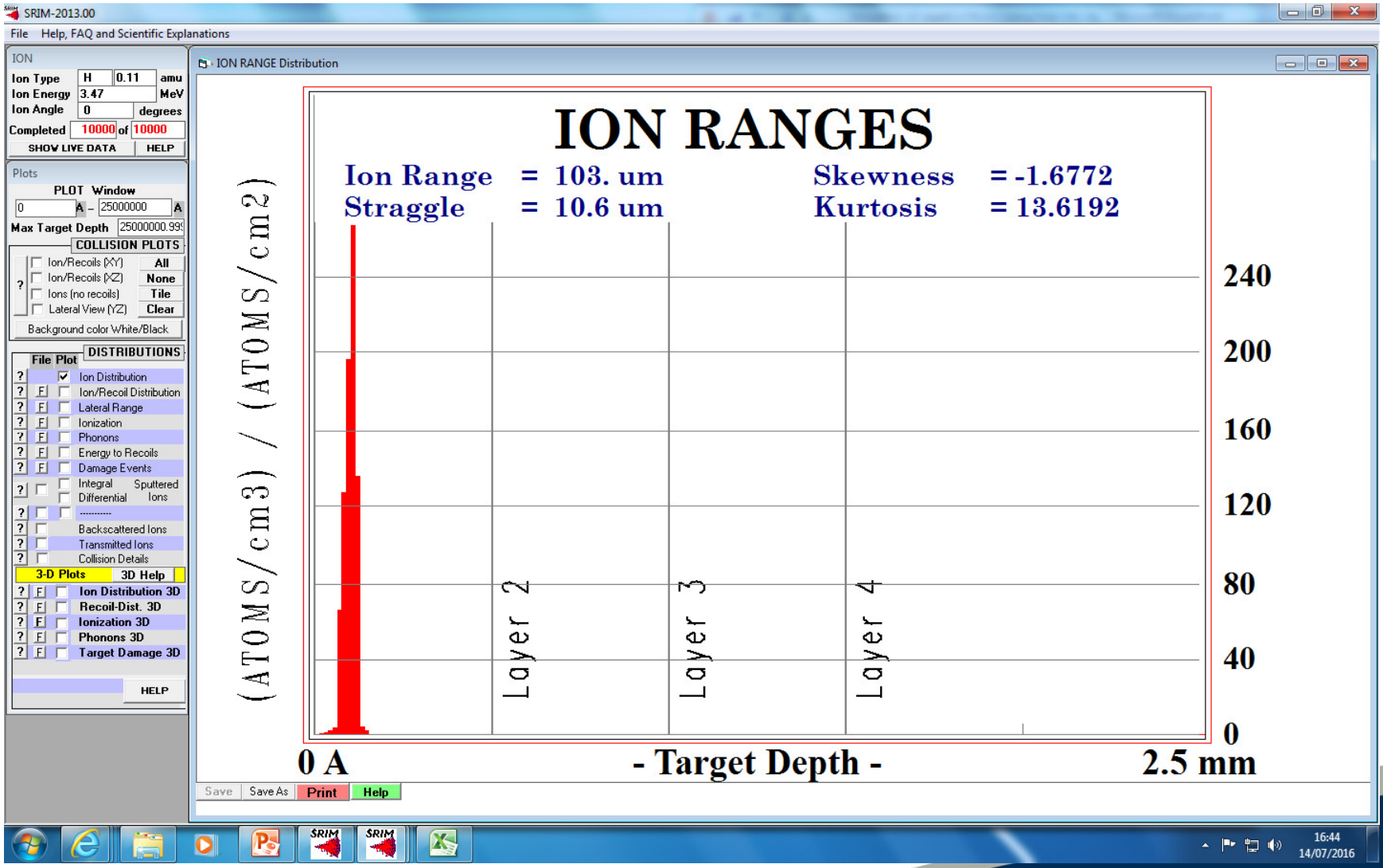

Science & Technology Facilities Council
ISIS

Depth Profiling - Simulations

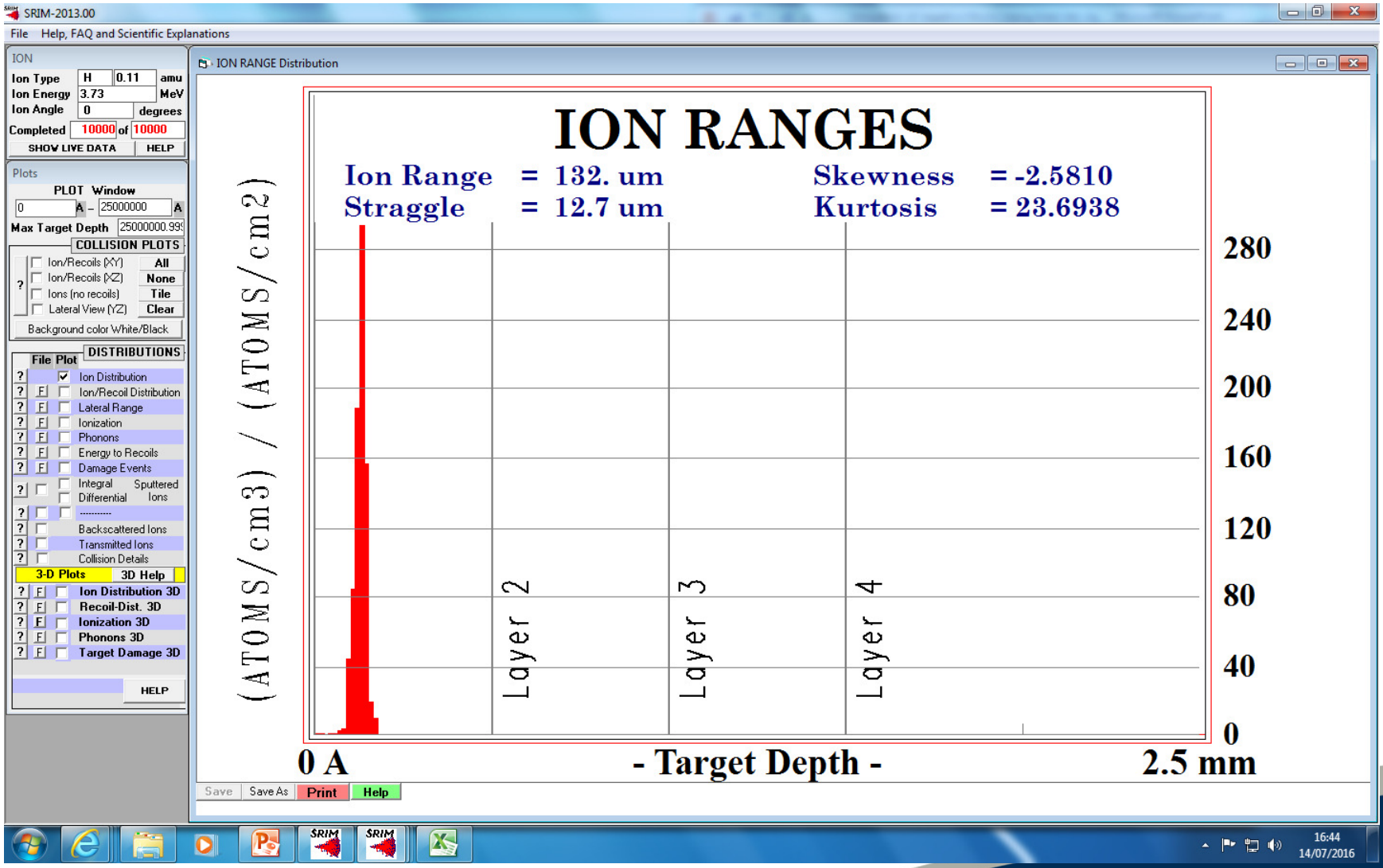

Science & Technology Facilities Council
ISIS

Depth Profiling - Simulations

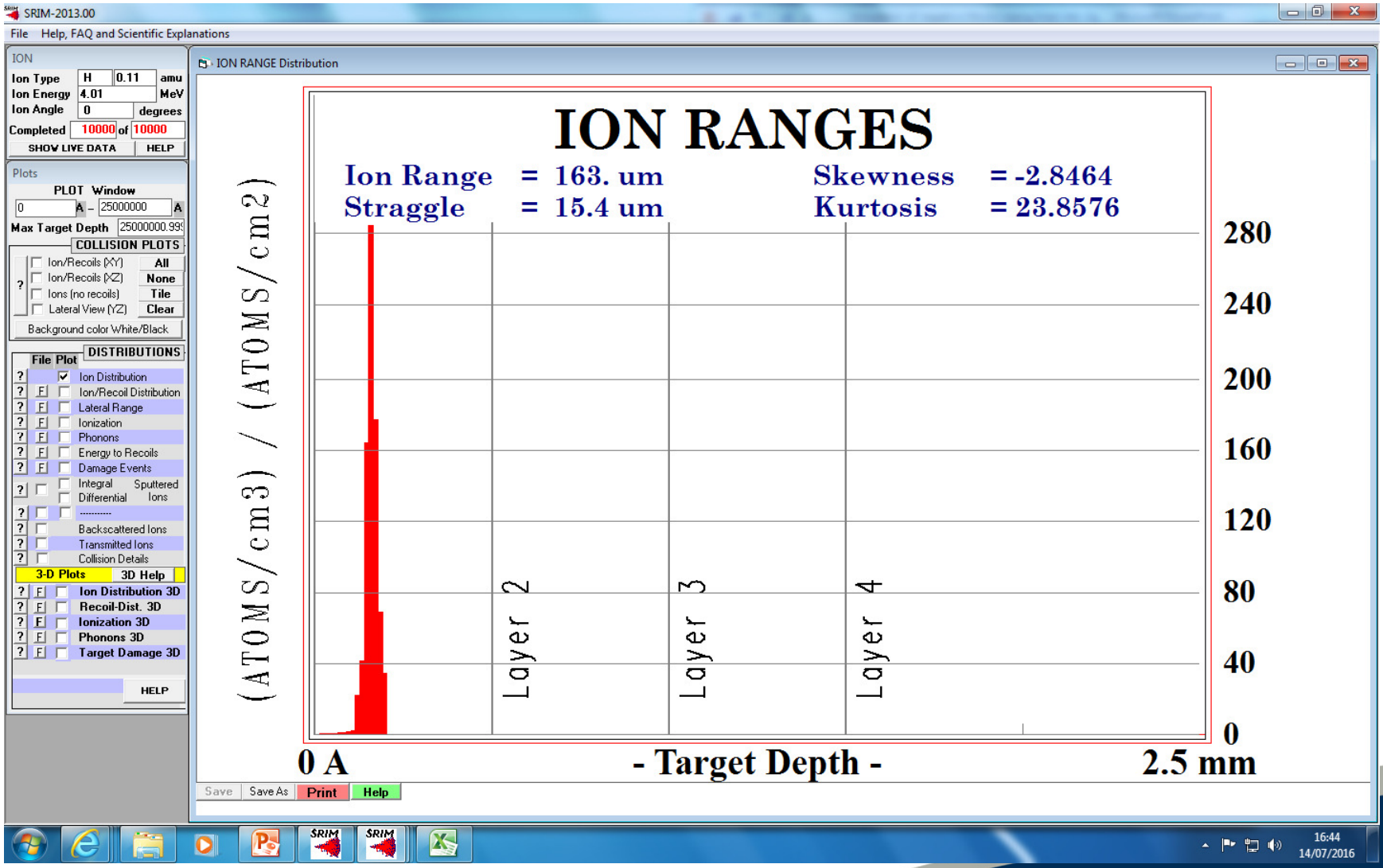

Science & Technology Facilities Council
ISIS

Depth Profiling - Simulations

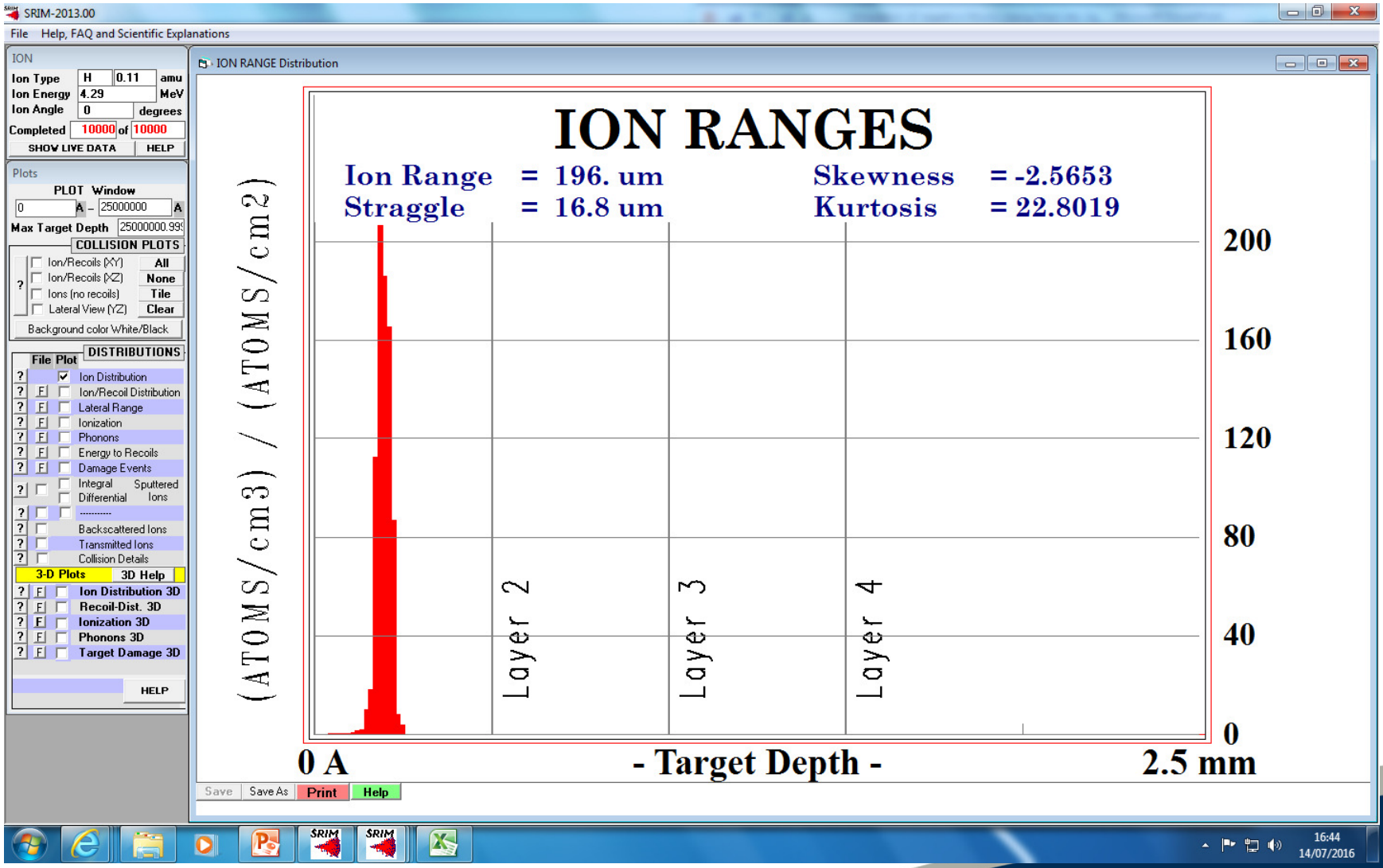

Science & Technology Facilities Council
ISIS

Depth Profiling - Simulations

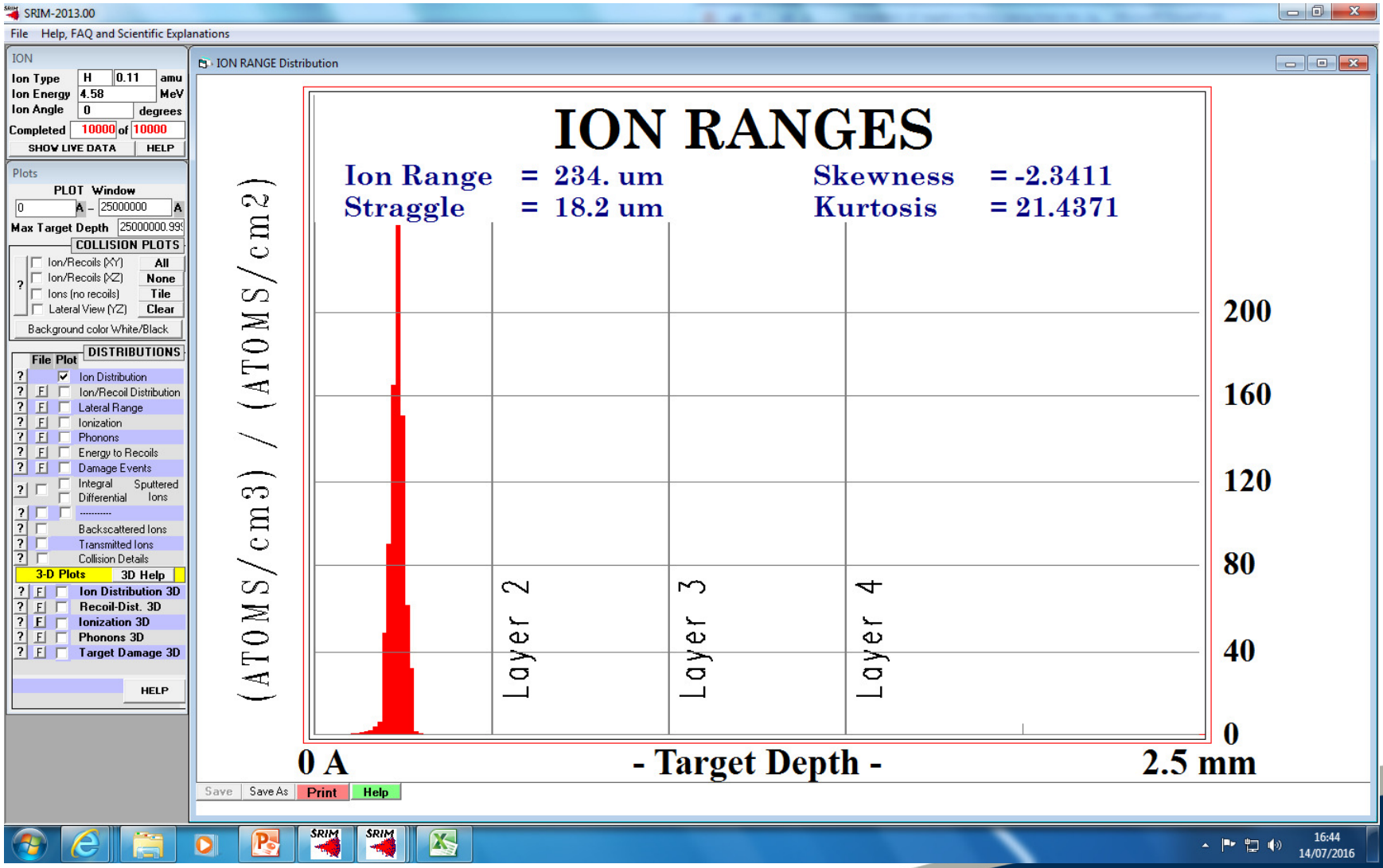

Science & Technology Facilities Council
ISIS

Depth Profiling - Simulations

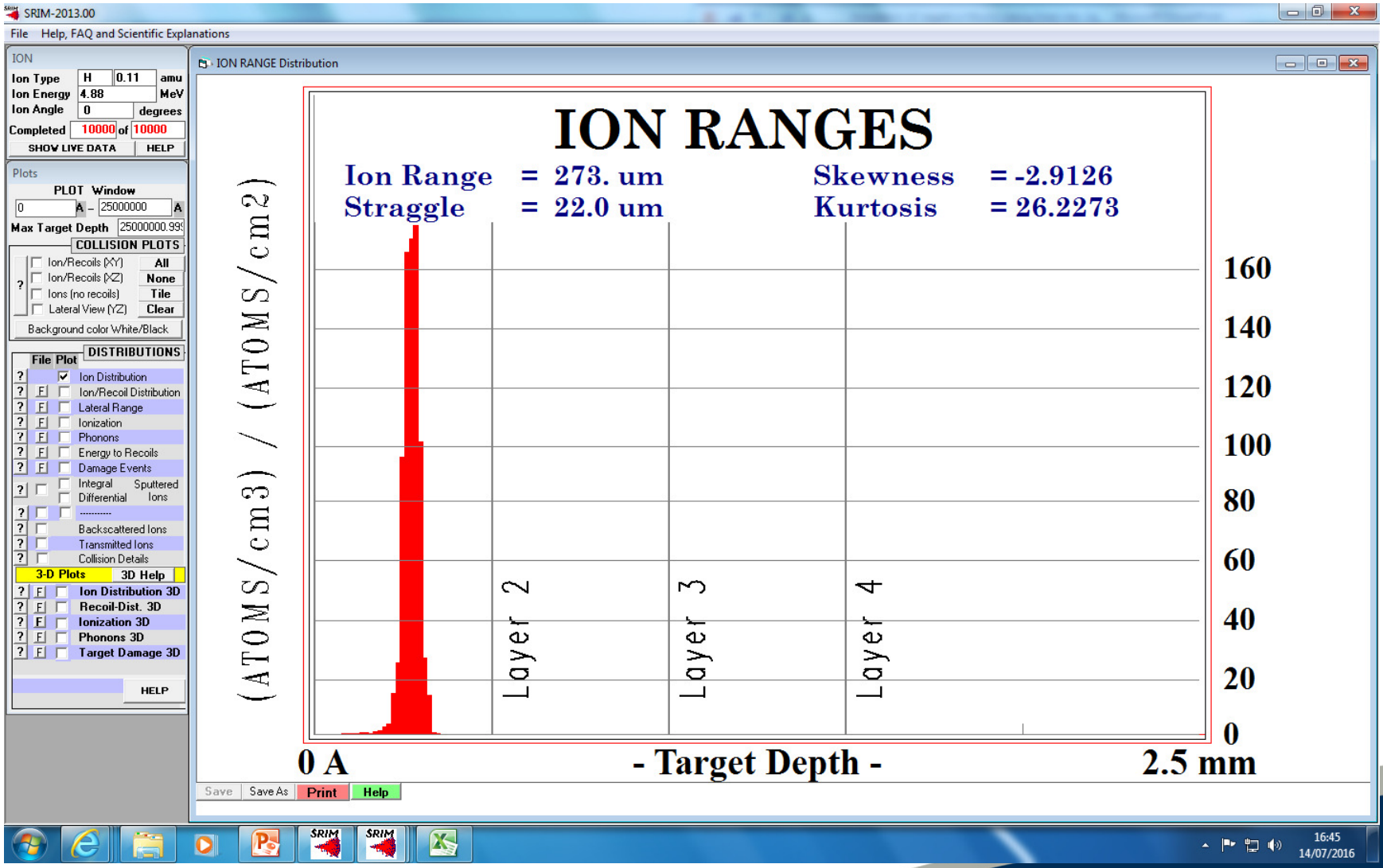

Science & Technology Facilities Council
ISIS

Depth Profiling - Simulations

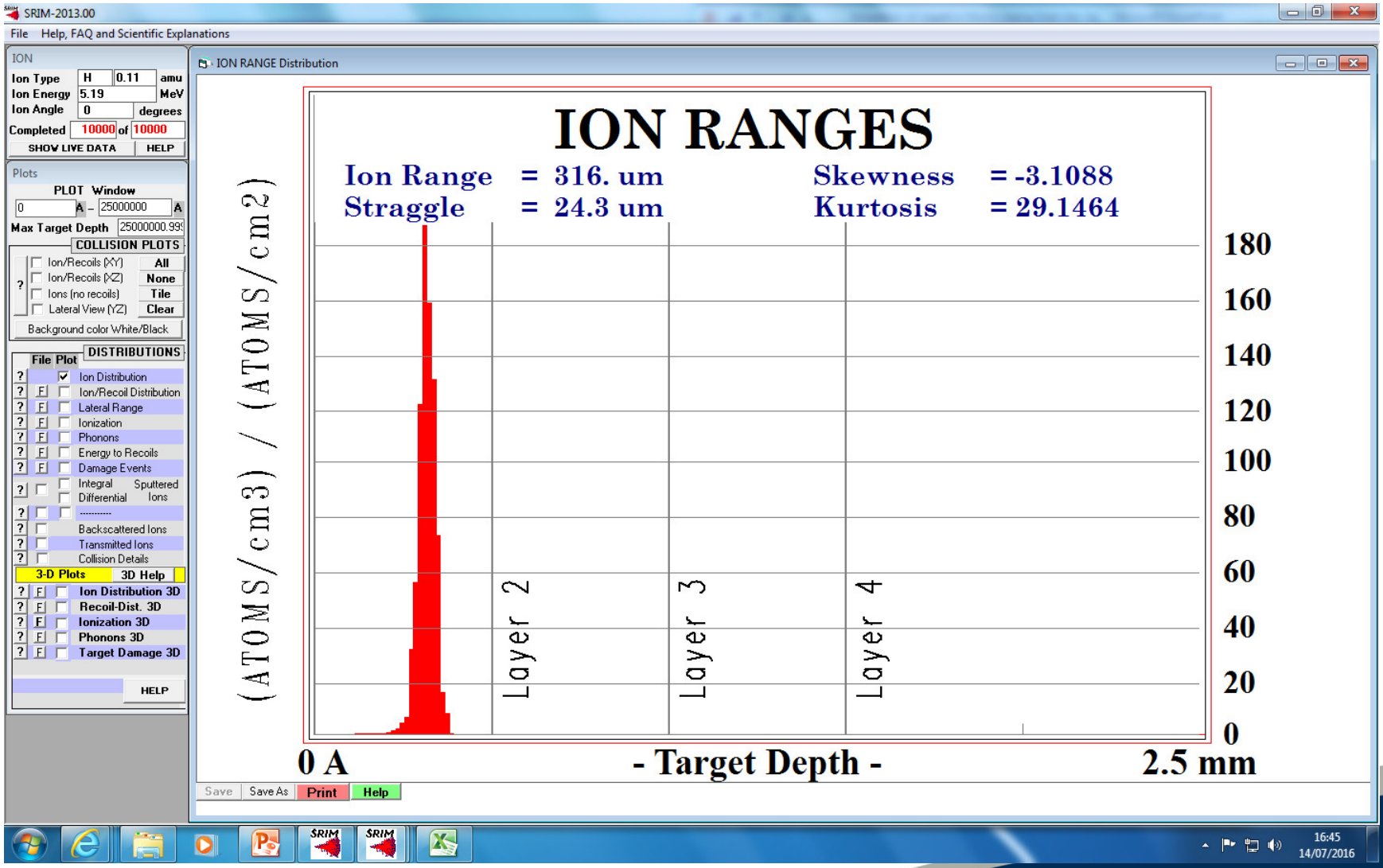

Depth Profiling - Simulations

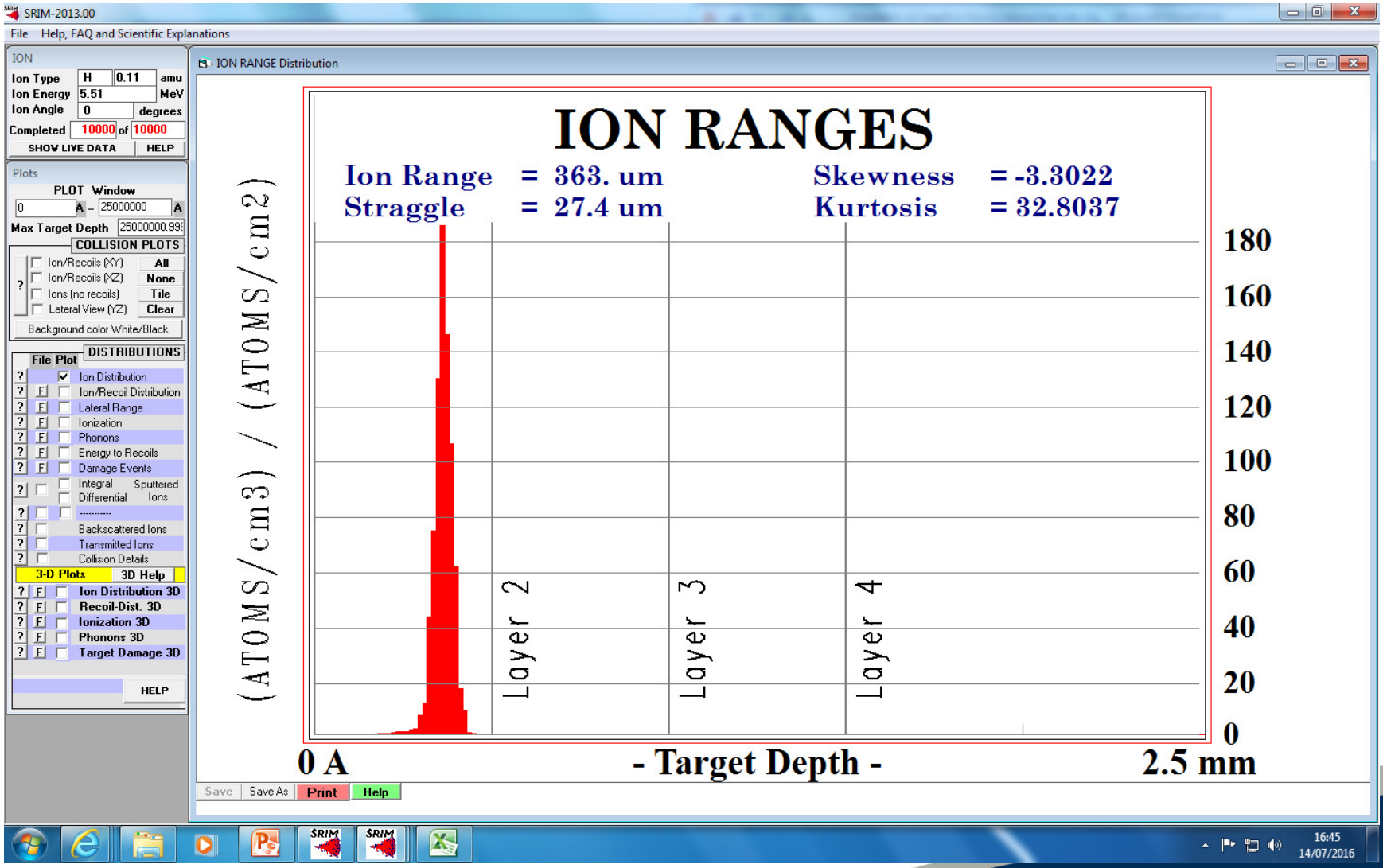

Depth Profiling - Simulations

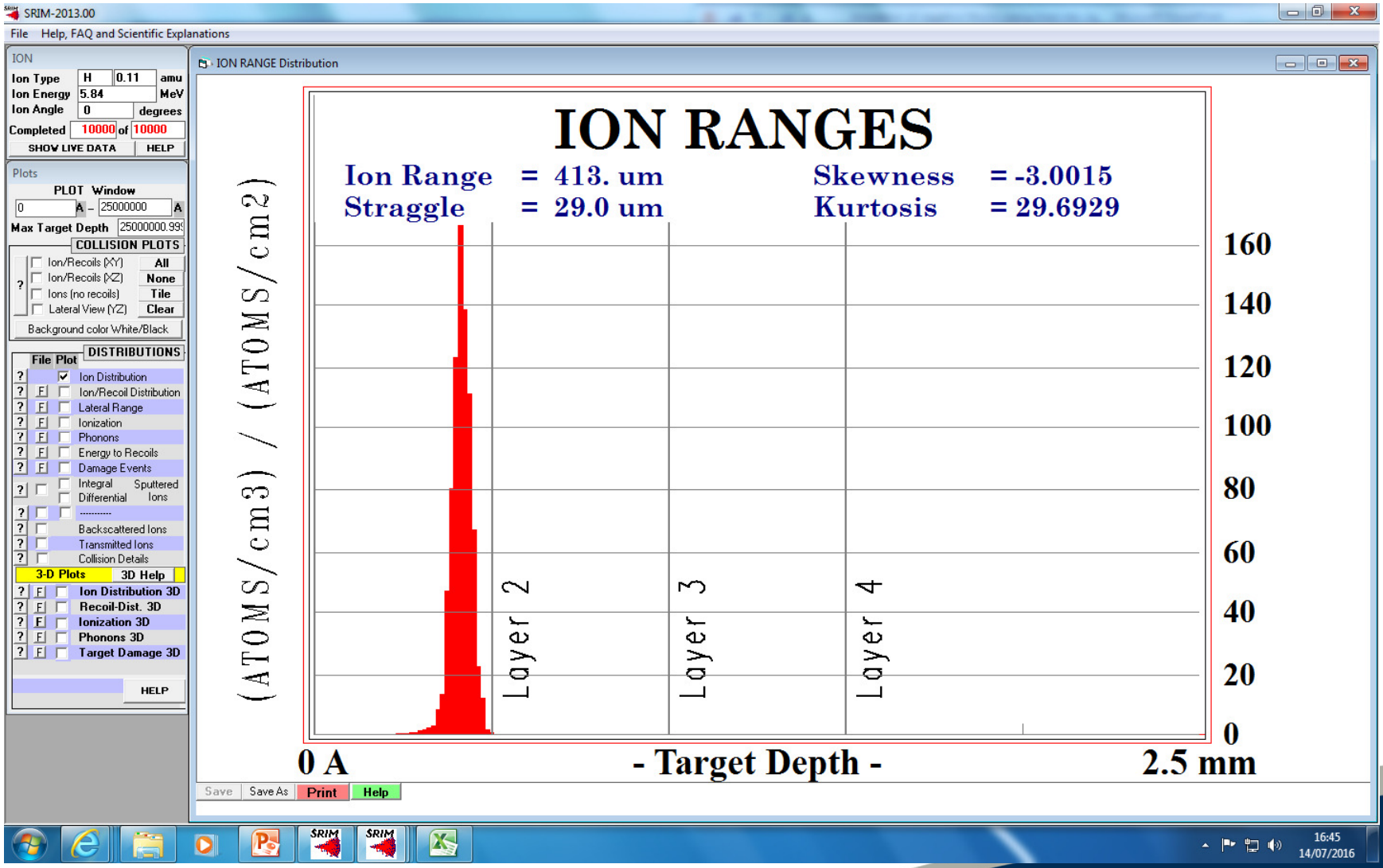

Science & Technology Facilities Council
ISIS

Depth Profiling - Simulations

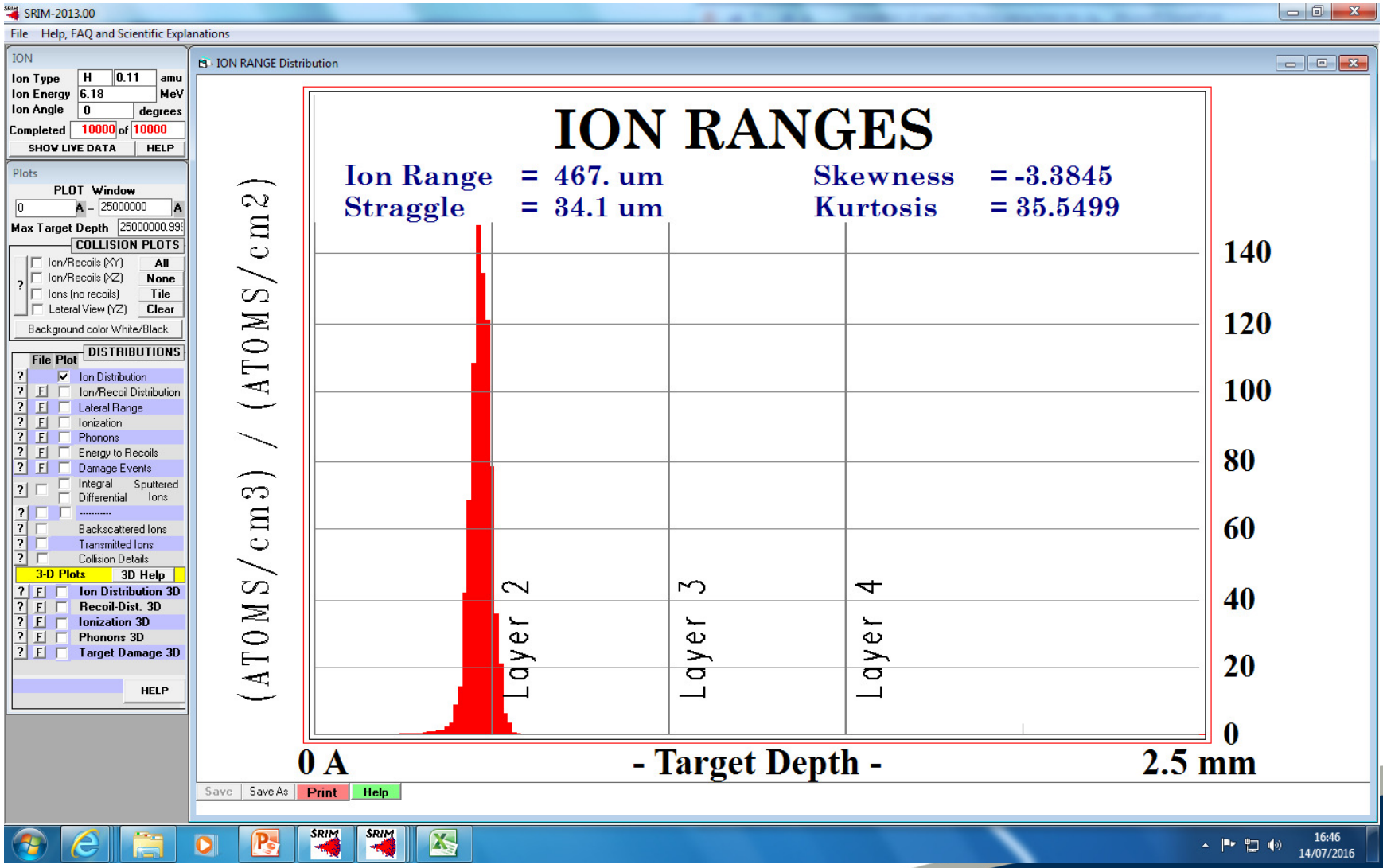

Science & Technology Facilities Council
ISIS

Depth Profiling - Simulations

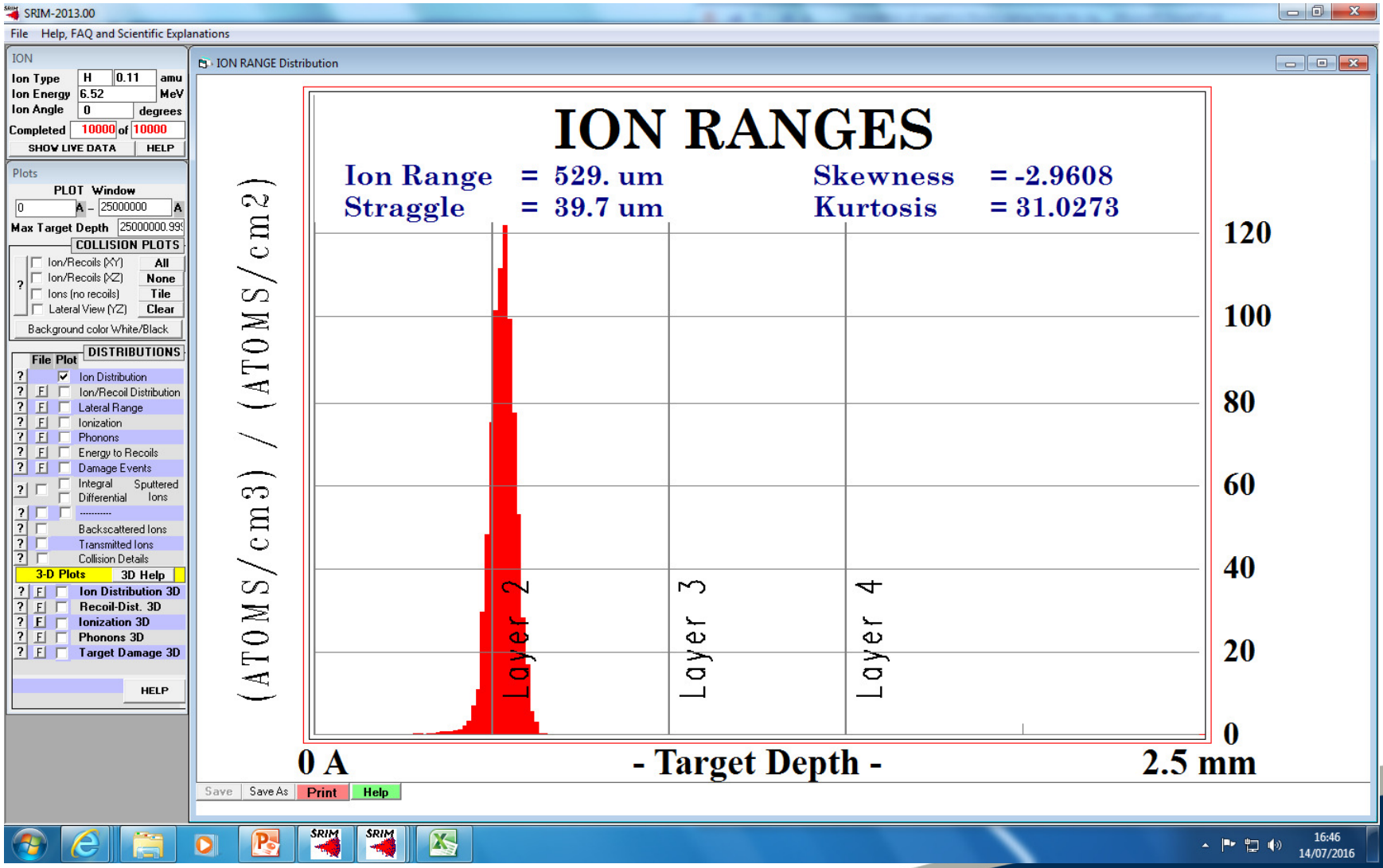

Science & Technology Facilities Council
ISIS

Depth Profiling - Simulations

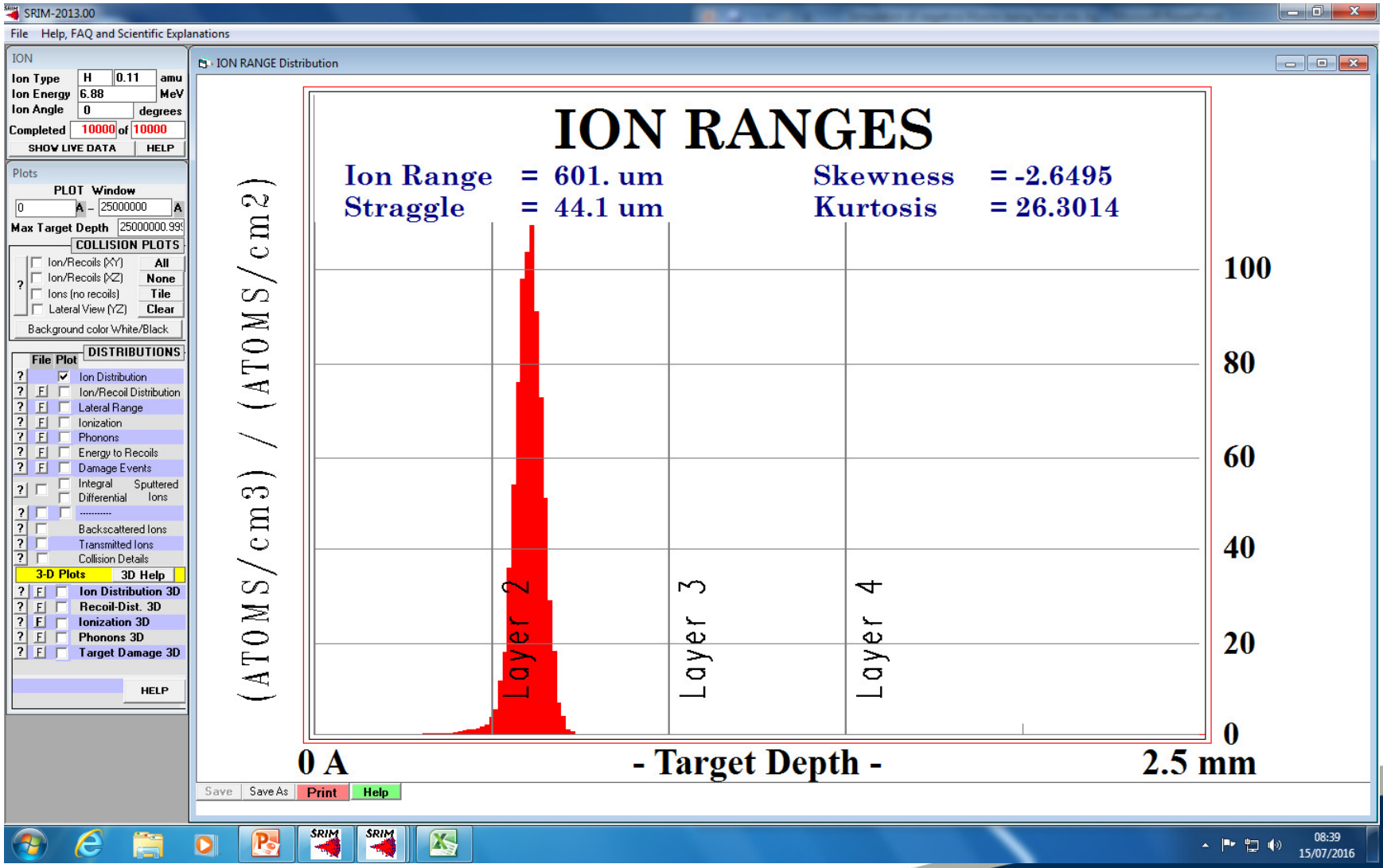

Depth Profiling - Simulations

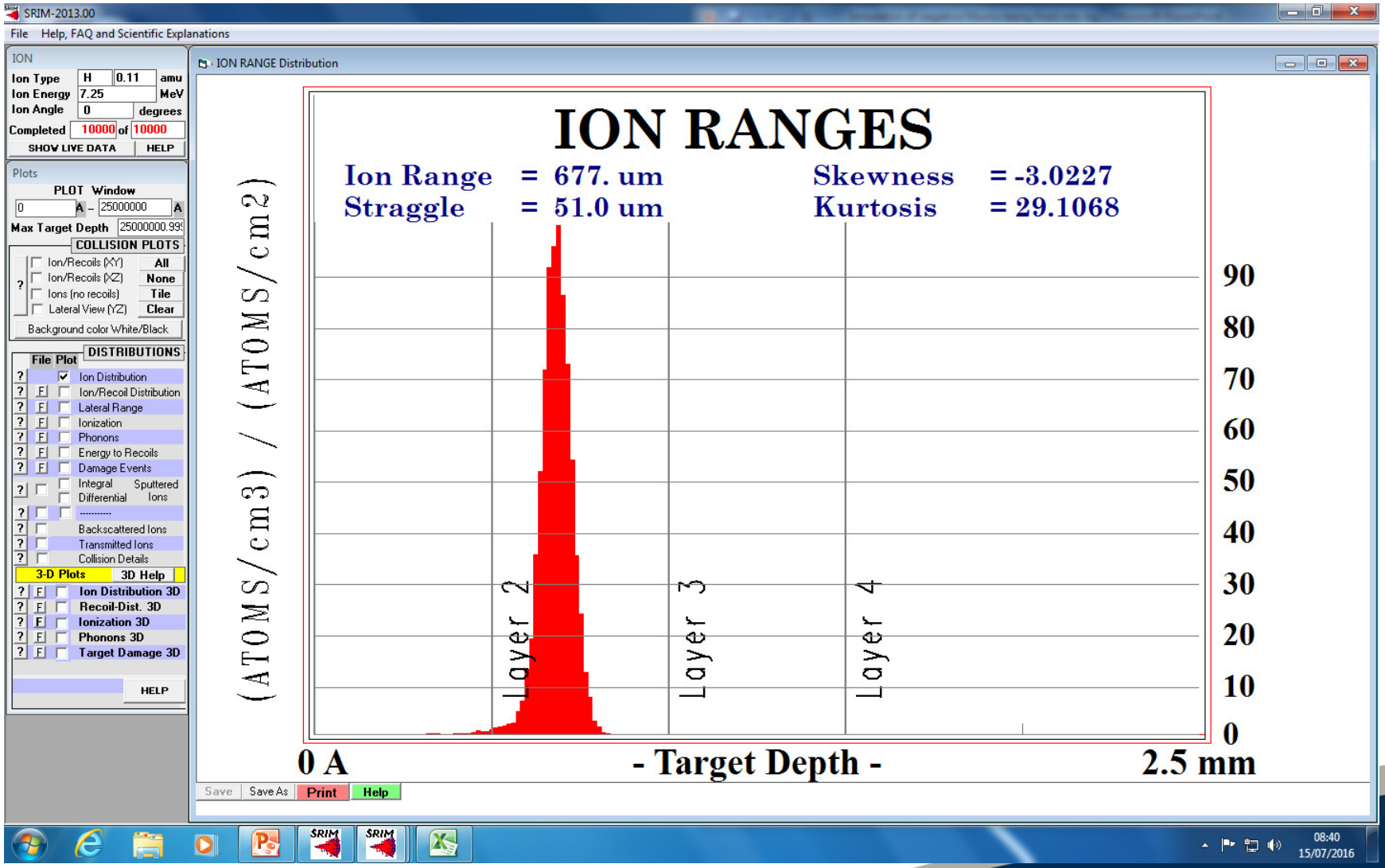

Science & Technology Facilities Council
ISIS

Depth Profiling - Simulations

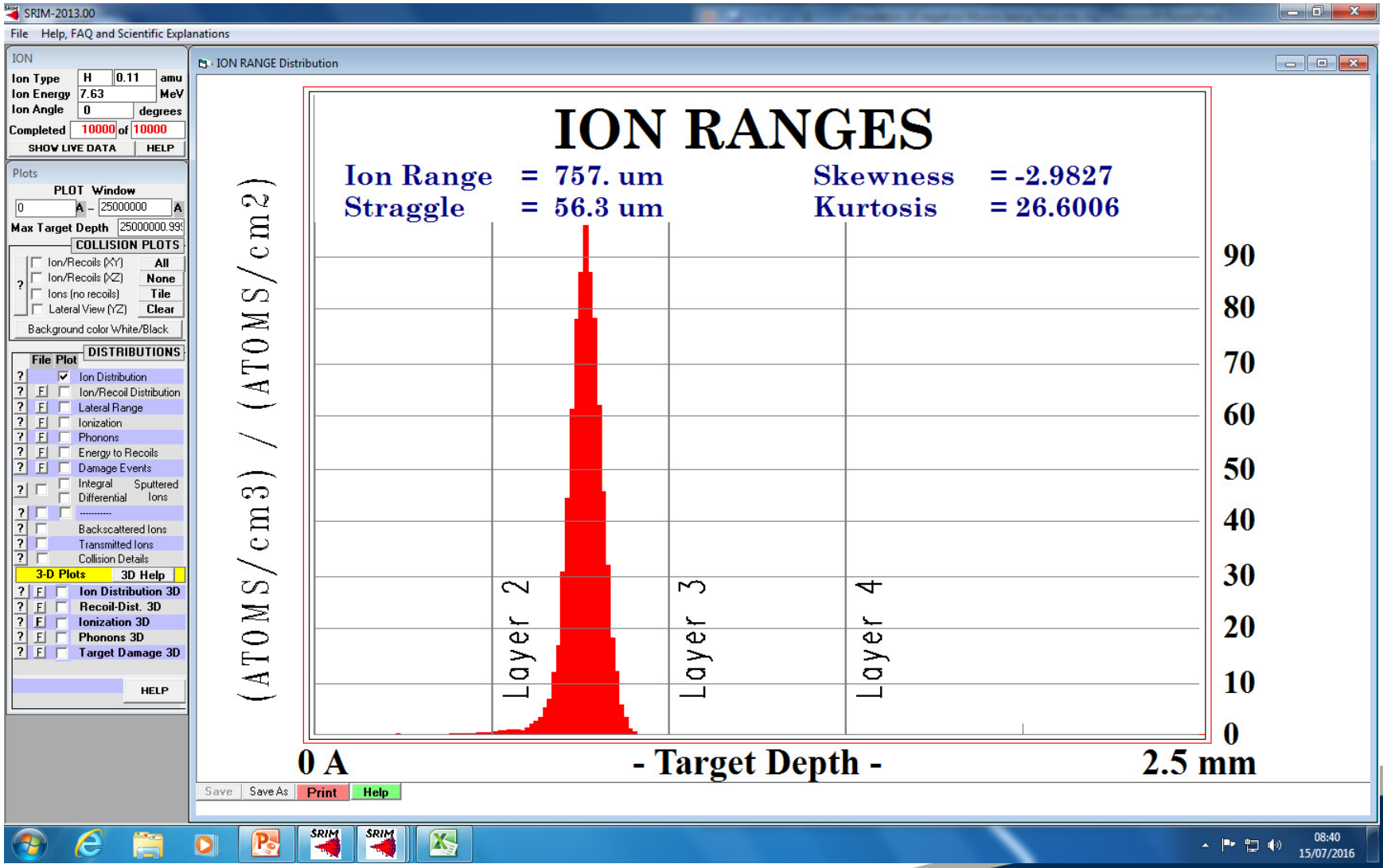

Science & Technology Facilities Council
ISIS

Depth Profiling - Simulations

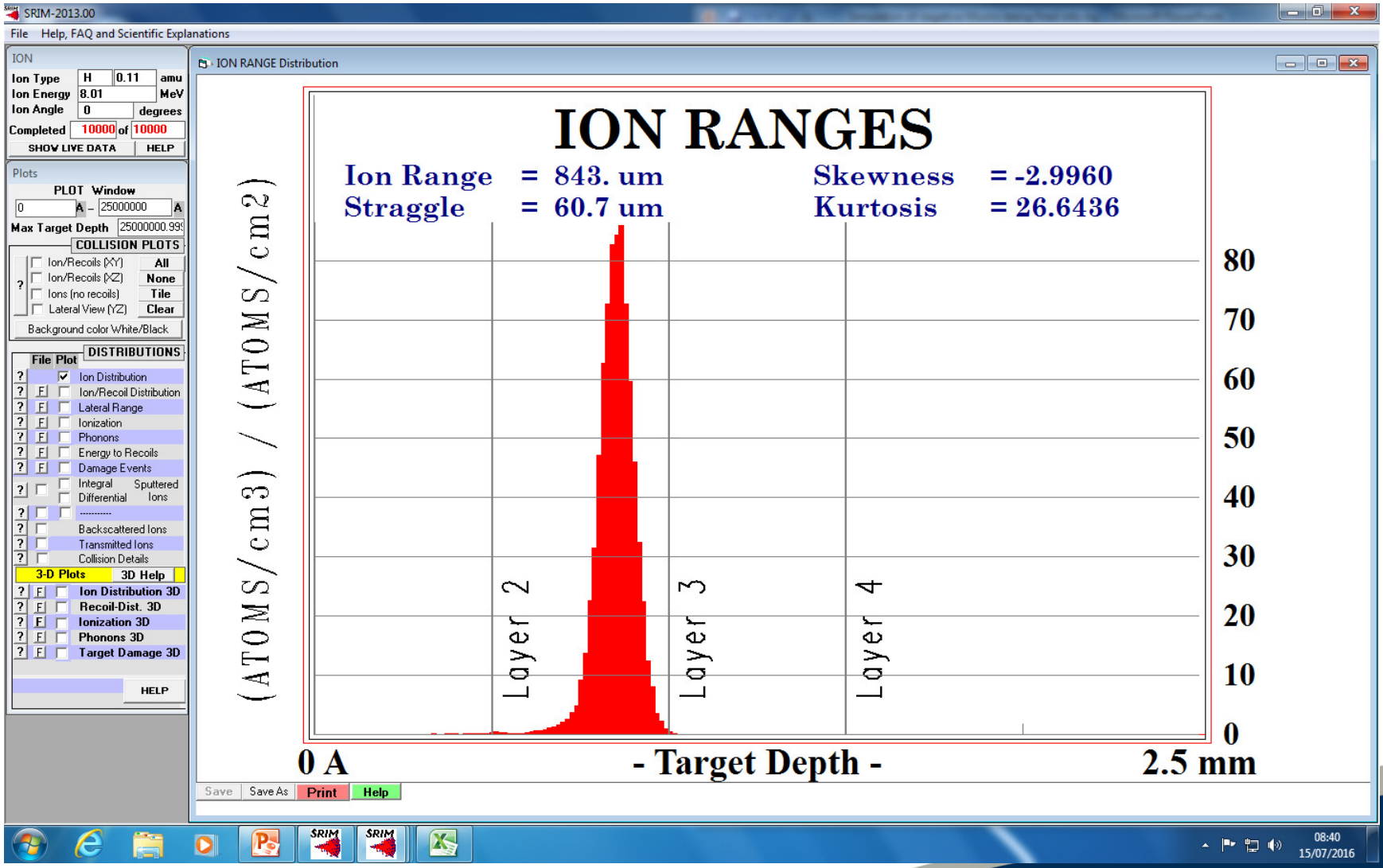

Science & Technology Facilities Council
ISIS

Depth Profiling - Simulations

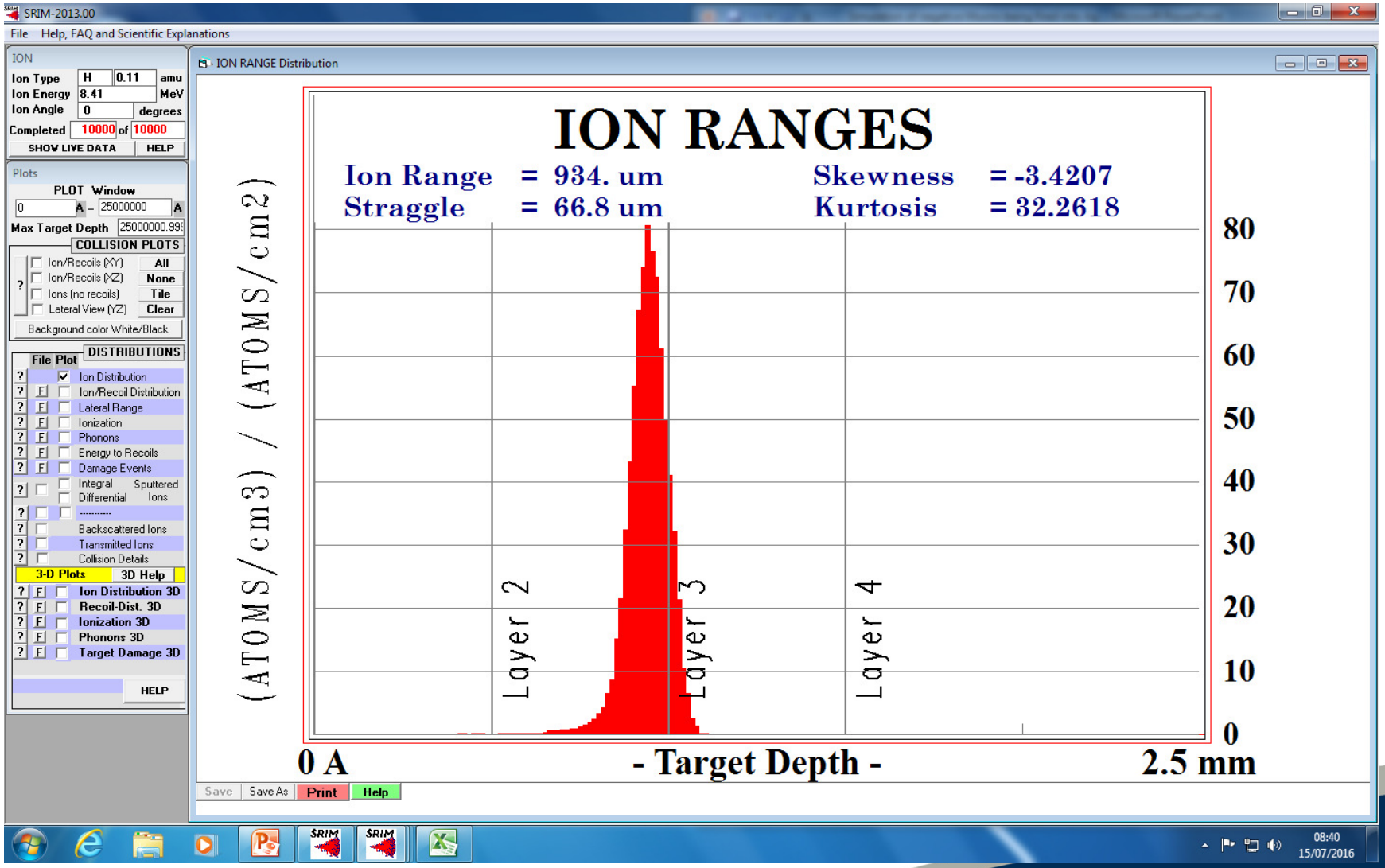

Science & Technology Facilities Council
ISIS

Depth Profiling - Simulations

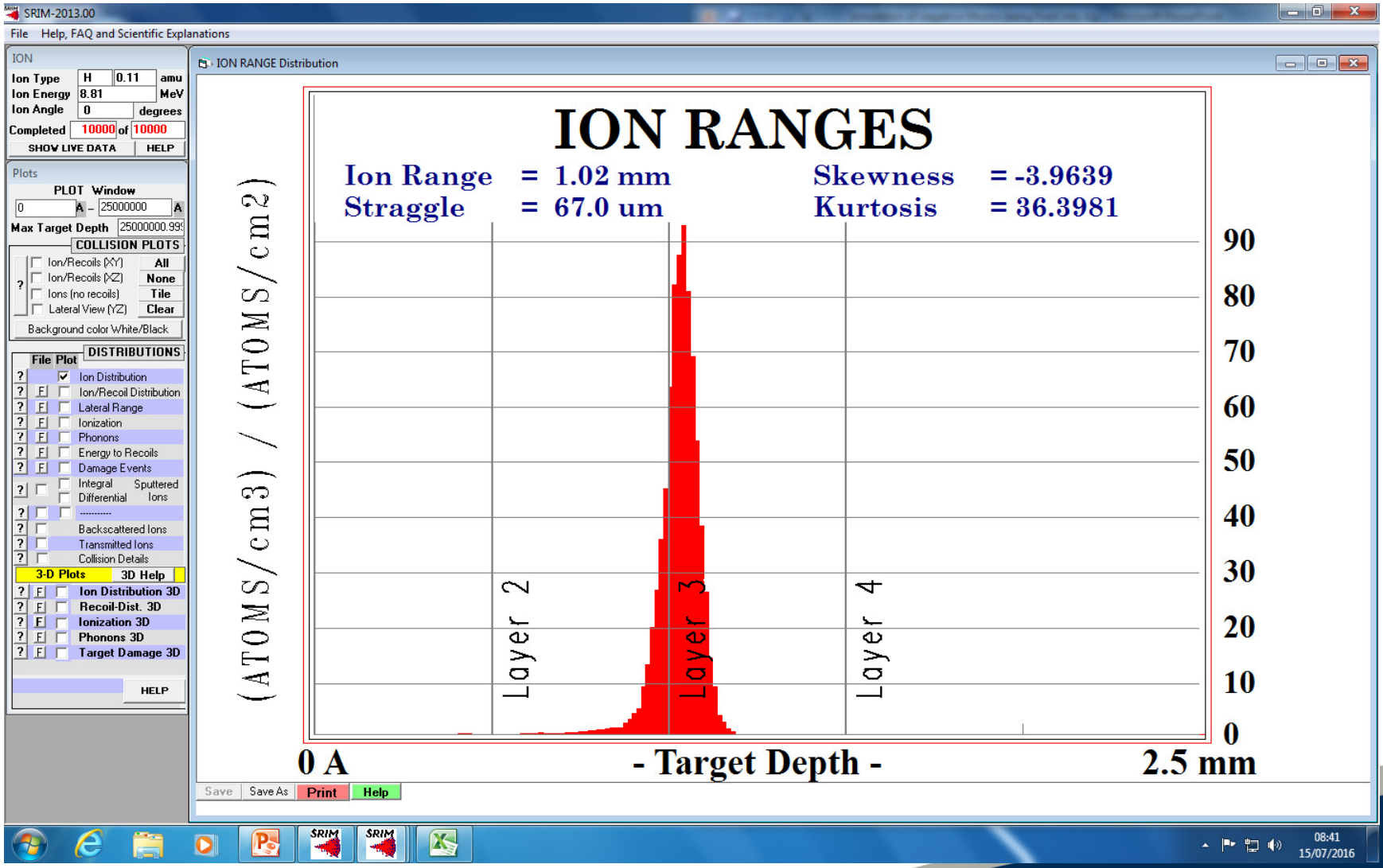

Science & Technology Facilities Council
ISIS

Depth Profiling - Simulations

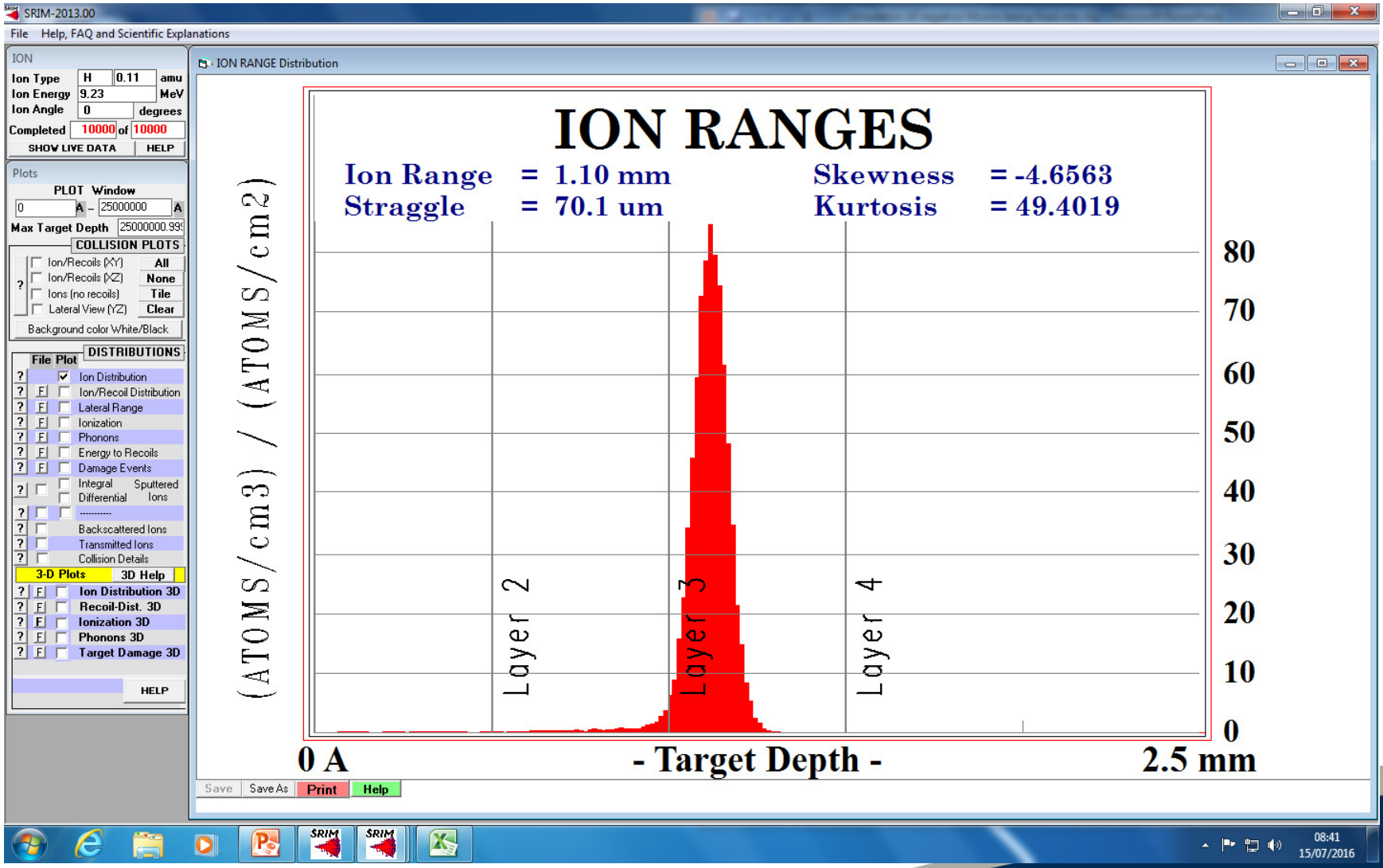

Science & Technology Facilities Council
ISIS

Depth Profiling - Simulations

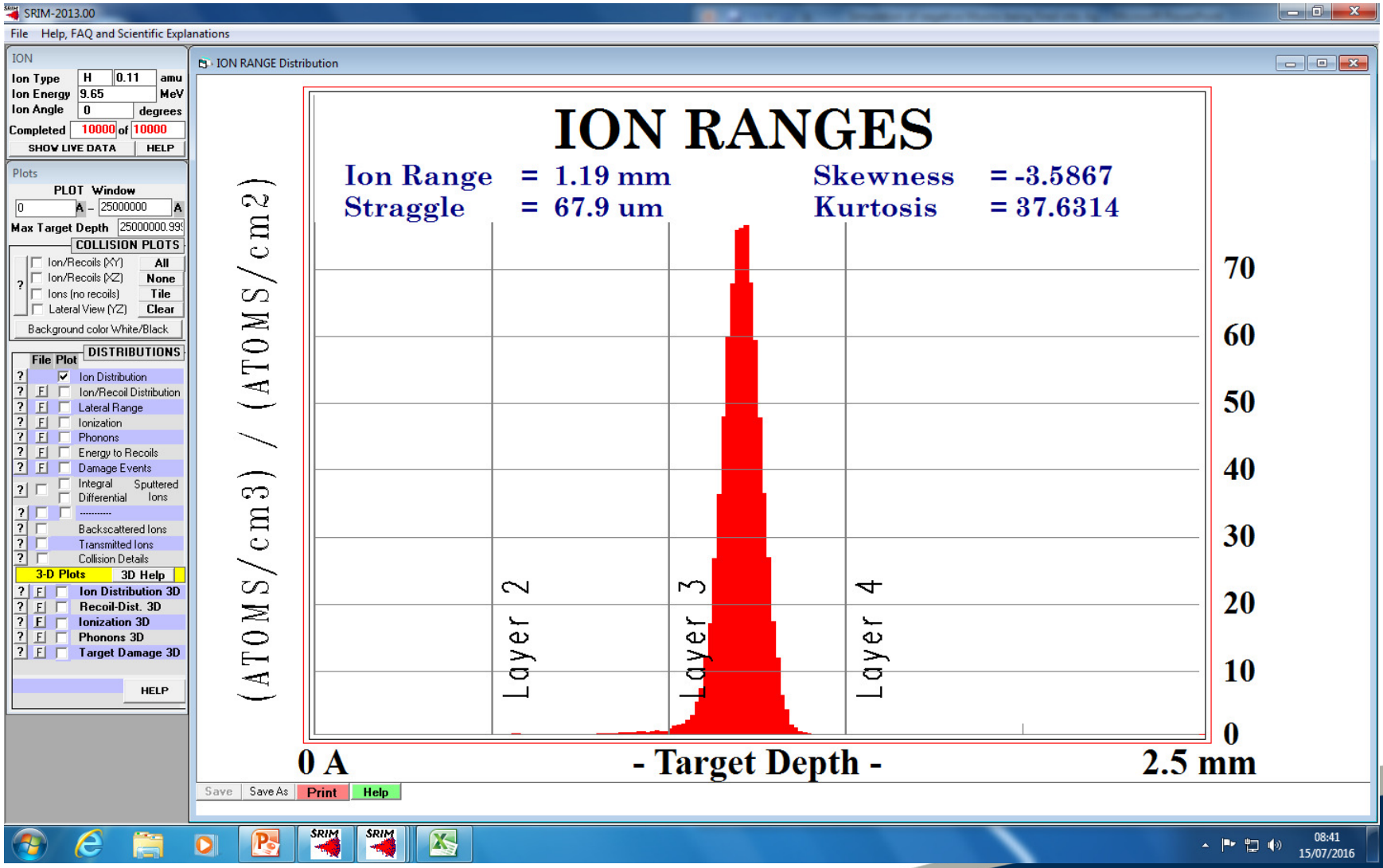

Science & Technology Facilities Council
ISIS

Depth Profiling - Simulations

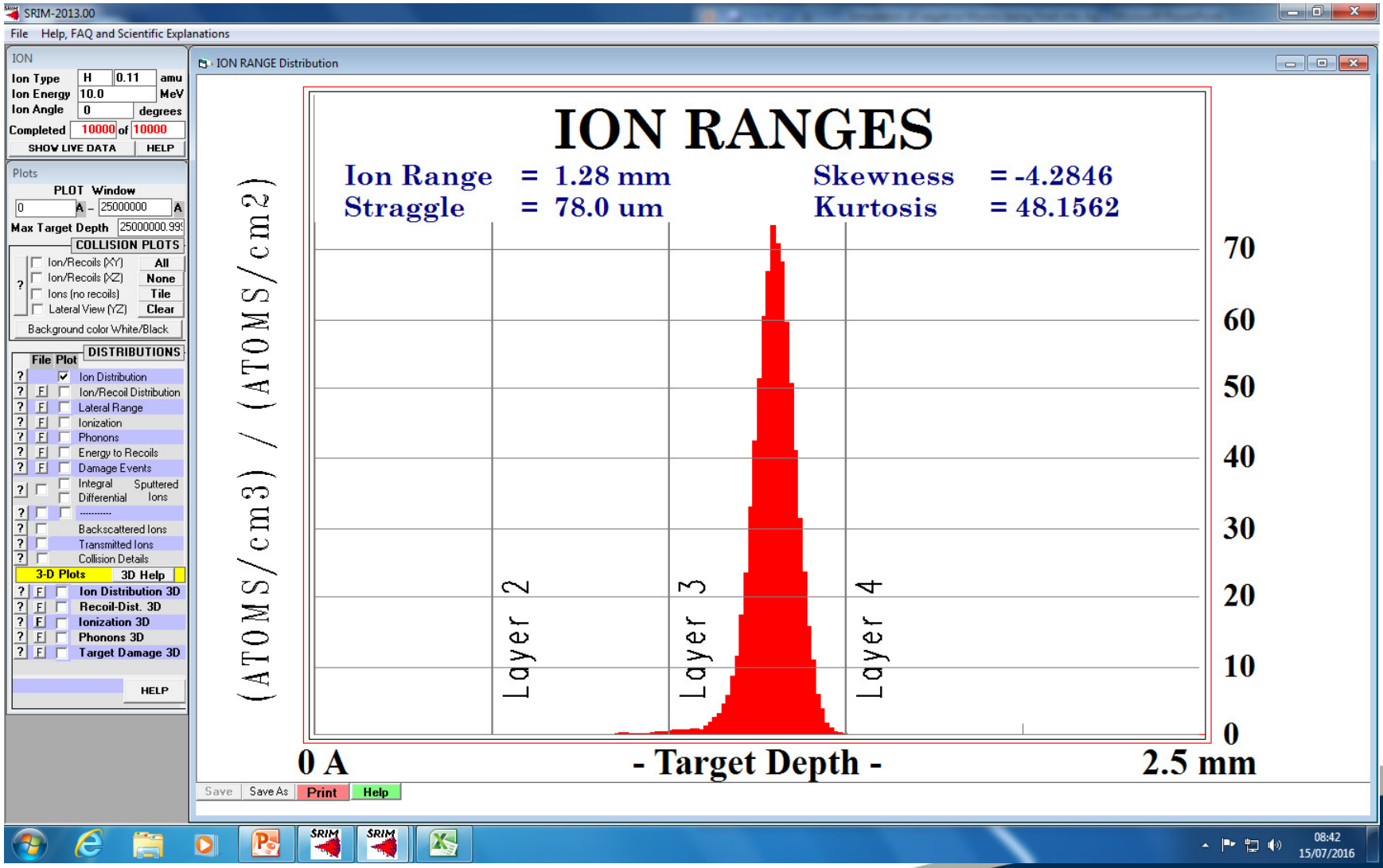

Science & Technology Facilities Council
ISIS

Depth Profiling - Simulations

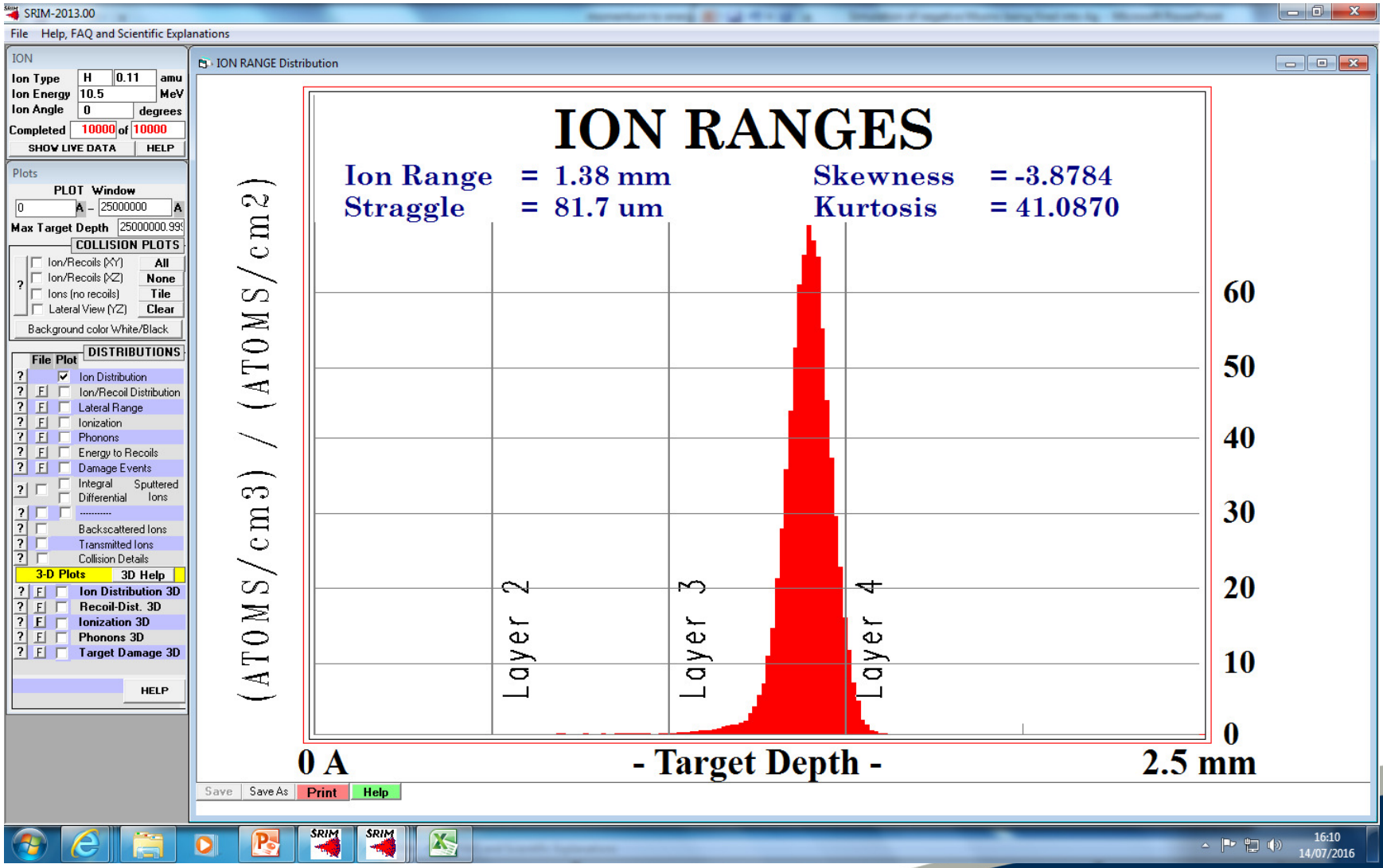

Depth Profiling - Simulations

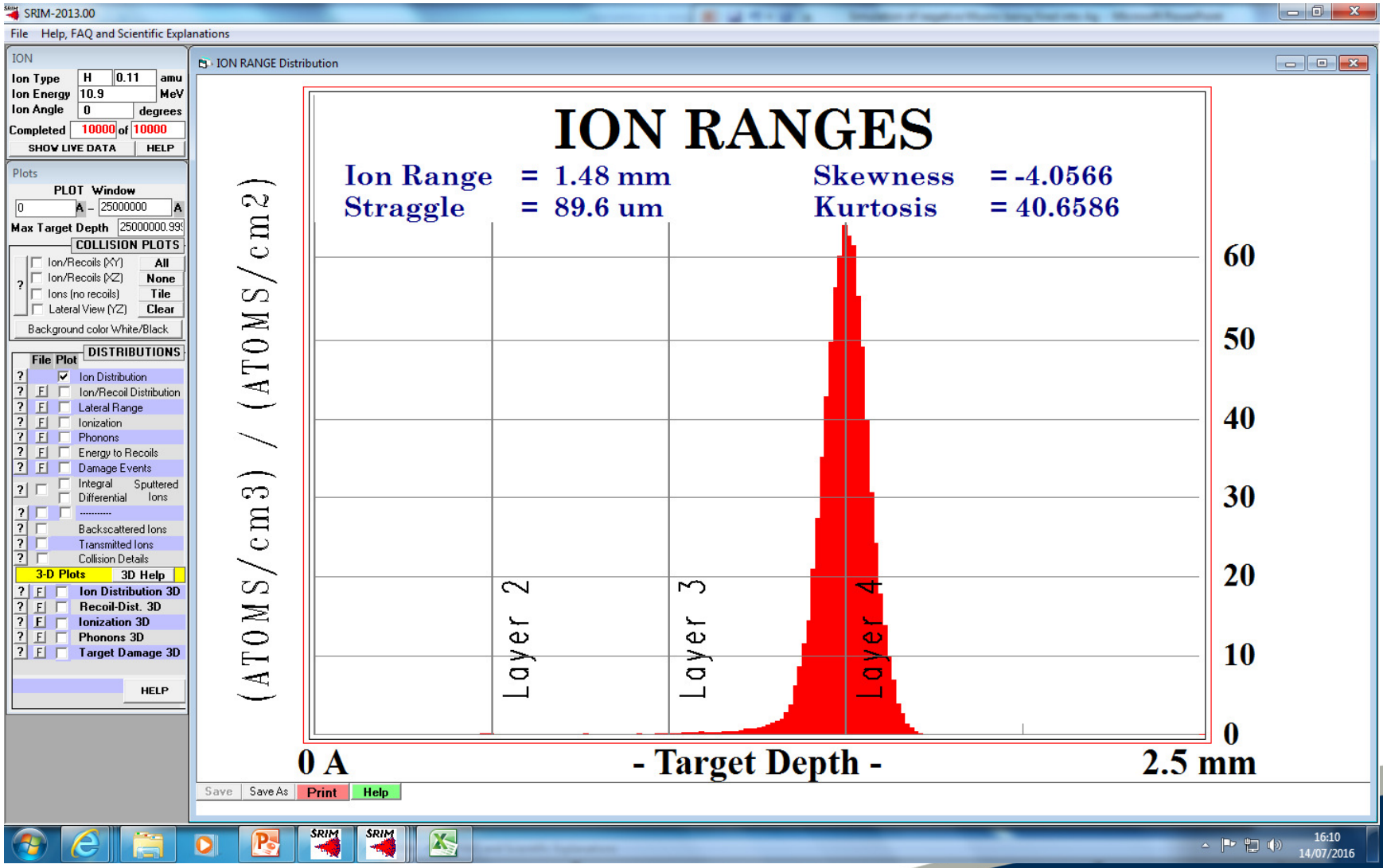

Science & Technology Facilities Council
ISIS

Depth Profiling - Simulations

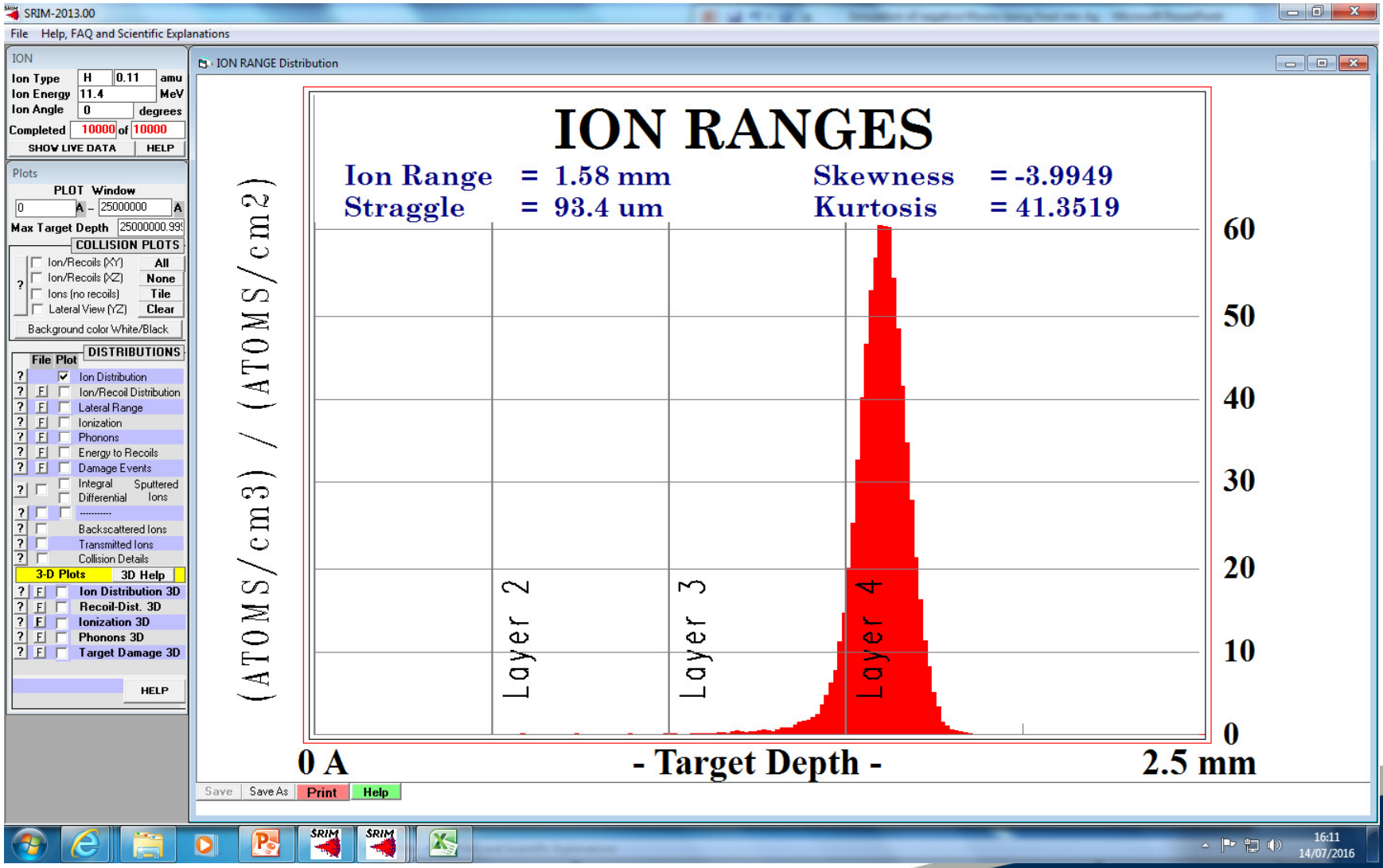

Science & Technology Facilities Council
ISIS

Depth Profiling - Simulations

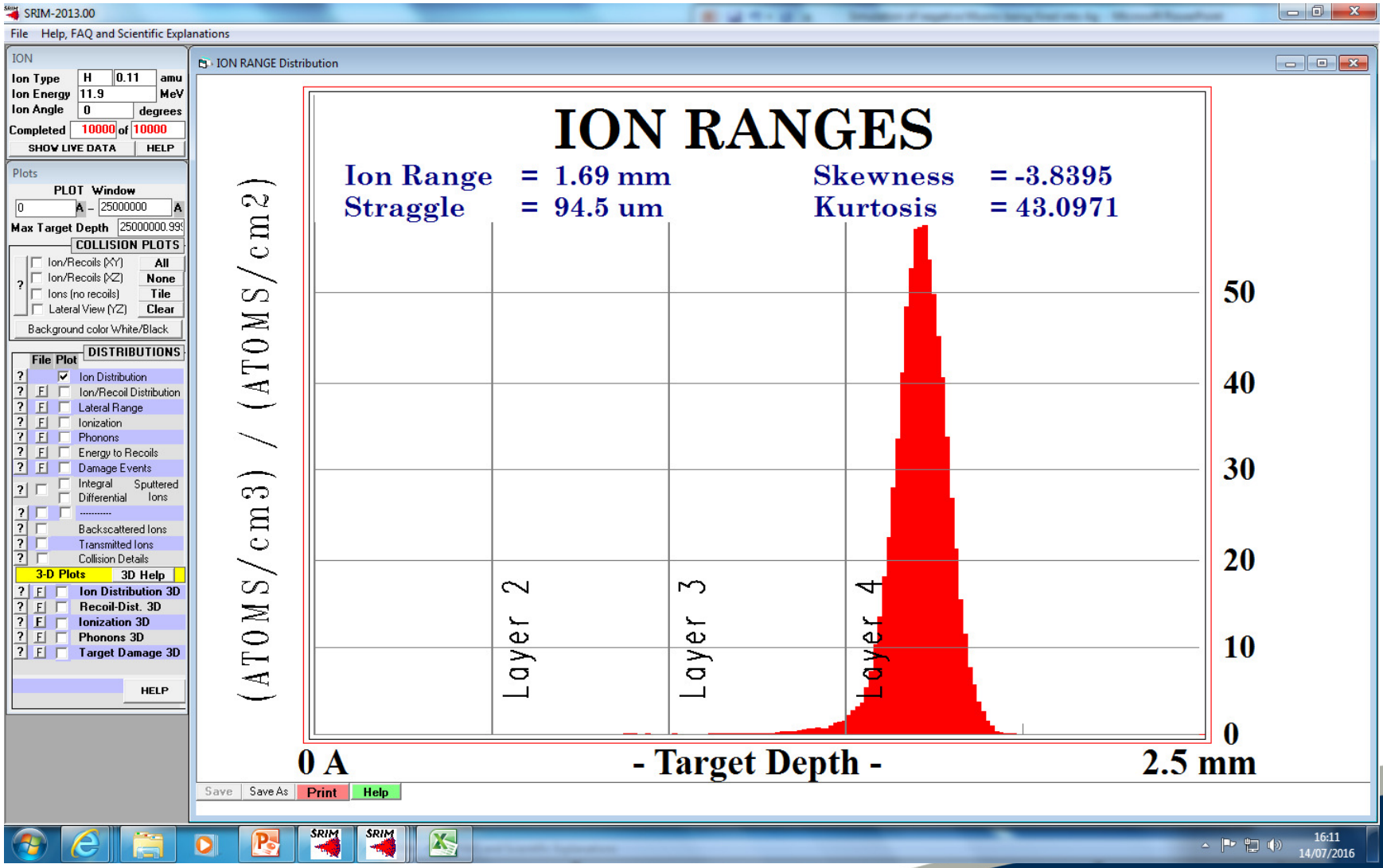

Depth Profiling - Simulations

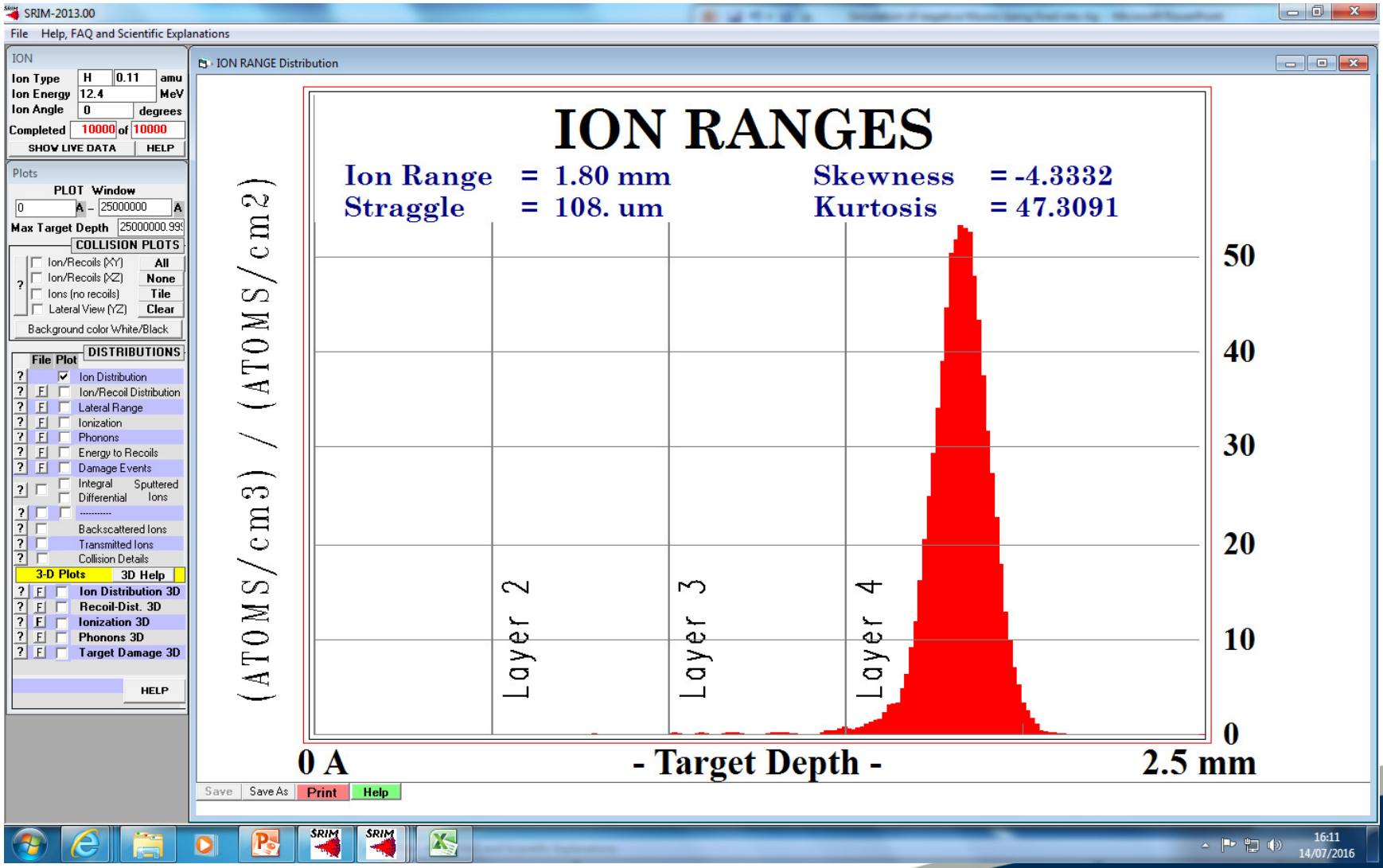

Depth Profiling - Simulations

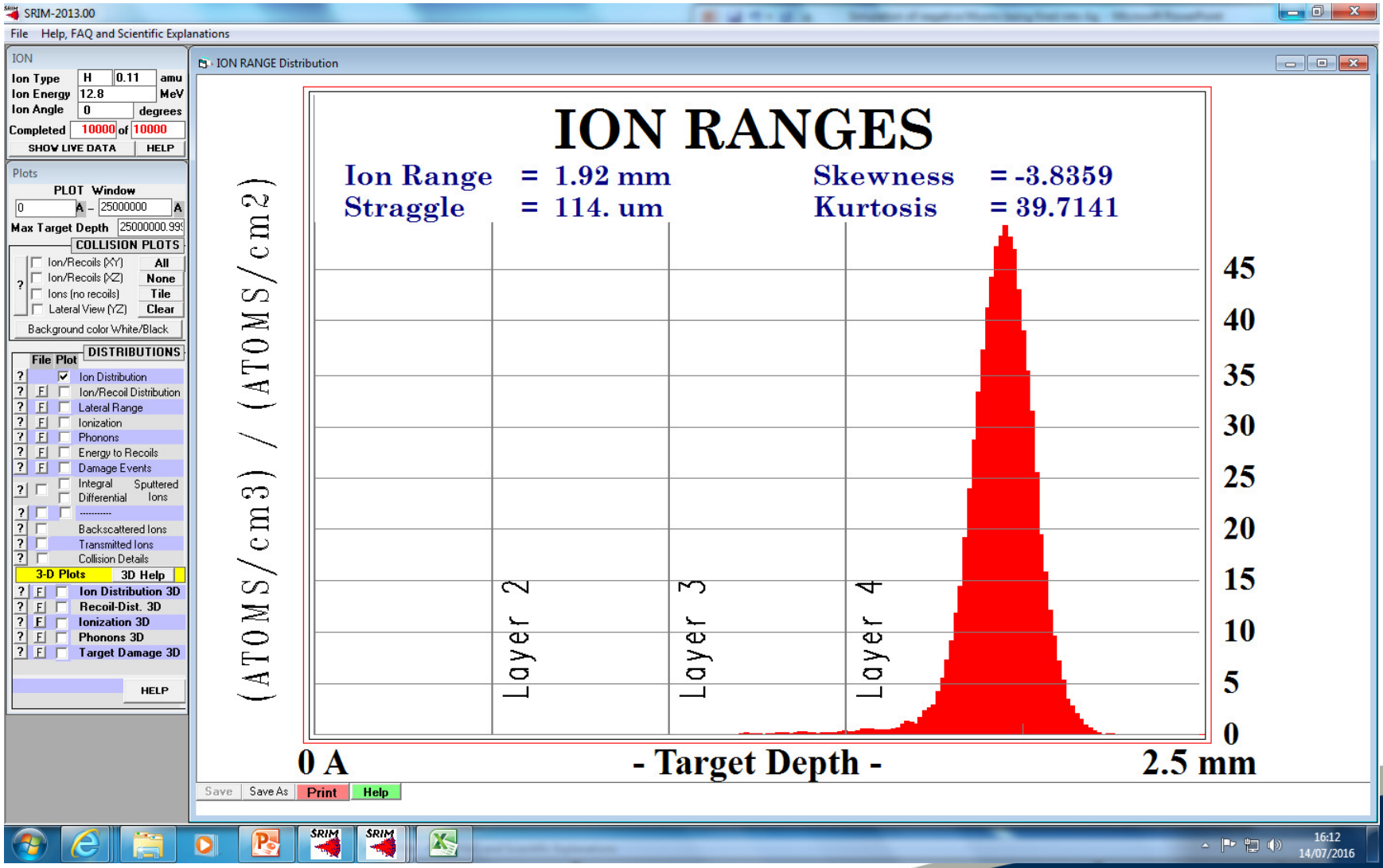

Science & Technology Facilities Council
ISIS

Depth Profiling - Simulations

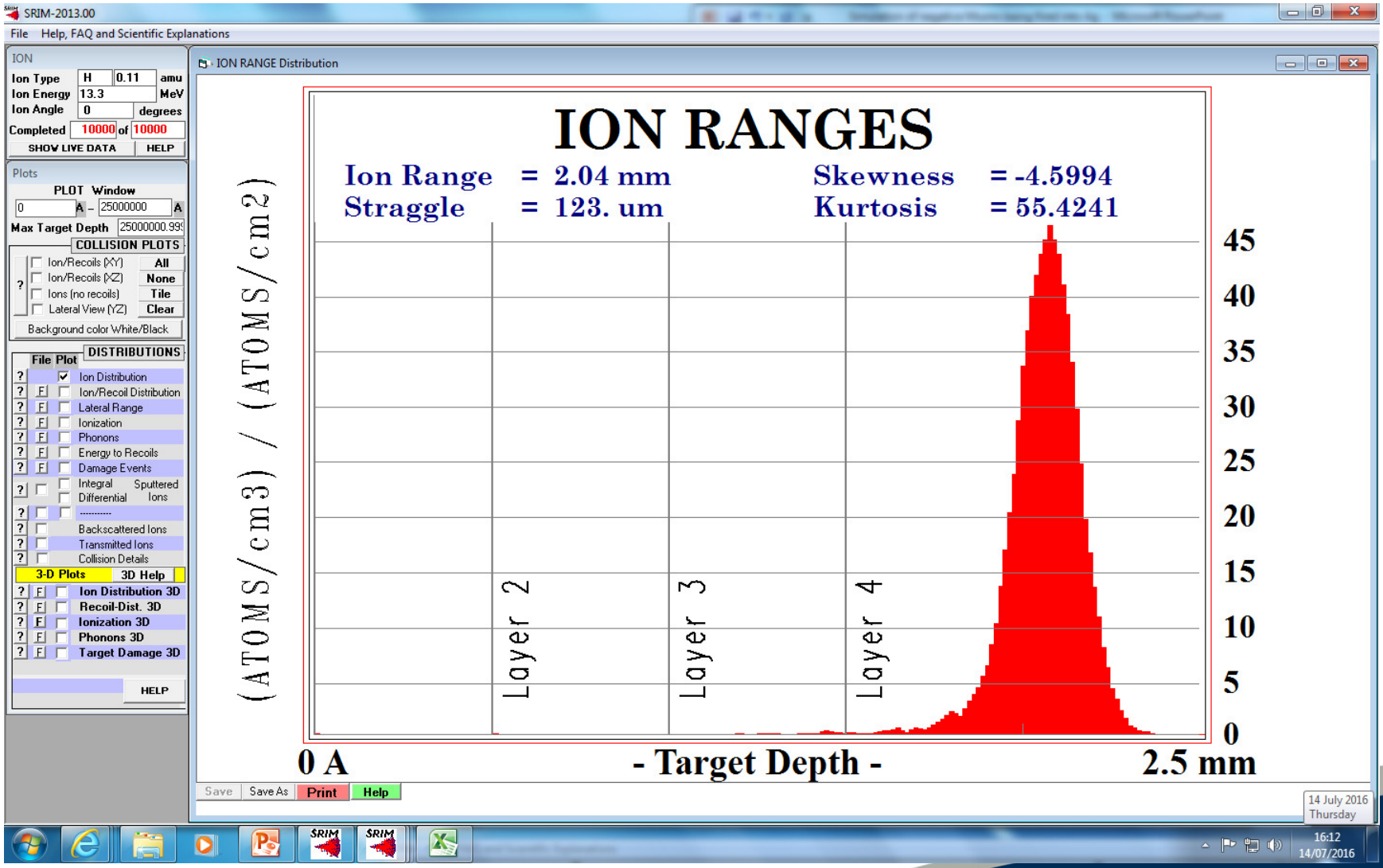

Science & Technology Facilities Council
ISIS

Depth Profiling - Simulations

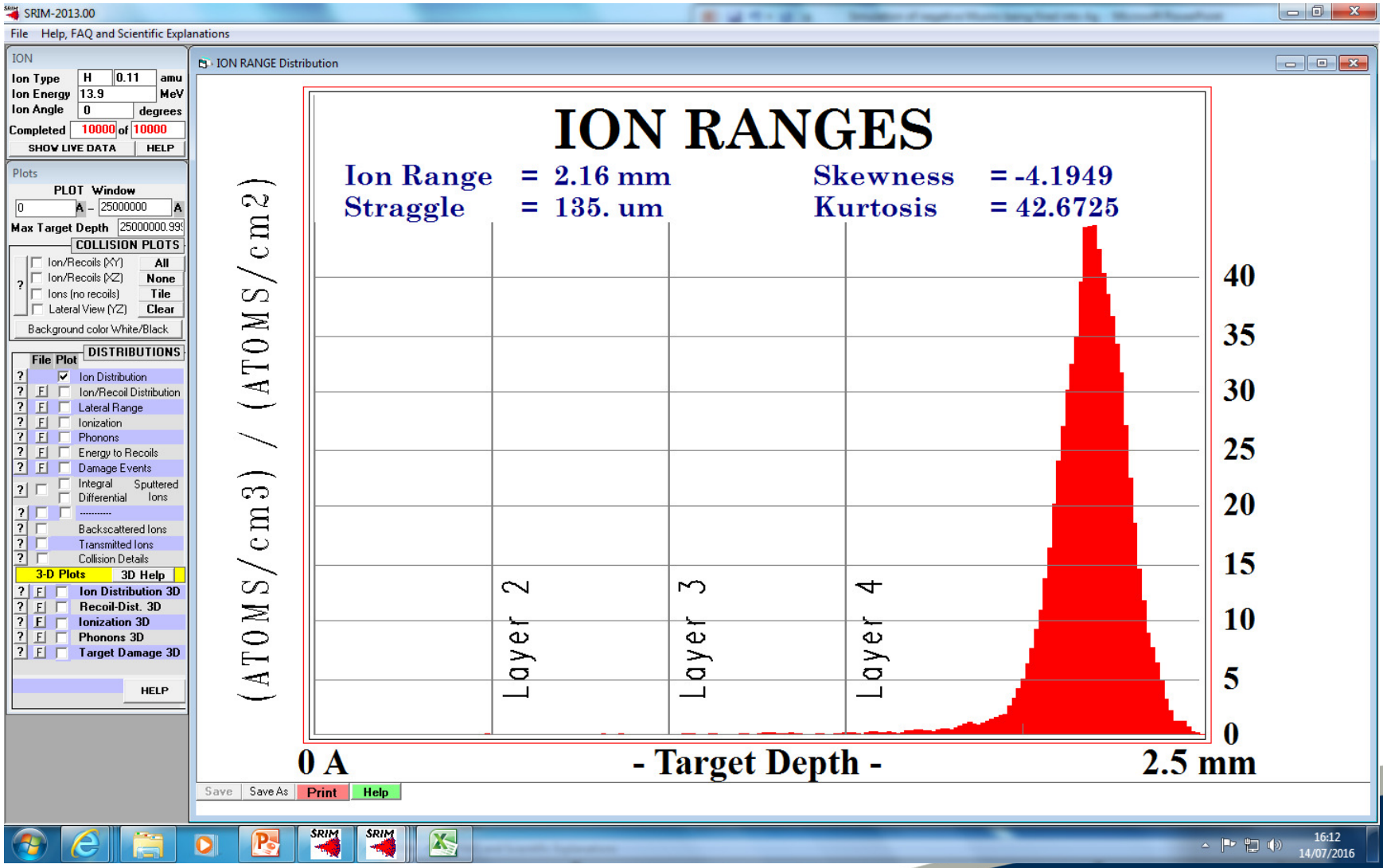

Science & Technology Facilities Council
ISIS

Depth Profiling - Simulations

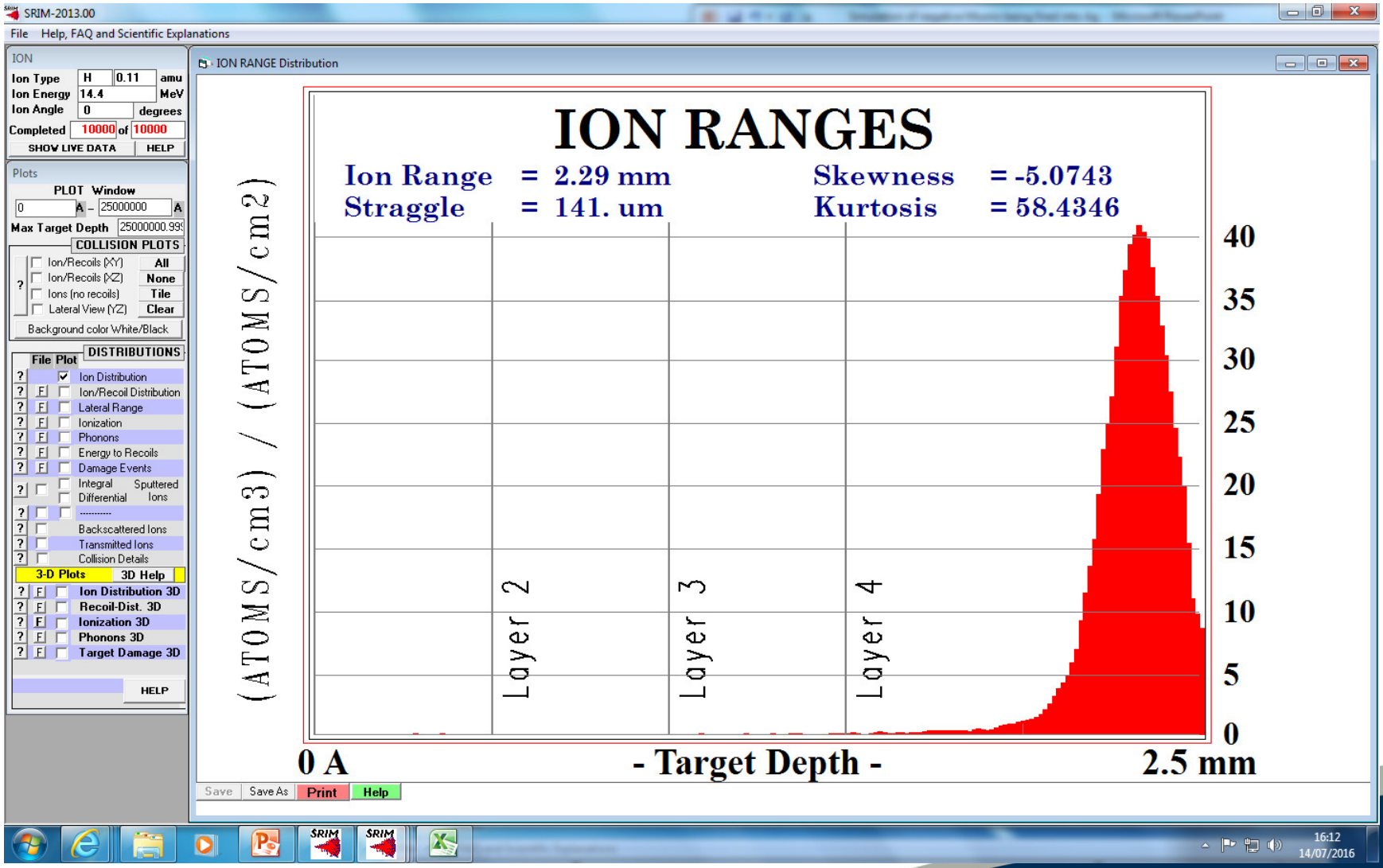

Depth Profiling - Simulations

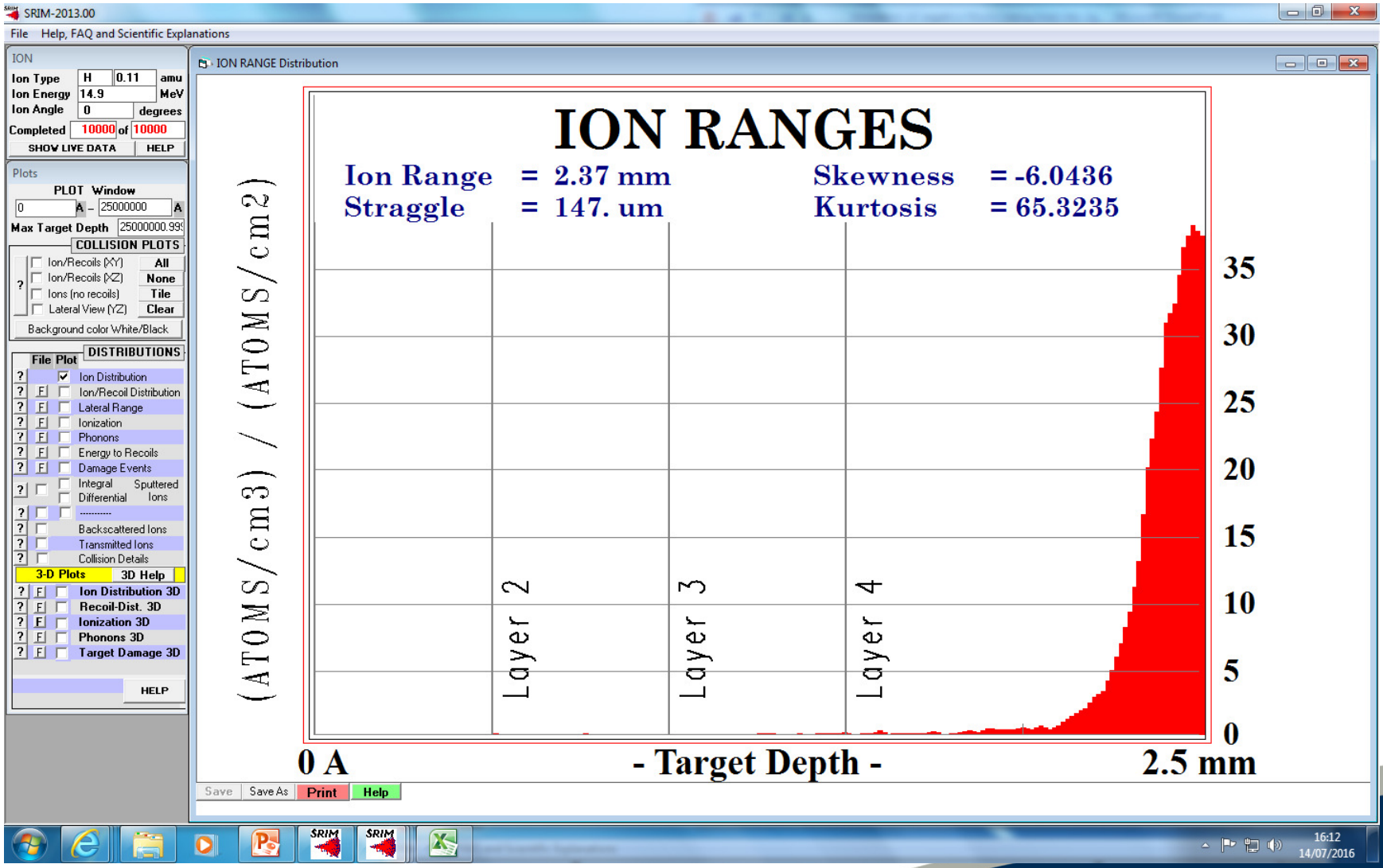

Science & Technology Facilities Council
ISIS

Depth Profiling - Simulations

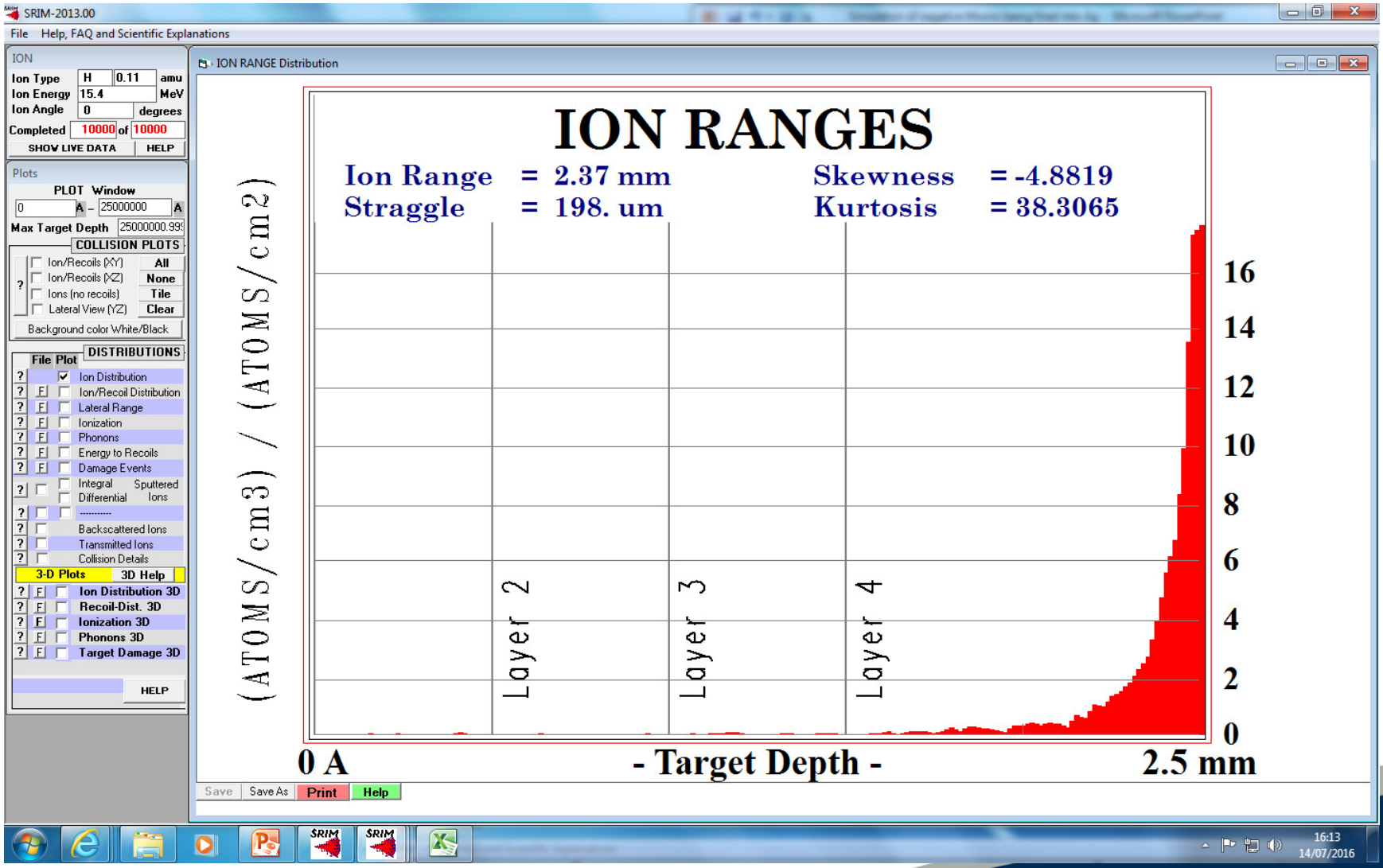

Depth Profiling

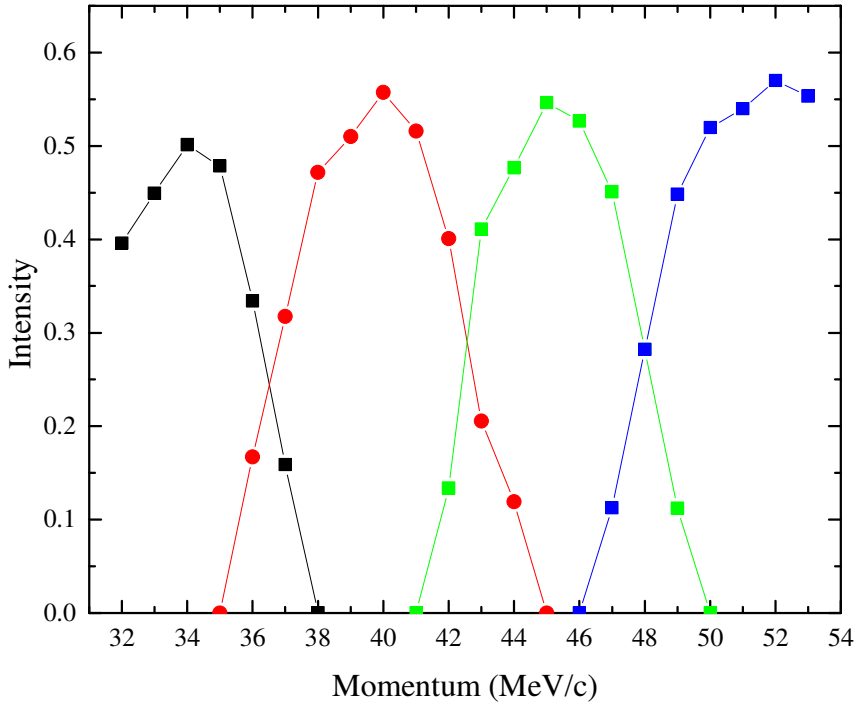

Amount of muons in each layer for a given momentum

Depth Profiling

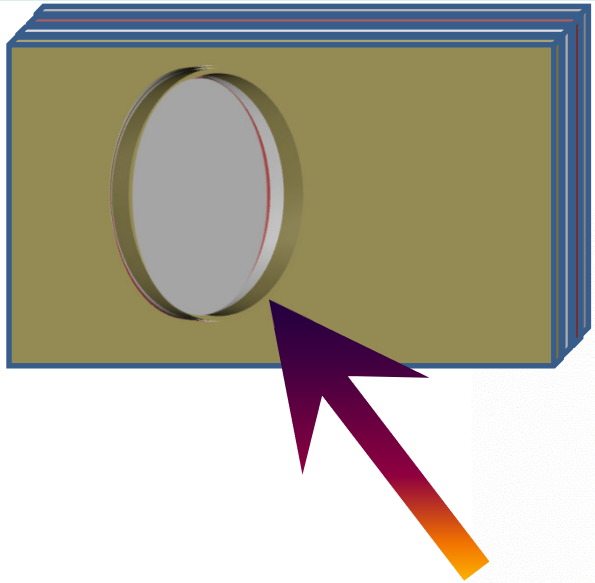

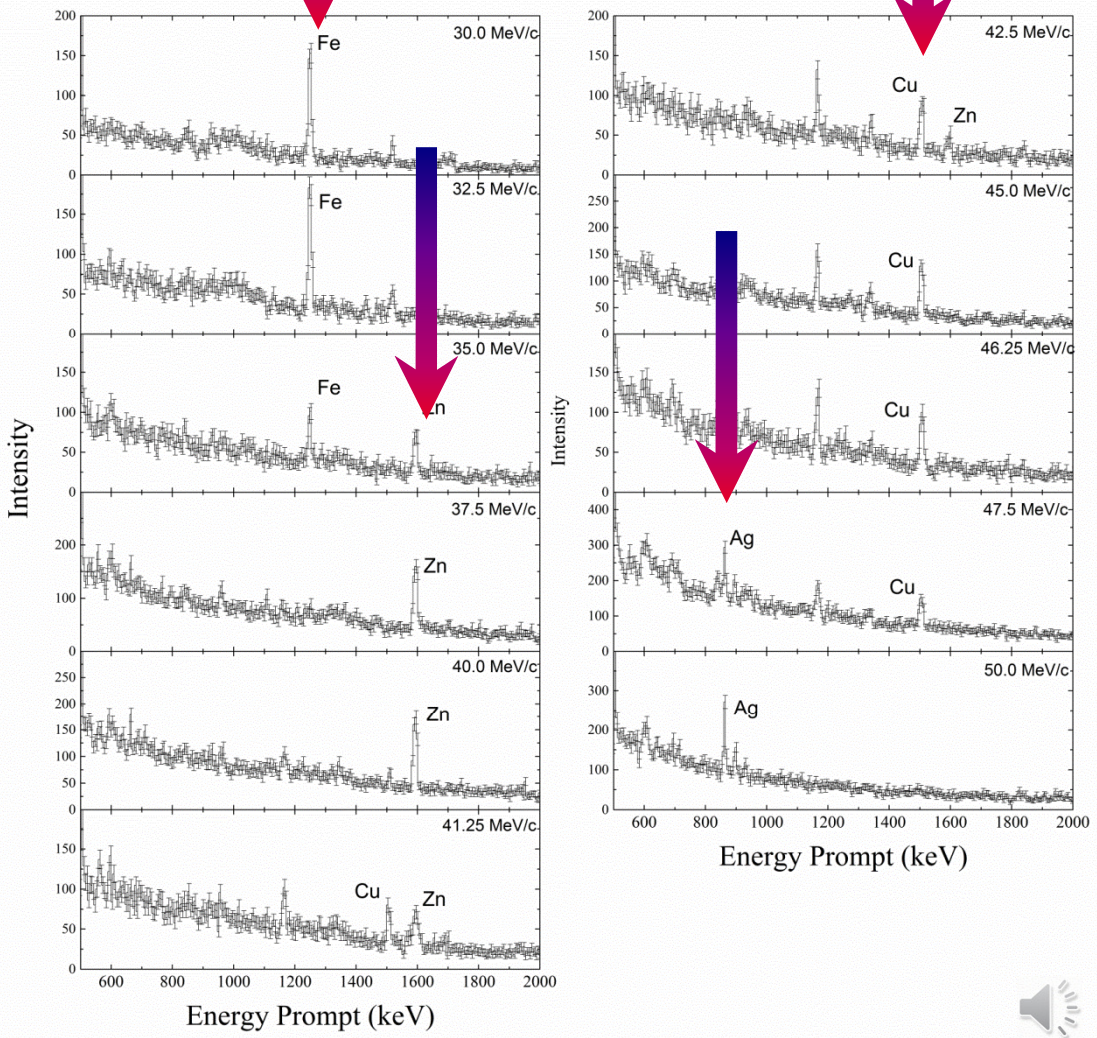

Depth Profiling

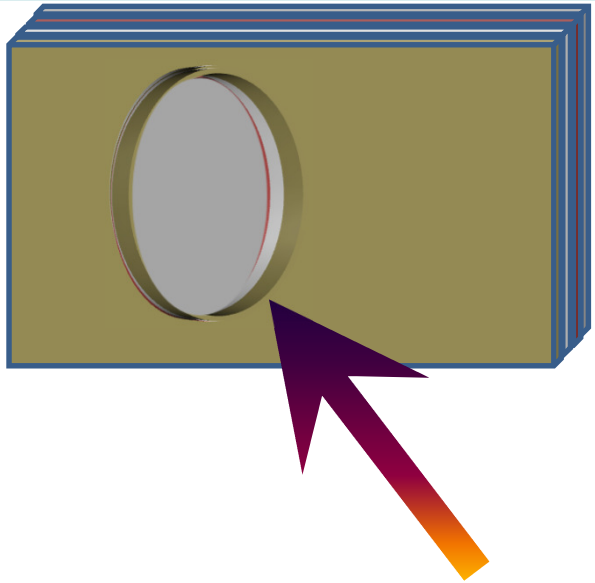

μ^-

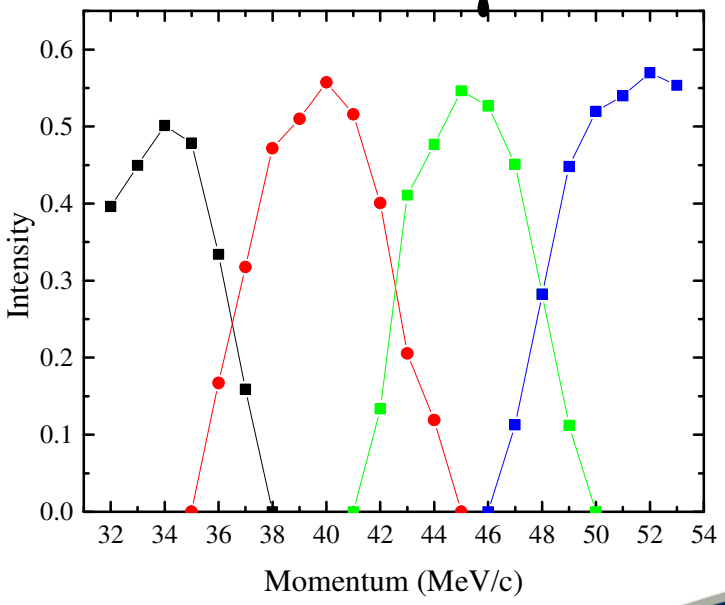

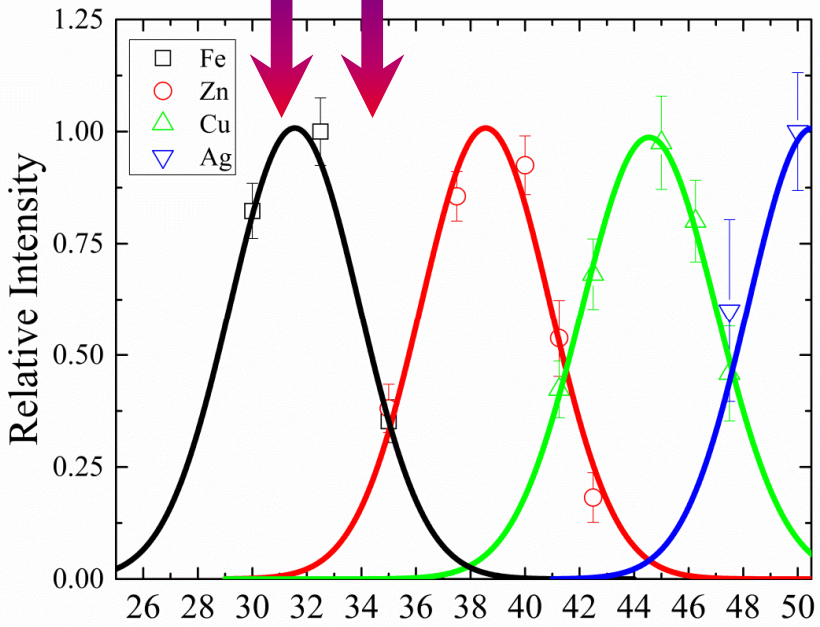

Science & Technology Facilities Council
ISIS

Depth Profiling - Simulations

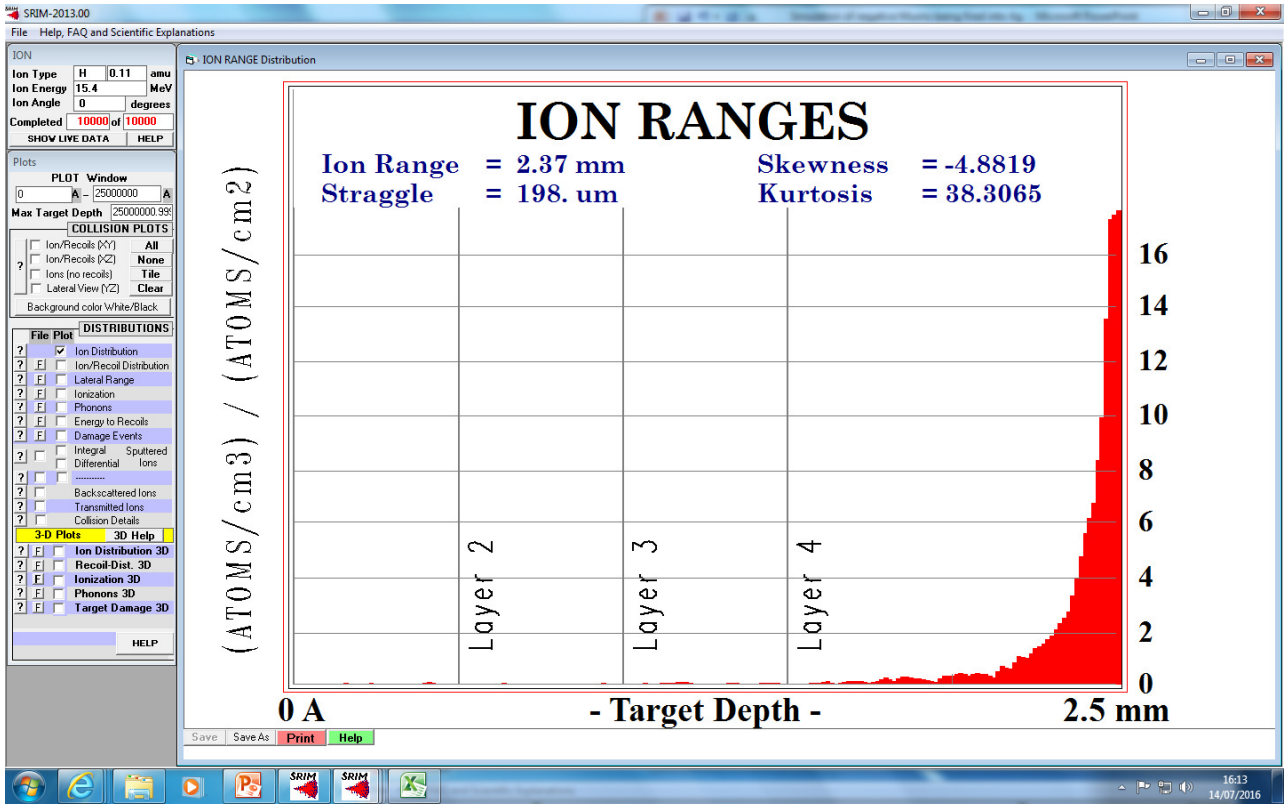

Implantation Energy 15.4 MeV, Max available 38 MeV

Depth Profiling

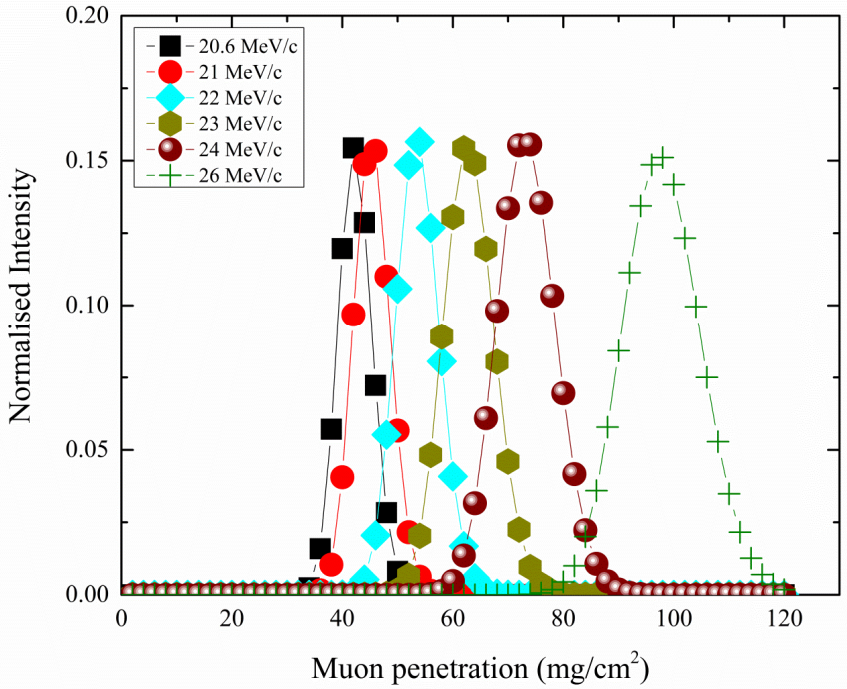

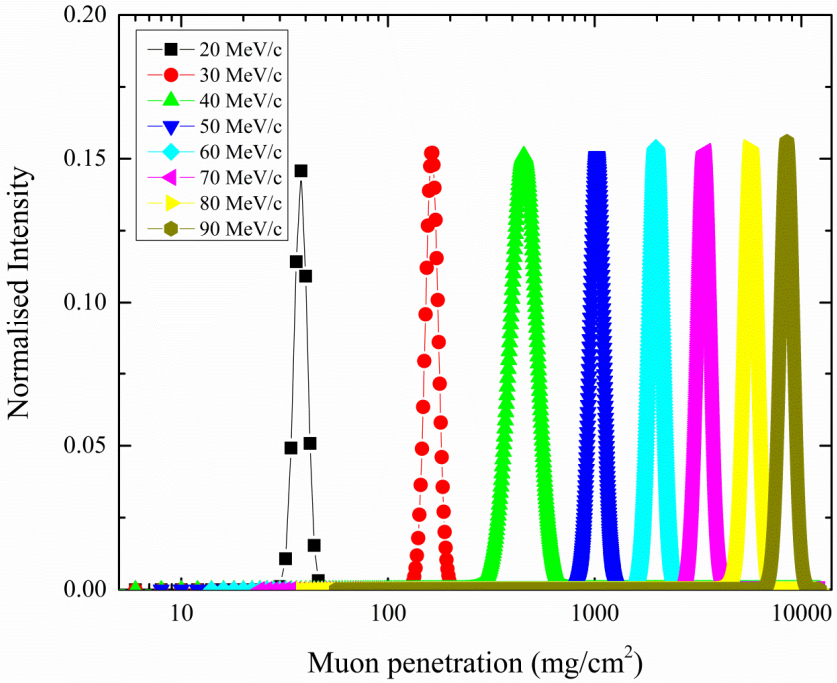

Stopping range is momentum and density dependent

Max available is ~8.5g/cm^2

In Cu ~1cm

In Ag ~0.8 cm

In Fe ~1.1cm,

In C ~3.8 cm

and ~8.5 cm in Water

Science & Technology Facilities Council
ISIS

Au Standards

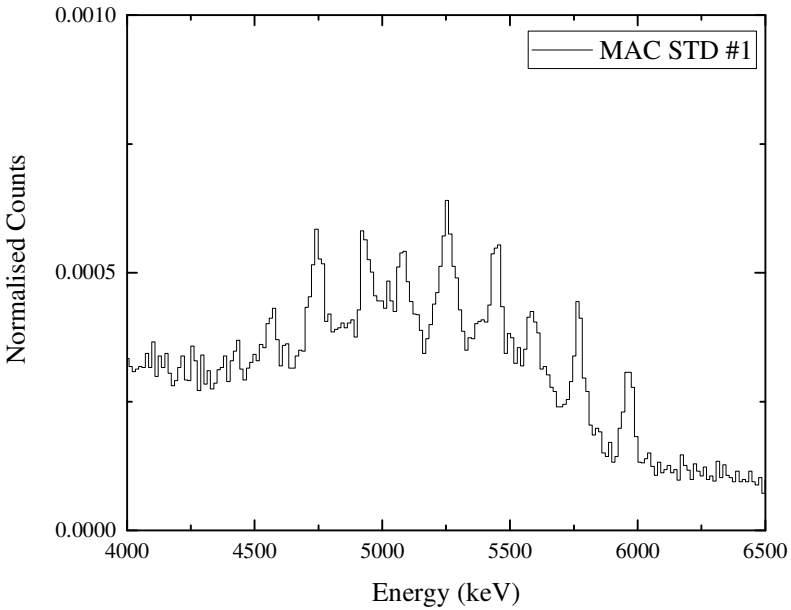

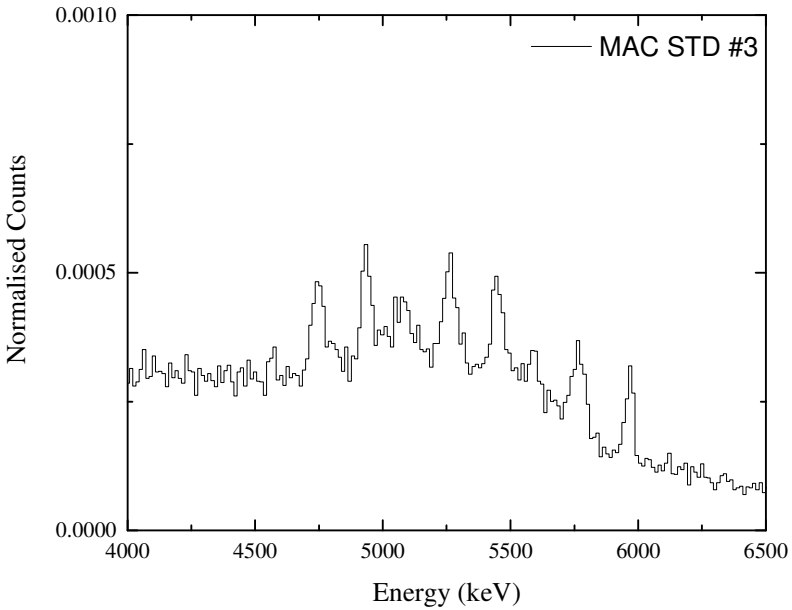

Au 94%
Ag 4.13%
Cu 1.3%
Sn 0.54%

Au 60.9%
Ag 28.8%
Cu 8.75%
Sn 1.65%

Science & Technology Facilities Council
ISIS

Au Standards

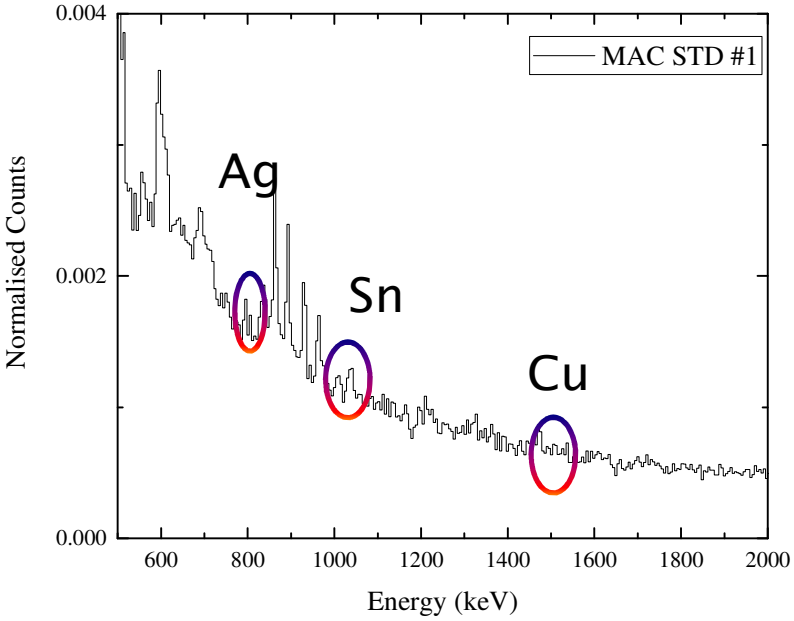

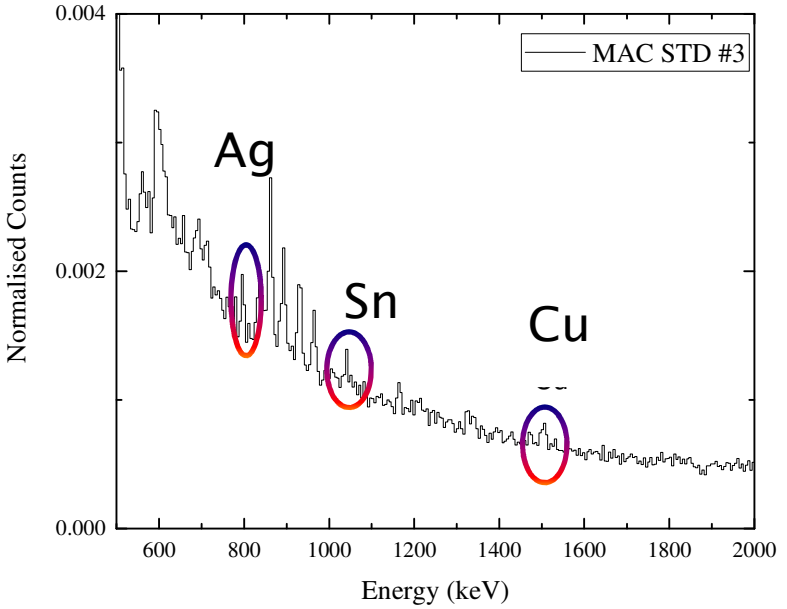

Au 94%
Ag 4.13%
Cu 1.3%
Sn 0.54%

Au 60.9%
Ag 28.8%
Cu 8.75%
Sn 1.65%

Science & Technology Facilities Council
ISIS

Bronze Standards

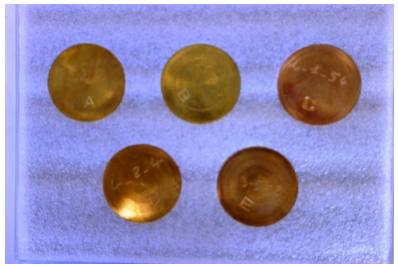

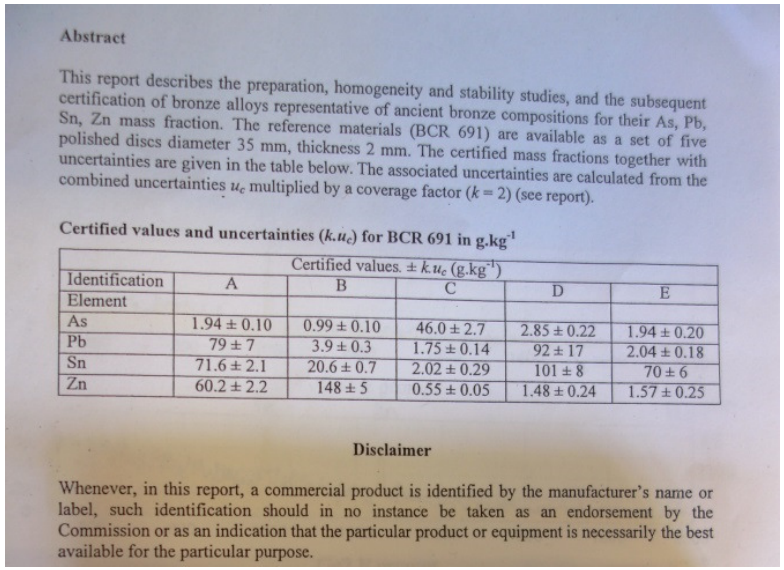

Abstract

This report describes the preparation, homogeneity and stability studies, and the subsequent certification of bronze alloys representative of ancient bronze compositions for their As, Pb, Sn, Zn mass fraction. The reference materials (BCR 691) are available as a set of five polished discs diameter 35 mm, thickness 2 mm. The certified mass fractions together with uncertainties are given in the table below. The associated uncertainties are calculated from the combined uncertainties u_c multiplied by a coverage factor ($k = 2$) (see report).

Certified values and uncertainties ($k.u_c$) for BCR 691 in g.kg^{-1}

	Certified values $\pm k.u_c$ (g.kg^{-1})				
Identification	A	B	C	D	E
Element					
As	1.94 ± 0.10	0.99 ± 0.10	46.0 ± 2.7	2.85 ± 0.22	1.94 ± 0.20
Pb	79 ± 7	3.9 ± 0.3	1.75 ± 0.14	92 ± 17	2.04 ± 0.18
Sn	71.6 ± 2.1	20.6 ± 0.7	2.02 ± 0.29	101 ± 8	70 ± 6
Zn	60.2 ± 2.2	148 ± 5	0.55 ± 0.05	1.48 ± 0.24	1.57 ± 0.25

Disclaimer

Whenever, in this report, a commercial product is identified by the manufacturer's name or label, such identification should in no instance be taken as an endorsement by the Commission or as an indication that the particular product or equipment is necessarily the best available for the particular purpose.

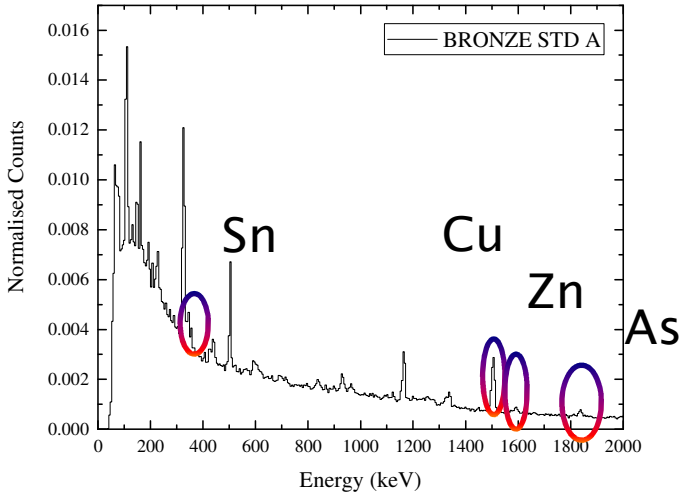

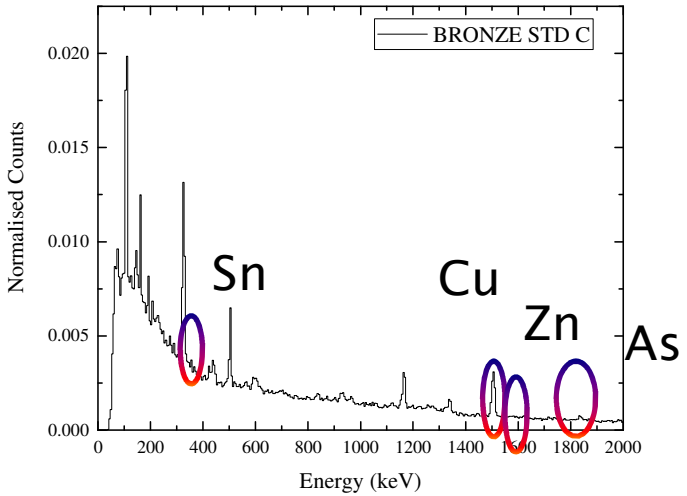

Science & Technology Facilities Council
ISIS

Bronze Standards

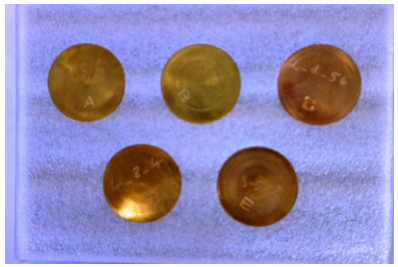

Abstract

This report describes the preparation, homogeneity and stability studies, and the subsequent certification of bronze alloys representative of ancient bronze compositions for their As, Pb, Sn, Zn mass fraction. The reference materials (BCR 691) are available as a set of five polished discs diameter 35 mm, thickness 2 mm. The certified mass fractions together with uncertainties are given in the table below. The associated uncertainties are calculated from the combined uncertainties u_c multiplied by a coverage factor ($k = 2$) (see report).

Certified values and uncertainties ($k.u_c$) for BCR 691 in g.kg^{-1}

	Certified values. $\pm k.u_c$ (g.kg^{-1})				
Identification	A	B	C	D	E
Element					
As	1.94 ± 0.10	0.99 ± 0.10	46.0 ± 2.7	2.85 ± 0.22	1.94 ± 0.20
Pb	79 ± 7	3.9 ± 0.3	1.75 ± 0.14	92 ± 17	2.04 ± 0.18
Sn	71.6 ± 2.1	20.6 ± 0.7	2.02 ± 0.29	101 ± 8	70 ± 6
Zn	60.2 ± 2.2	148 ± 5	0.55 ± 0.05	1.48 ± 0.24	1.57 ± 0.25

Disclaimer

Whenever, in this report, a commercial product is identified by the manufacturer's name or label, such identification should in no instance be taken as an endorsement by the Commission or as an indication that the particular product or equipment is necessarily the best available for the particular purpose.

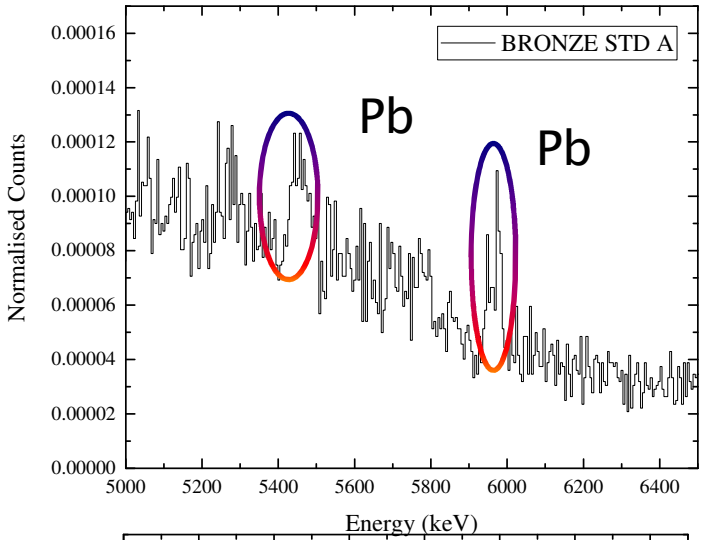

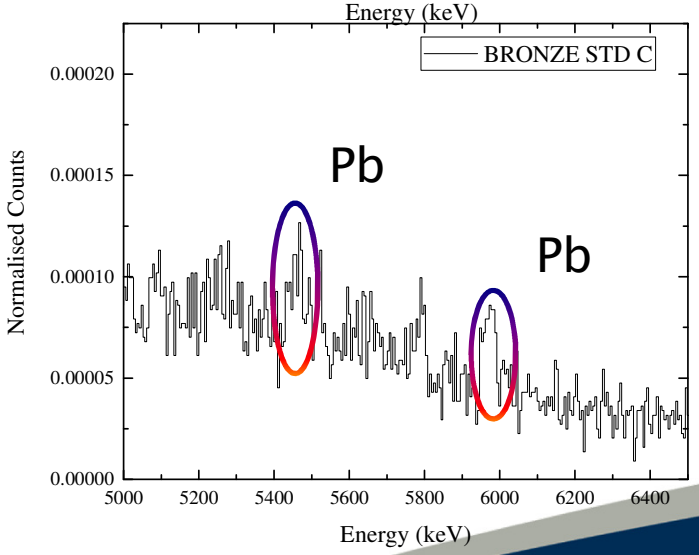

Science & Technology Facilities Council
ISIS

Bronze Standards

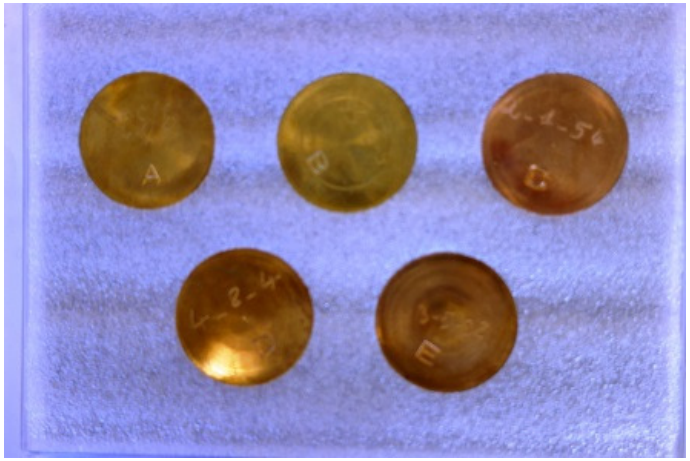

	Standard A		Standard C	
Element	Certified composition (%)	Ratio of peak intensity to Cu (%)	Certified composition (%)	Ratio of peak intensity to Cu (%)
As	0.194 ± 0.1	0.5 ± 0.3	4.60 ± 0.27	4.4 ± 0.5
Pb	7.9 ± 0.7	n.c.	0.175 ± 0.014	n.c.
Sn	7.16 ± 0.21	7.5 ± 0.5	0.202 ± 0.029	0.6 ± 0.3
Zn	6.02 ± 0.22	6.1 ± 0.5	0.055 ± 0.005	n.d.

Table 1: The certified composition for the two bronze standards. The ratio of the peak intensities from the muonic X-rays. This shows a remarkably good argeement. The abbreviations n.d. indicates not detected and n.c. not calcaulated. This is due to the potential contamination of the data due to the lead beam snout.

Hillier et al, Microchemical Journal 125 203 (2016)

Roman Coins - High Energy X-rays

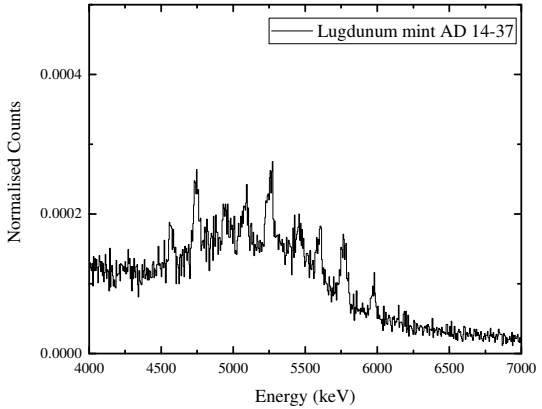

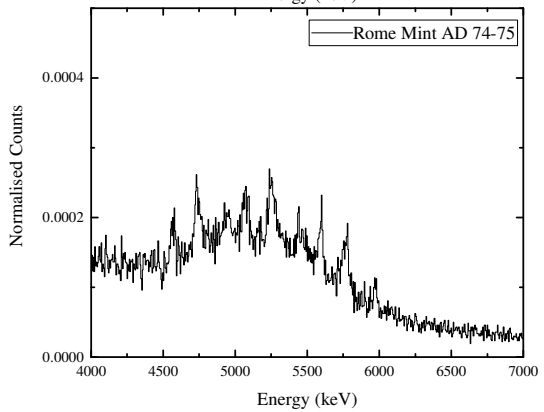

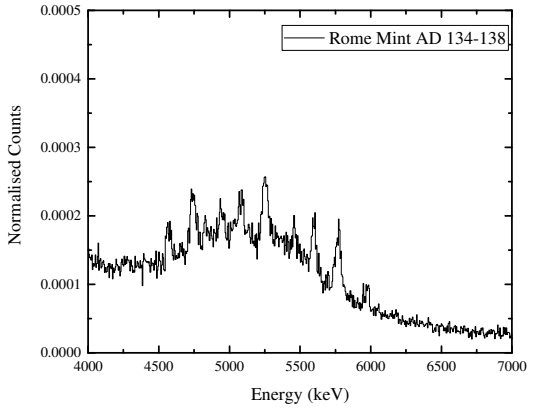

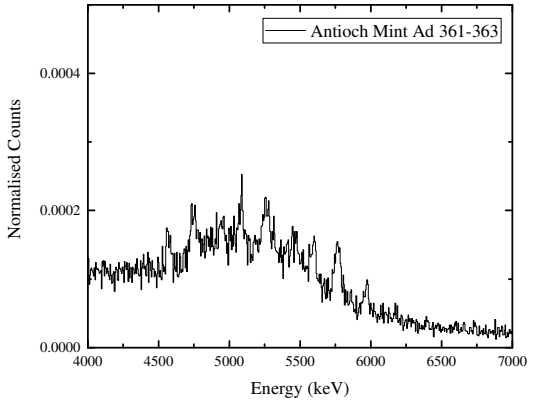

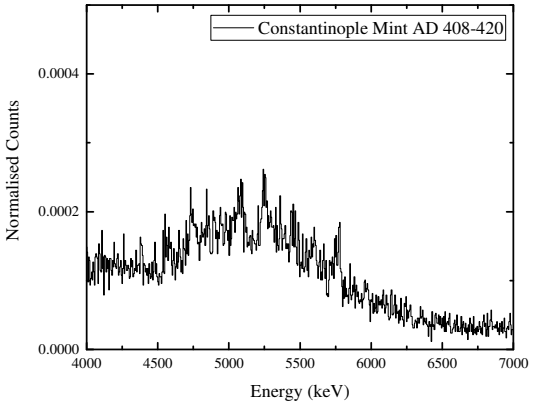

Au peaks
Peaks clearer on the earlier coins

Science & Technology Facilities Council
ISIS

Roman Coins - Low Energy X-rays

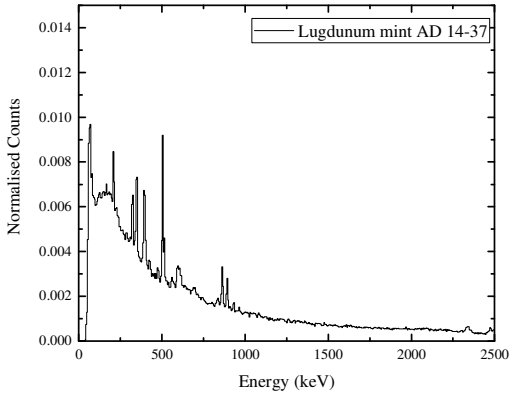

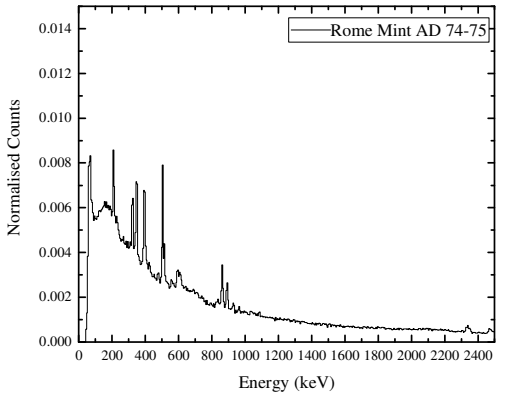

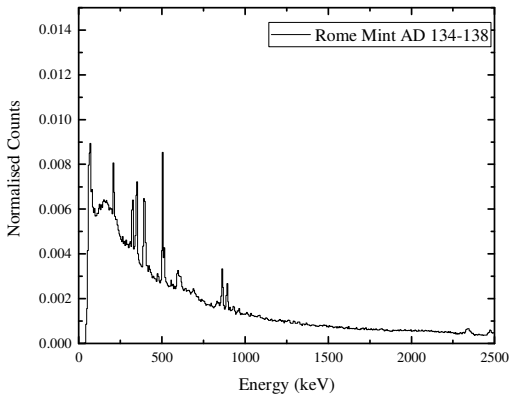

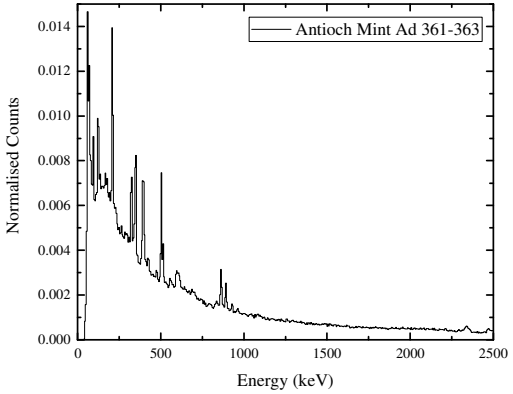

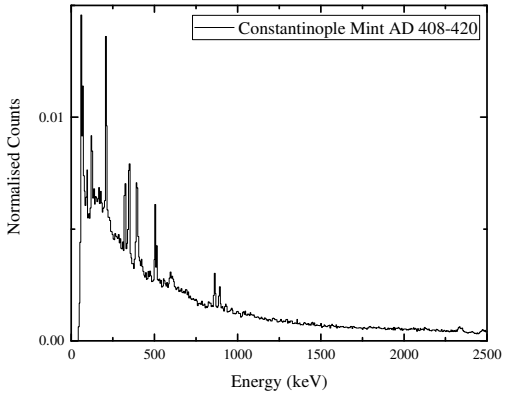

Early coins appear to be high purity

Later coins have additional peaks

Science & Technology Facilities Council
ISIS

Roman Coins - the differences

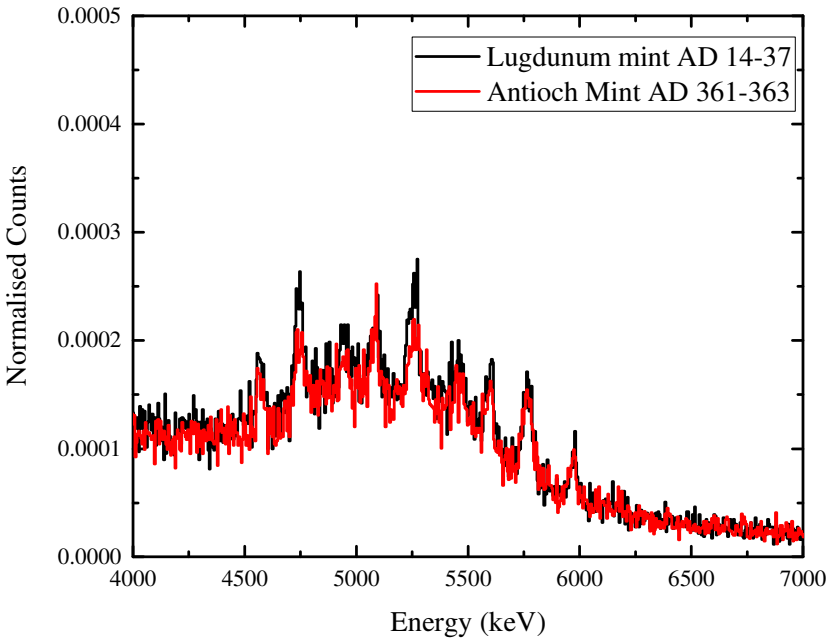

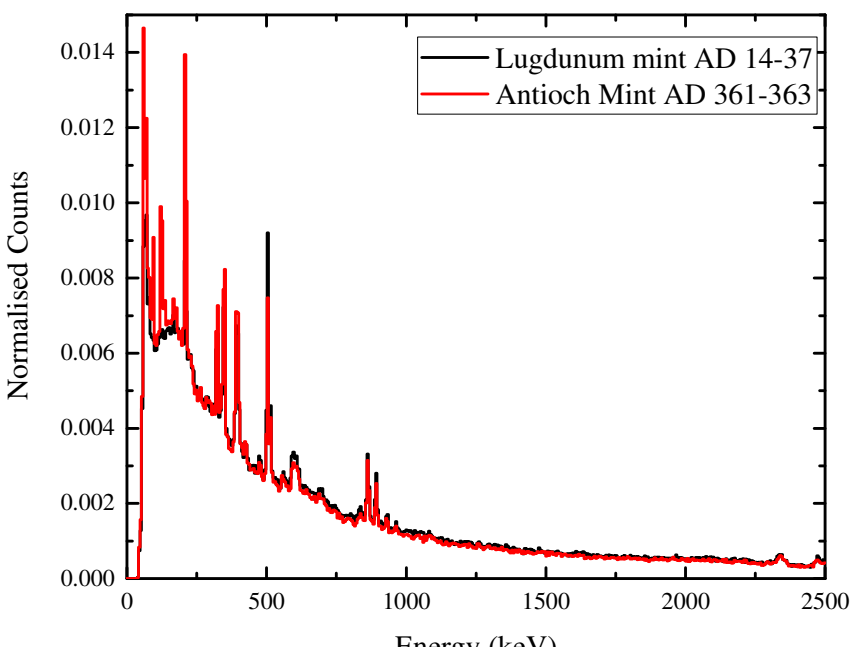

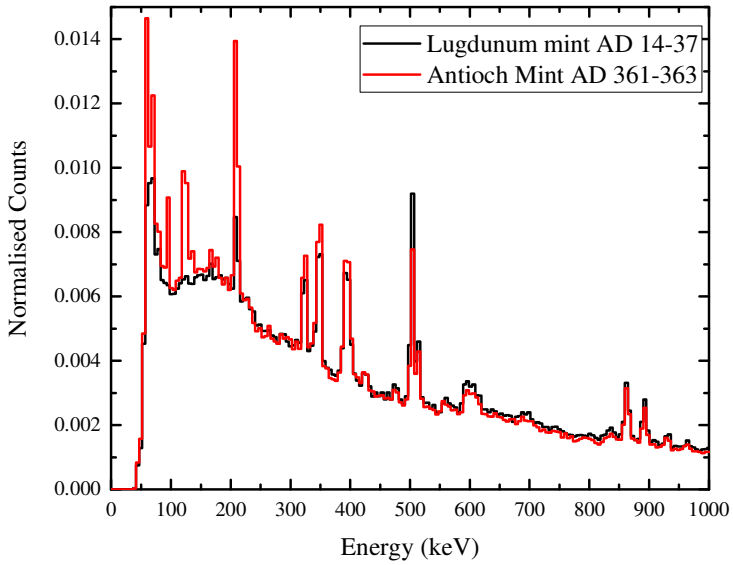

Roman Coins – debased silver coin

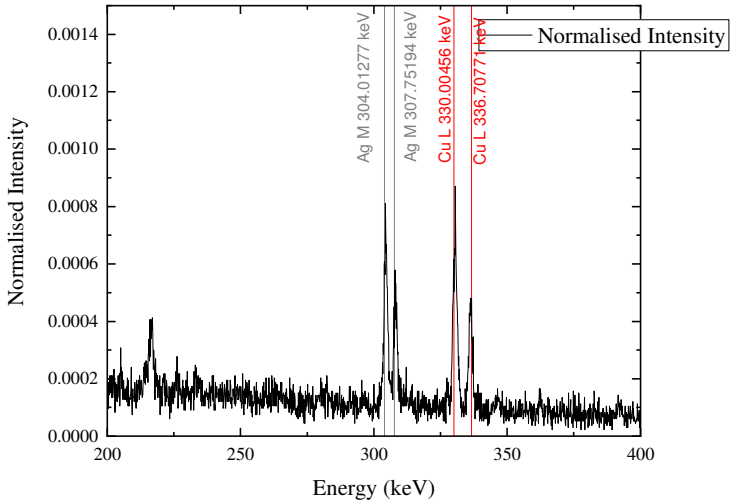

Julia Domna – 3rd Century

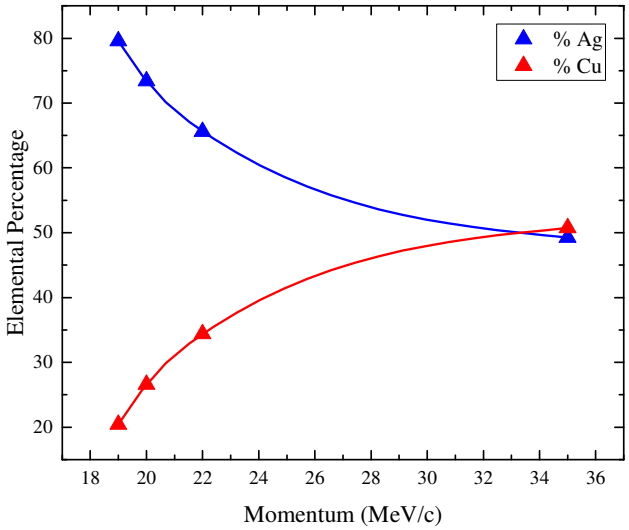

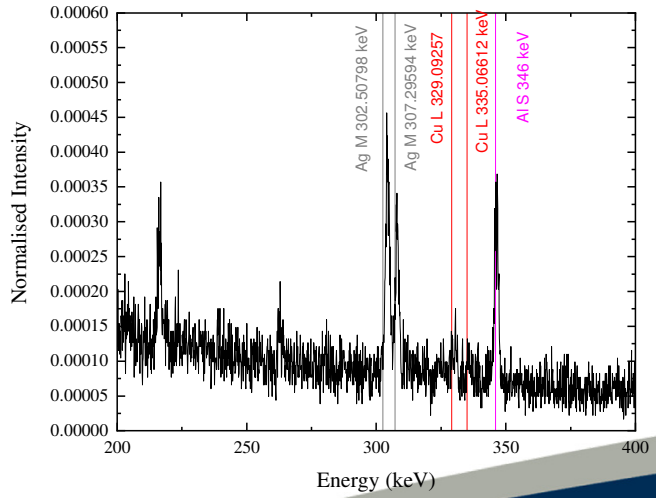

Science & Technology Facilities Council
ISIS

Islamic Silver Coins

LT 262
UMAYYAD
Dimasha mint

LT 169
Ghaznavid
Bahramshab mint

Islamic Silver Coins

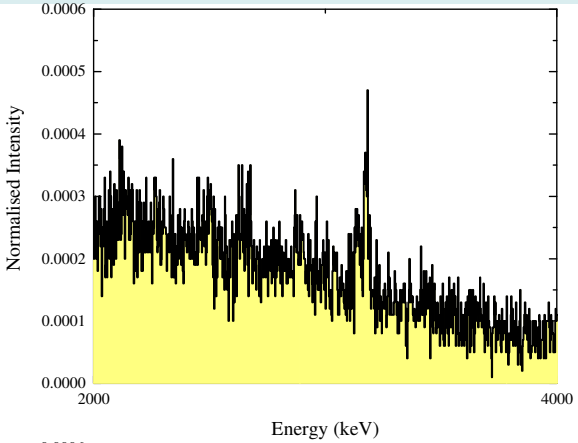

Pure Ag

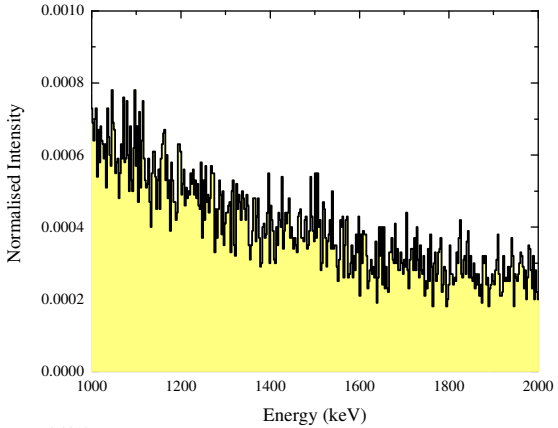

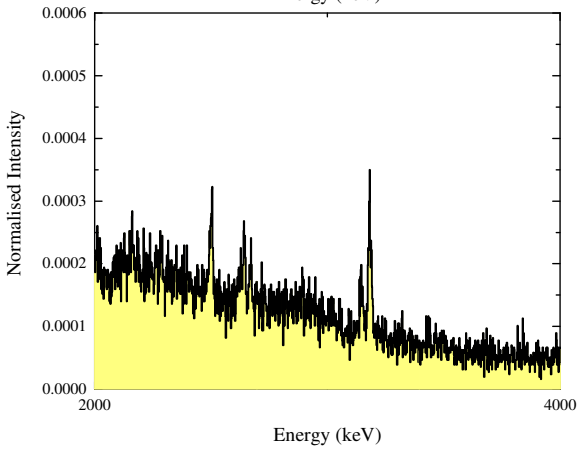

LT 262
UMAYYAD
Dimasha mint

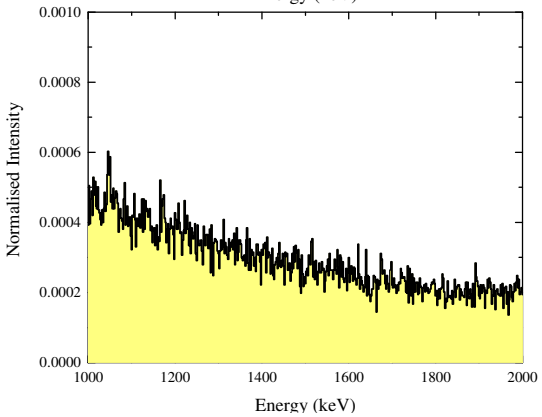

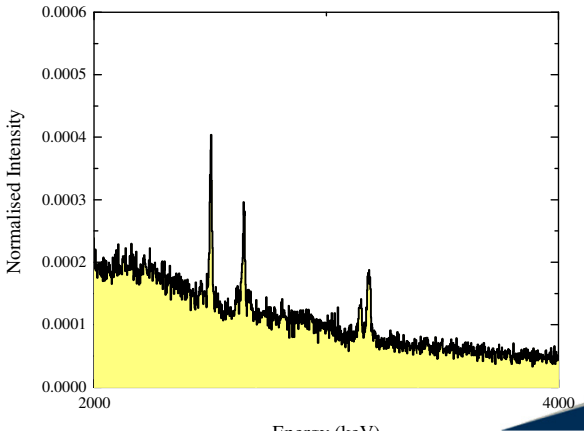

LT 169
Ghaznavid
Bahramshab mint

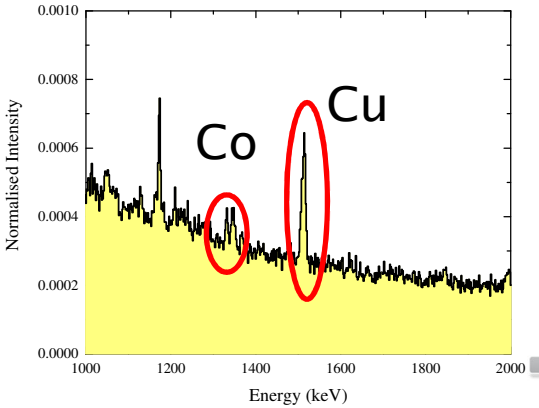

Islamic Silver Coins

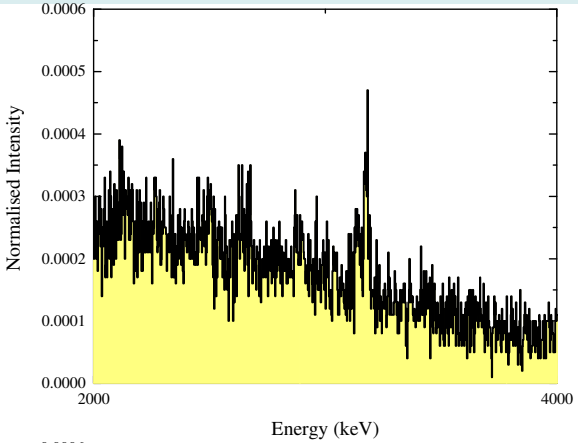

Pure Ag

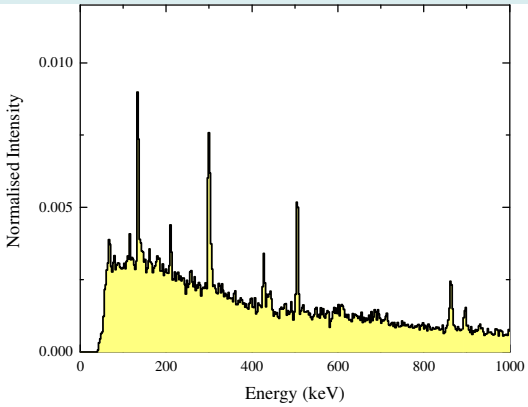

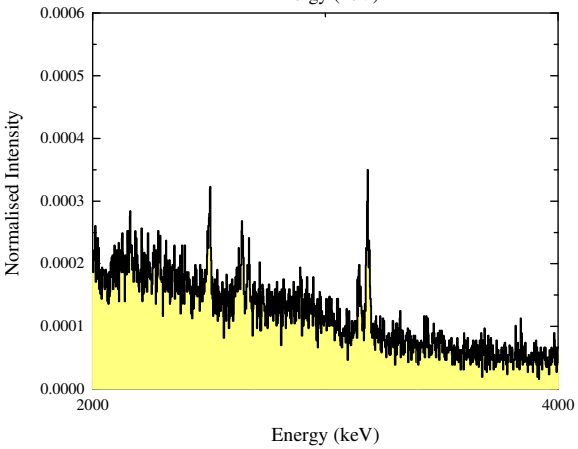

LT 262
UMAYYAD
Dimasha mint

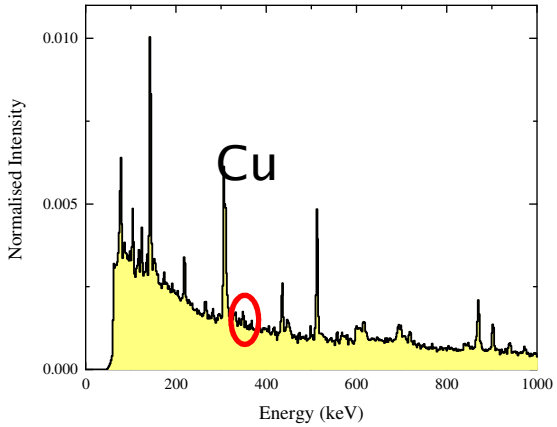

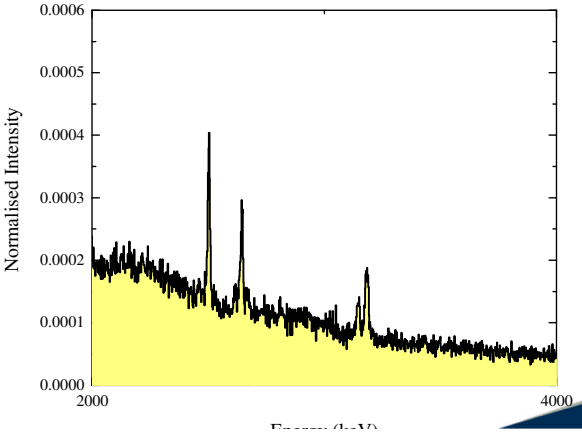

LT 169
Ghaznavid
Bahramshab mint

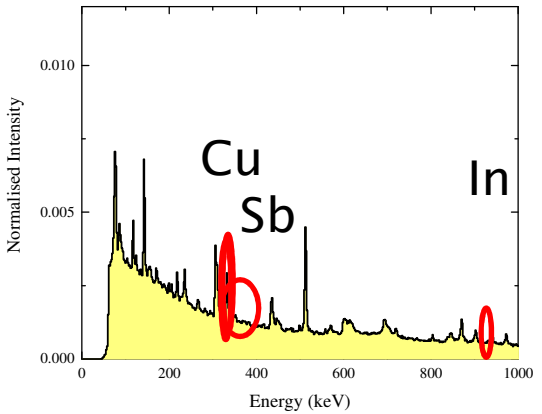

Coin from the Mary Rose

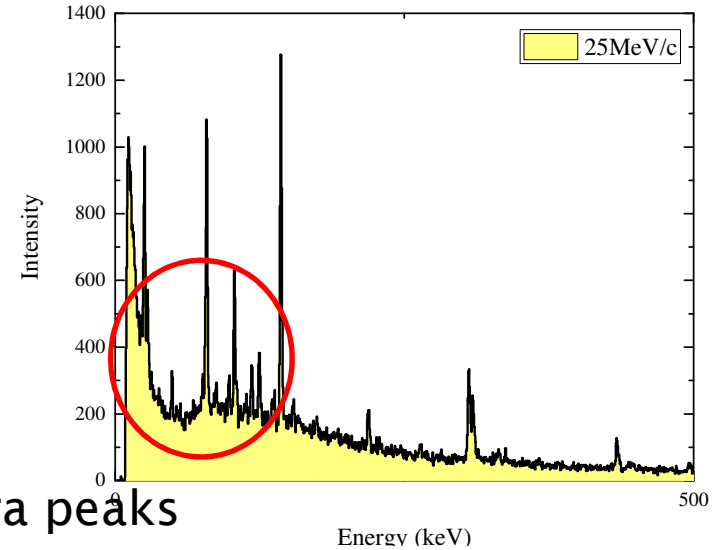

Extra peaks

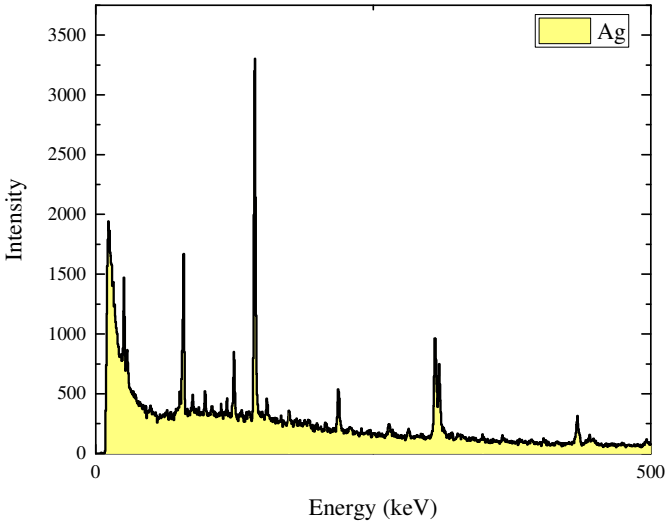

Coin from the Mary Rose

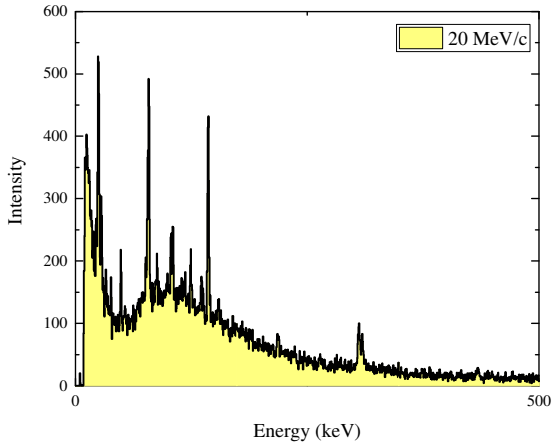

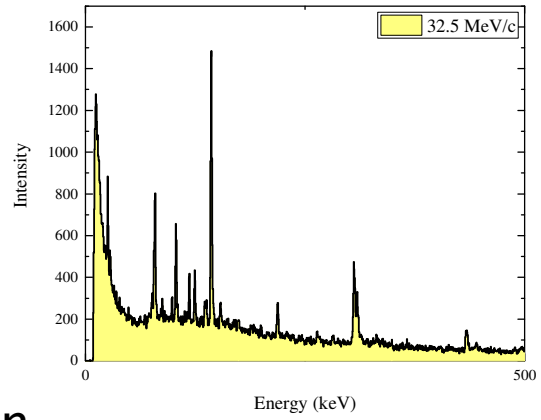

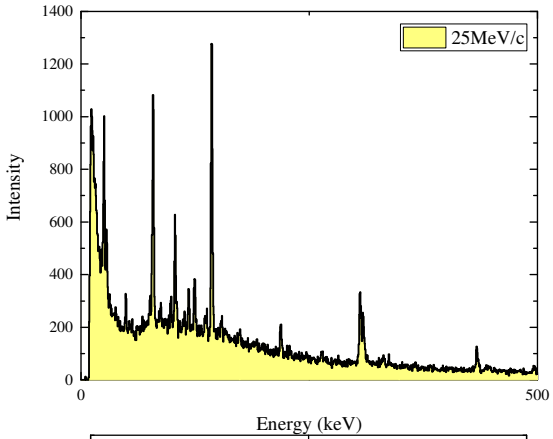

Extra peaks seen
Copper?
Nitrogen
Oxygen
Carbon

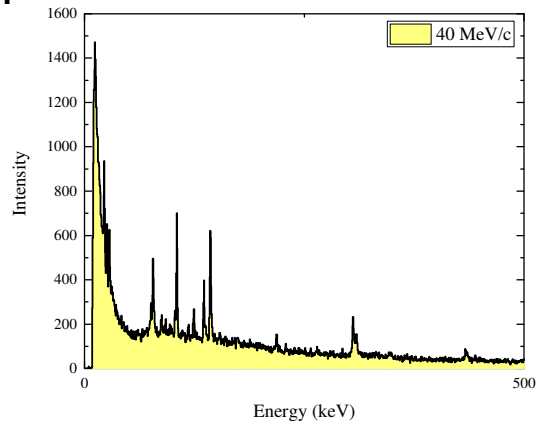

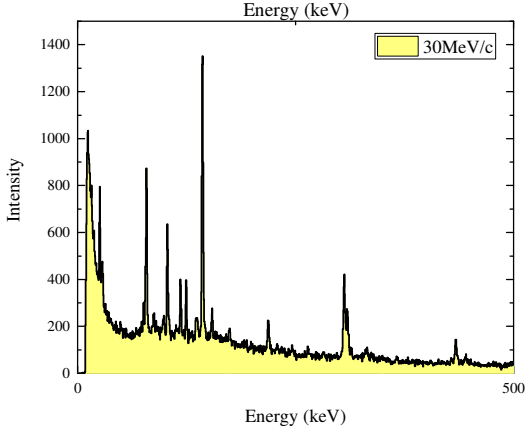

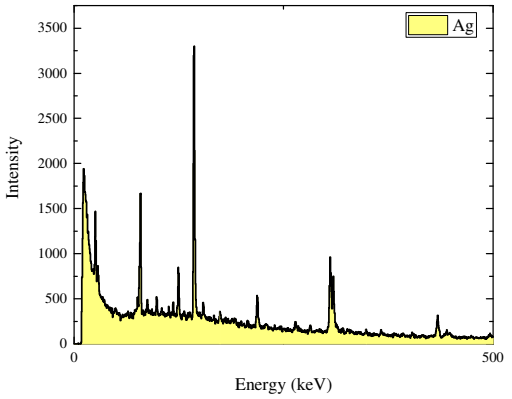

cilities Council

Lithium amide imide ($LiNH_2$ - Li_2NH)

HYDROGEN STORAGE: $LiNH_2 + LiH \leftrightarrow Li_2NH + H_2$

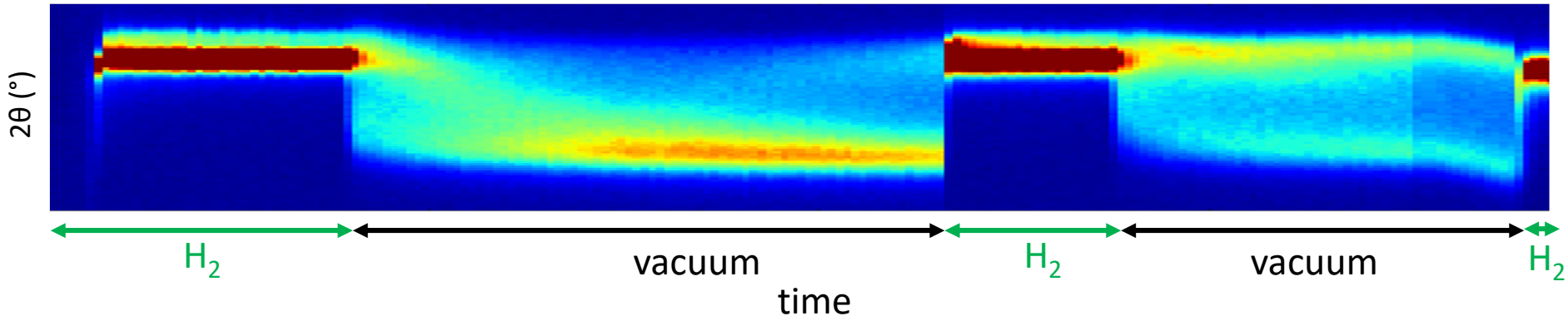

Synchrotron X-ray powder diffraction shows hydrogen release occurs via range of intermediate stoichiometry values – key to easily reversible hydrogen storage

AMMONIA CRACKING: $2NH_3 \rightarrow N_2 + 3H_2$ using Li_2NH

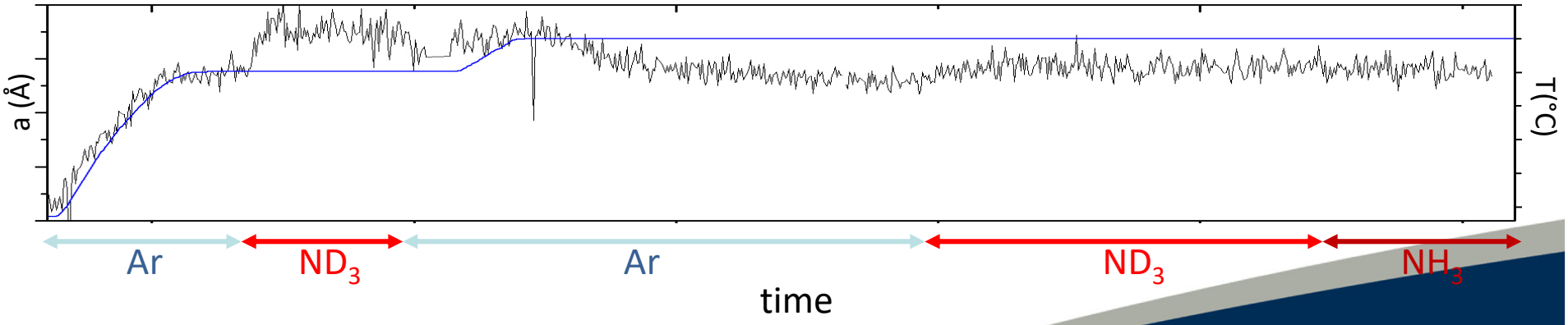

Variation in lattice parameter of Li_2ND on exposure to ND_3 indicates non-stoichiometry during ammonia decomposition reaction – active form of the catalyst is non-stoichiometric

Lithium amide imide ($LiNH_2$ - Li_2NH)

Quantifying the stoichiometry is difficult. By diffraction the scattering (both X-ray and neutron) is dominated by the nitrogen.

QUANTIFYING STOICHIOMETRY WITH NEGATIVE MUONS

Synthesised a series of lithium amide-imide samples with varying stoichiometry:

$$xLi_3N + (2-x)LiNH_2 \rightarrow 2Li_{1+x}NH_{2-x}$$

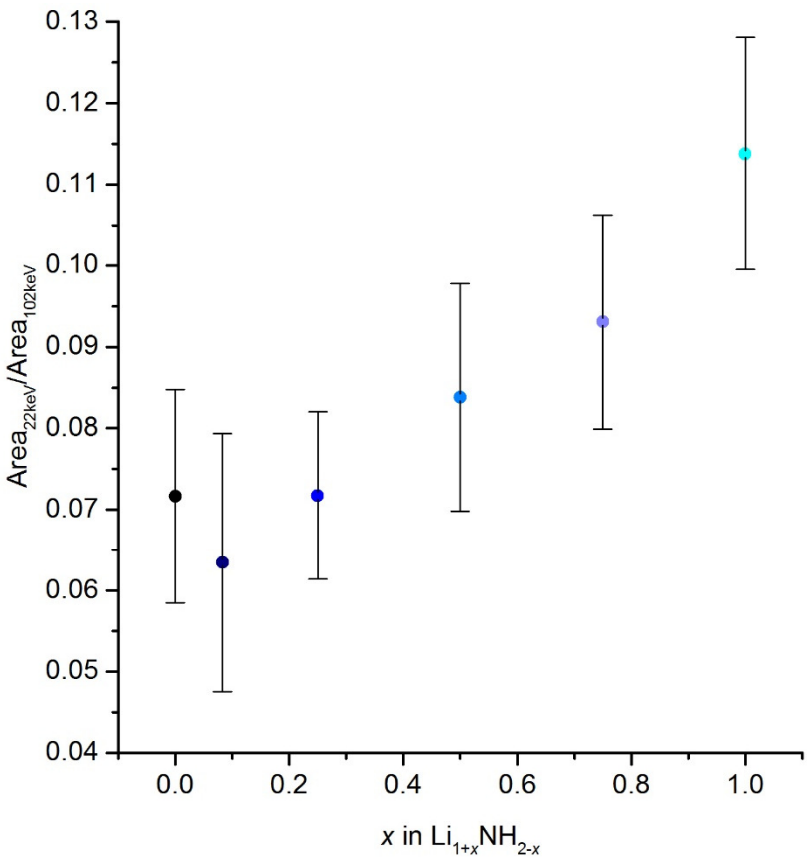

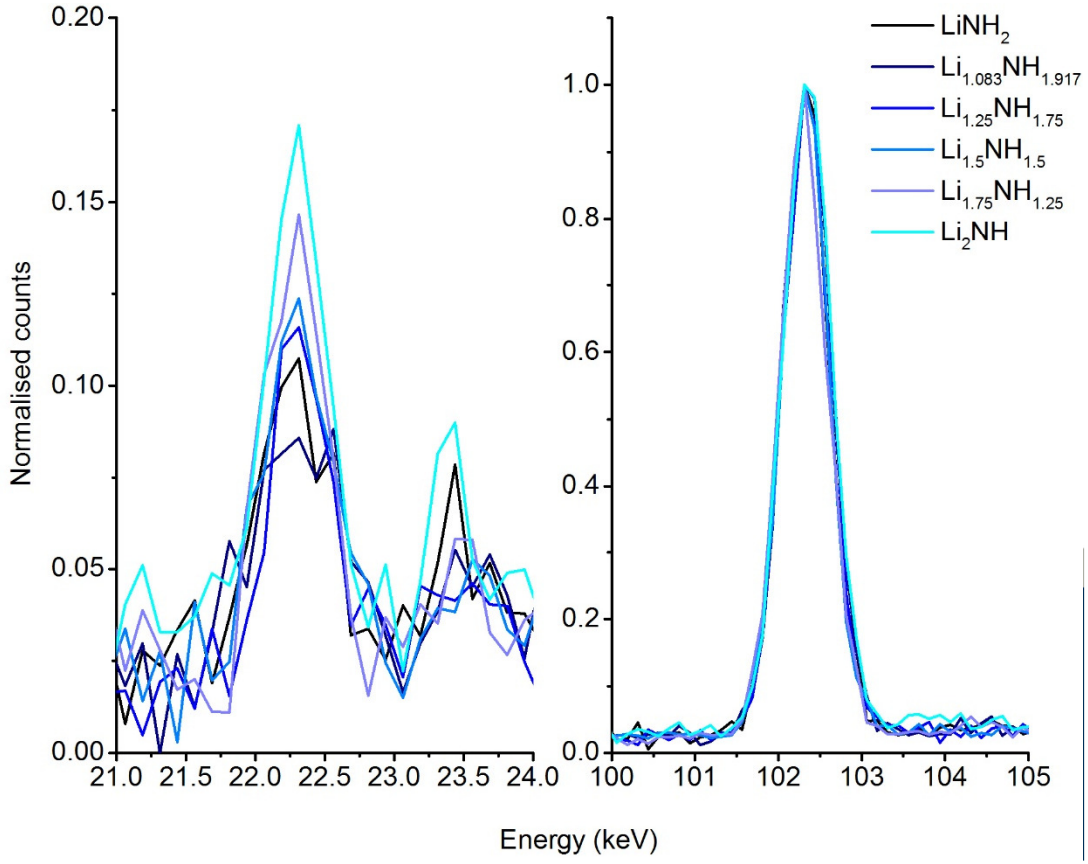

Ferro-electric relaxor

Different Structure in surface and bulk:

PHYSICAL REVIEW B **70**, 172204 (2004)

Direct observation of the near-surface layer in $Pb(Mg_{1/3}Nb_{2/3})O_3$ using neutron diffraction

K. H. Conlon,[1] H. Luo,[2] D. Viehland,[3] J. F. Li,[3] T. Whan,[1] J. H. Fox,[1] C. Stock,[4] and G. Shirane[5]
[1]*National Research Council, Chalk River, Ontario, Canada K0J 1J0*
[2]*Shanghai Institute of Ceramics, Chinese Academy of Sciences, Shanghai, China 201800*
[3]*Department of Materials Science and Engineering, Virginia Tech., Blacksburg, Virginia 24061, USA*
[4]*Department of Physics, University of Toronto, 60 St. George, Ontario, Canada M5S 1A7*
[5]*Physics Department, Brookhaven National Laboratory, Upton, New York 11973, USA*
(Received 5 July 2004; published 19 November 2004)

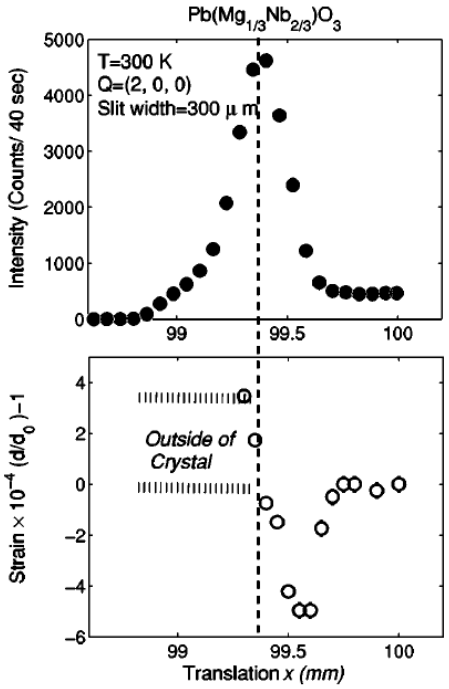

Relaxors display different properties in the bulk and surface – strain (neutrons) and x-rays (32 keV/surface and 67 keV/bulk)

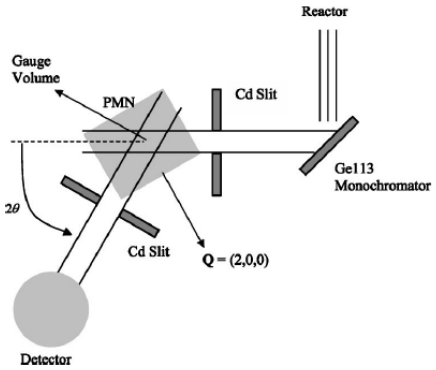

PHYSICAL REVIEW B **67**, 104102 (2003)

Ground state of the relaxor ferroelectric $Pb(Zn_{1/3}Nb_{2/3})O_3$

Guangyong Xu,[1] Z. Zhong,[2] Y. Bing,[3] Z.-G. Ye,[3] C. Stock,[4] and G. Shirane[1]
[1]*Physics Department, Brookhaven National Laboratory, Upton, New York 11973*
[2]*National Synchrotron Light Source, Brookhaven National Laboratory, Upton, New York 11973*
[3]*Department of Chemistry, Simon Fraser University, Burnaby, British Columbia, Canada, V5A 1S6*
[4]*Department of Physics, University of Toronto, Toronto, Ontario, Canada M5S 1A7*
(Received 4 November 2002; revised manuscript received 13 January 2003; published 17 March 2003)

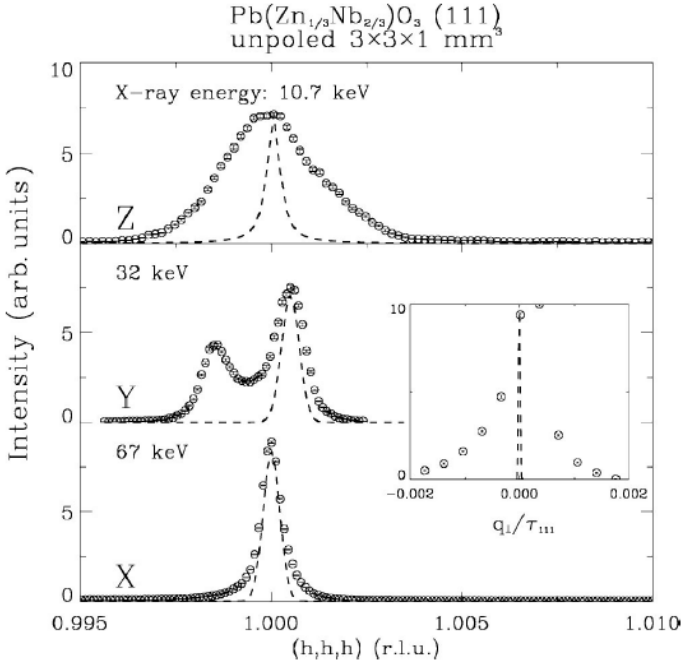

Ferro-electric relaxor

Chemical Homogeneity near surface?

Research Article

Journal of RAMAN SPECTROSCOPY

Received: 24 March 2010 Accepted: 4 June 2010 Published online in Wiley Online Library: 20 July 2010

(wileyonlinelibrary.com) DOI 10.1002/jrs.2746

Raman scattering study of the soft mode in $Pb(Mg_{1/3}Nb_{2/3})O_3$

Hiroki Taniguchi,[a]* Mitsuru Itoh[a] and Desheng Fu[b]

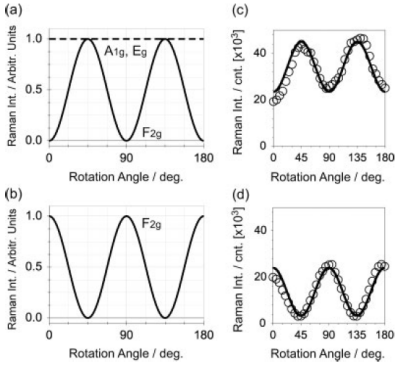

Raman suggestive of gradient between Mg and Nb near crystal surface (angular dependence)

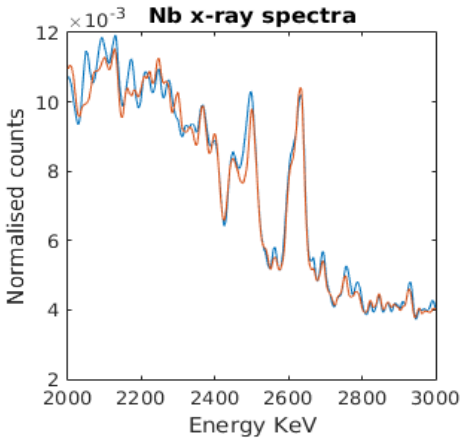

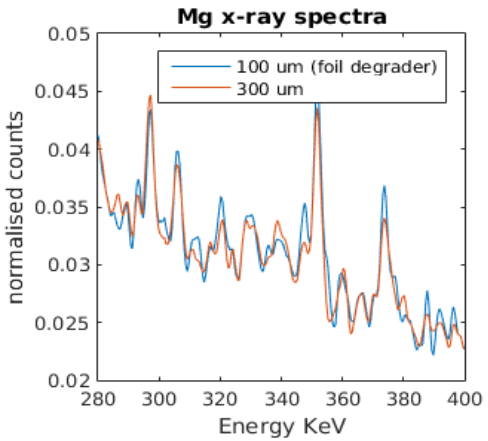

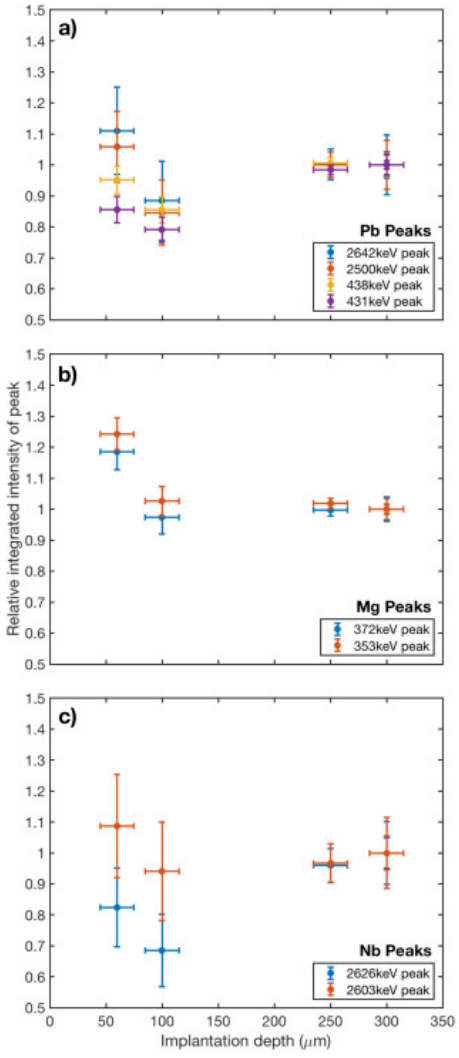

Negative Muons find no different between Mg and Nb from 100 – 300 microns, but below 100 microns a change in intensity is observed.

Muonic X-rays Emission: beyond elemental analysis

Chemical States?

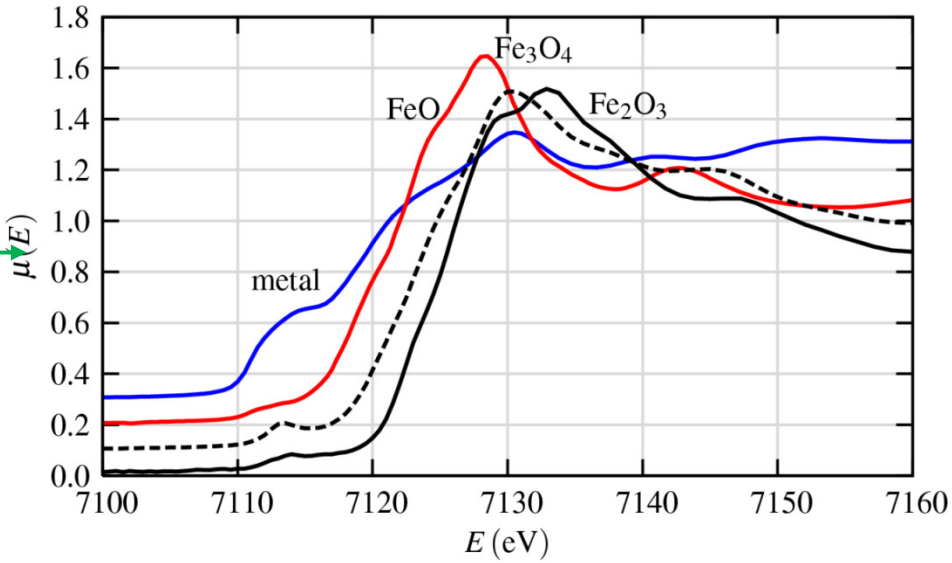

Limited by…

- Dipole selection rules $\Delta j/l/s = \pm 1$
- X-ray attenuation length
- Atomic number
- Sensitivity to Hybridization, Valence, Charge transfer.

While μ-X-ray Emission…

- Particle interaction = No selection rules
- Emission in Hard X-ray region (no overlap)
- Bulk sensitivity
- Sensitivity to Oxidation state, Valence, Charge transfer, Quantitative fractions, Spin-orbit coupling.

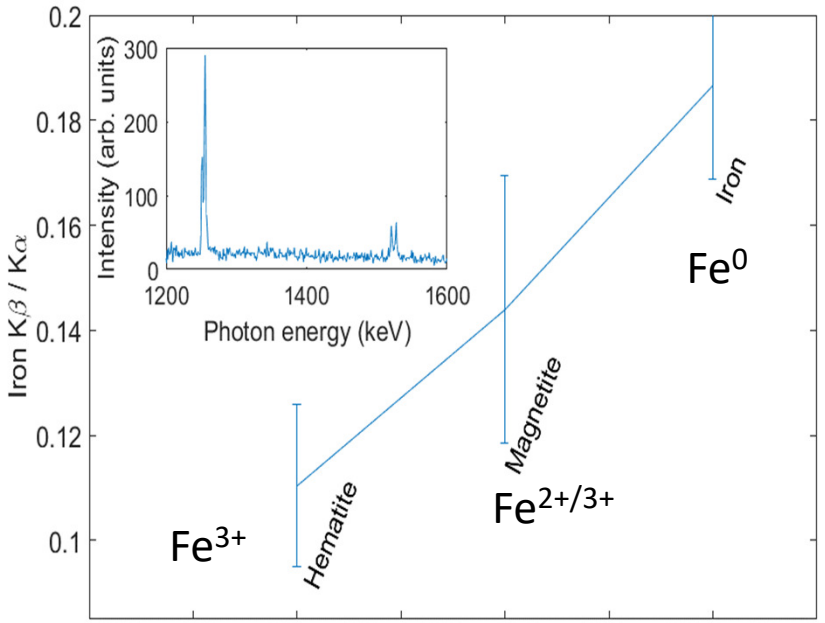

Real Space Imaging

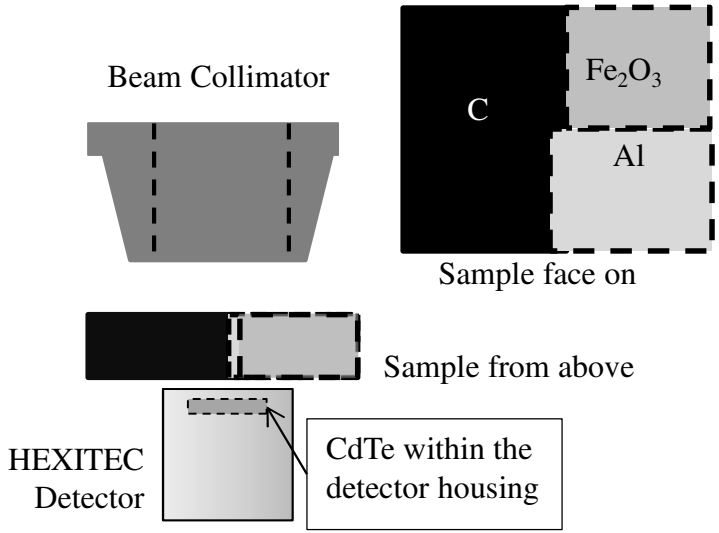

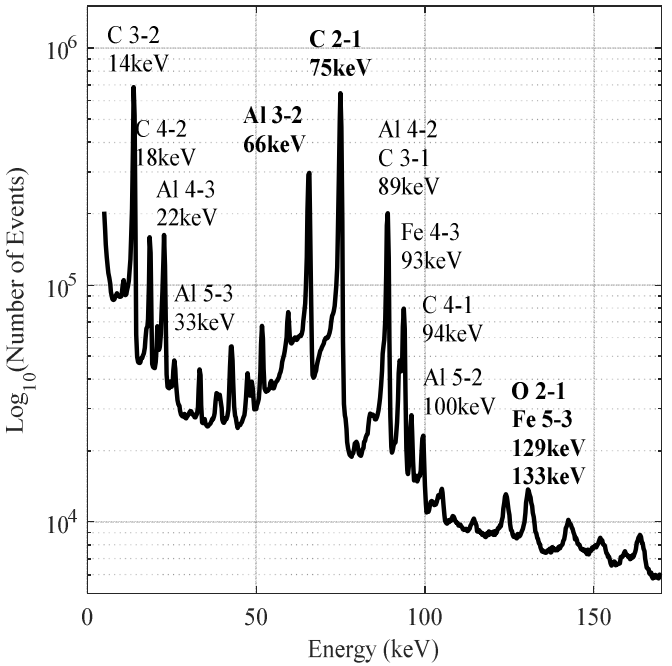

The spectrum from all pixels combined from a 10.5 hour exposure of the Al, C and Fe_2O_3 sample.

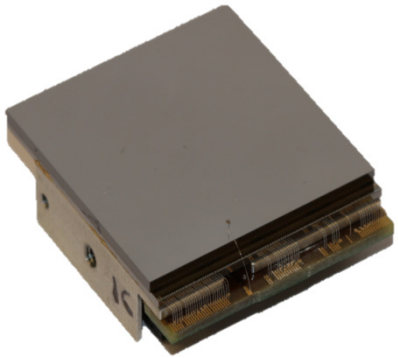

A HEXITEC detector module with 1mm thick CdTe mounted on the ASIC and mechanical block.

80 x 80 pixel 250 um pitch

Real Space Imaging

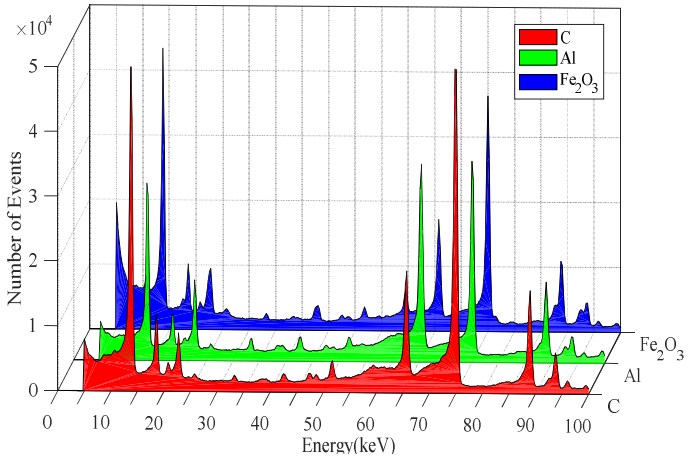

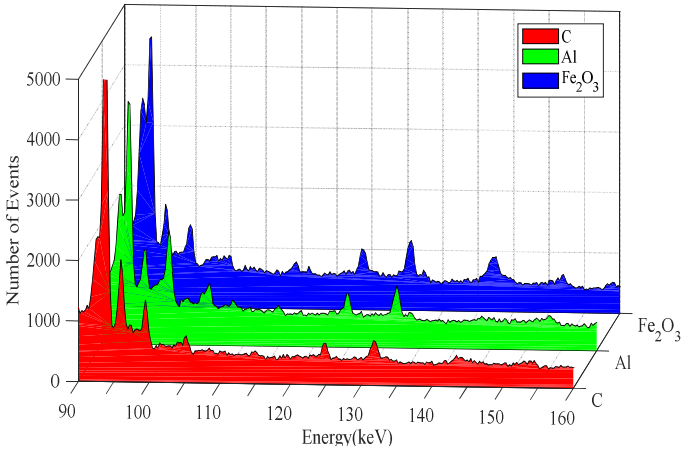

The spectrum from an area of 20x20 pixels next to the C, Al and Fe_2O

66 keV

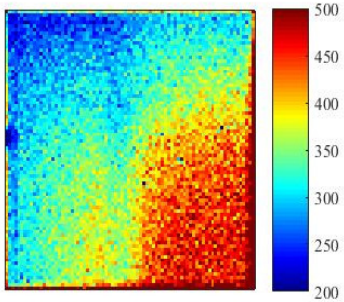

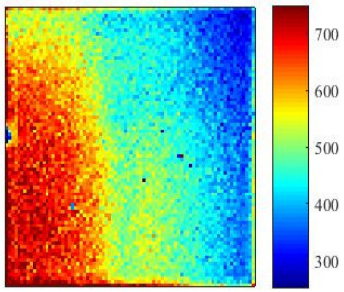

75 keV

130 keV

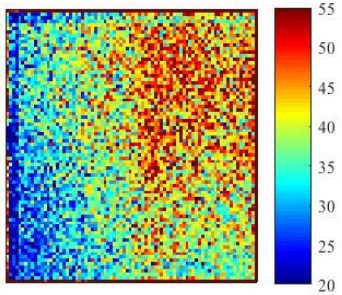

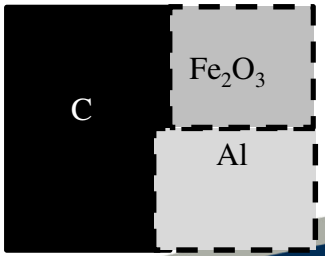

Science & Technology Facilities Council
ISIS

Real Space Imaging

Take slices of elemental composition by varying the momentum

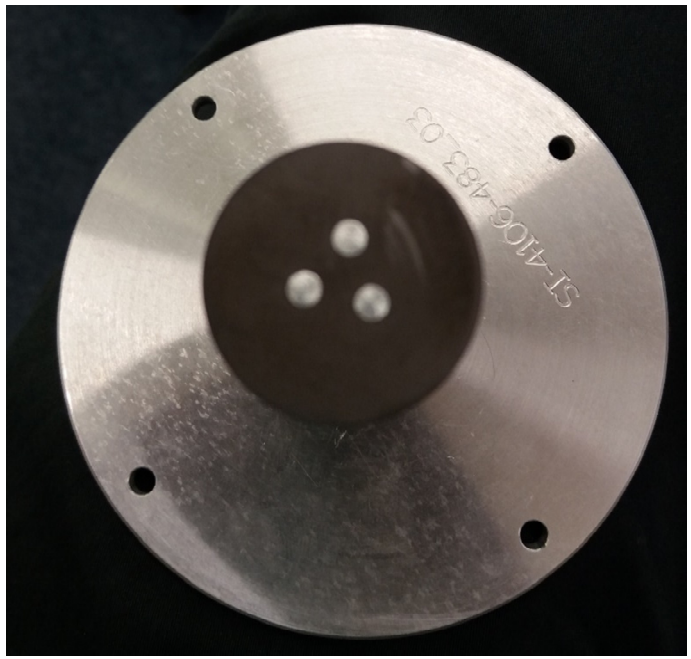

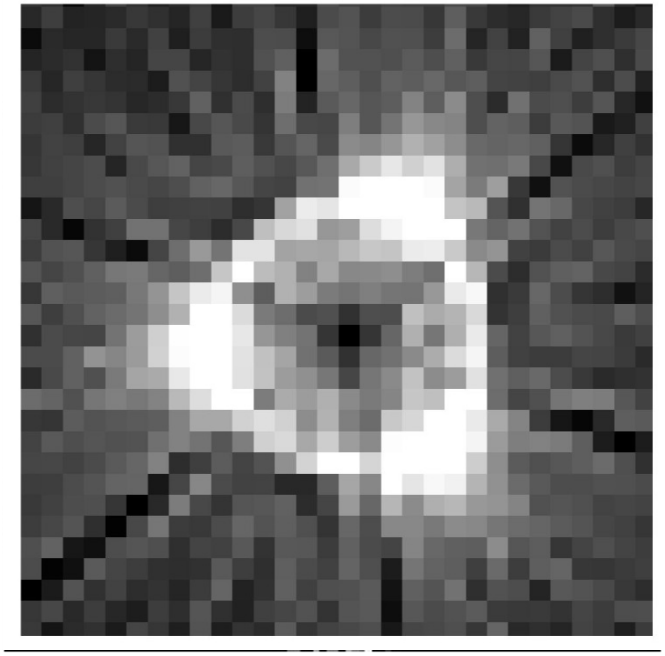

Inverse Randon transform gives the reconstructed image

Conclusions

- Elemental analysis is possible using negative muons
- Non destructive
- Depth can be easily controlled
- Can measure deep inside a sample
- Sensitive to all elements
- Imaging is possible
- Ideas?